Self-interacting Dark Matter of an SU(2) Gauged Dark Sector

by

Ruochuan Liu
B.Sc., University of Victoria, 2015

A Thesis Submitted in Partial Fulfillment of the
Requirements for the Degree of

Master of Science

in the Department of Physics and Astronomy

Self-interacting Dark Matter of an SU(2) Gauged Dark Sector

by

Ruochuan Liu
B.Sc., University of Victoria, 2015

Supervisory Committee

Dr. Pospelov, Supervisor
(Department of Physics and Astronomy)

Dr. Adam Ritz, Departmental Member
(Department of Physics and Astronomy)

Dr. Robert Kowalewski, Departmental Member
(Department of Physics and Astronomy)

Supervisory Committee

Dr. Pospelov, Supervisor
(Department of Physics and Astronomy)

Dr. Adam Ritz, Departmental Member
(Department of Physics and Astronomy)

Dr. Robert Kowalewski, Departmental Member
(Department of Physics and Astronomy)

ABSTRACT

This thesis investigates the possibility that the gauge boson in a certain hypothetical SU(2) gauged sector can constitute *all* the non-baryonic dark matter. The gauge bosons acquire mass from the Higgs mechanism as in the Standard Model and scatter *elastically* among themselves non-gravitationally. It is expected that this self-interaction of the dark gauge bosons would resolve the various discrepancies between the ΛCDM model and astrophysical observations on small (e.g. galactic or galaxy-cluster) scales. Parameter space within the domain of validity of perturbation theory satisfying the constraints of dark matter abundance, the elastic self-scattering momentum transfer cross-section suggested by recent astrophysical observations, and consideration of the Big-Bang nucleosynthesis was found to be non-empty in the "forbidden" regime where the mass of the dark Higgs boson is greater than the mass of the dark gauge boson.

Contents

List of Figures

ACKNOWLEDGEMENTS

I would like to thank:

Prof. Pavel Kovtun, Prof. Adam Ritz, for supporting me in the low moments.

Prof. Maxim Pospelov, for mentoring, support, encouragement, and patience.

University of Victoria, for funding me with a Scholarship.

But science can only be created by those who are thoroughly imbued with the aspiration toward truth and understanding. This source of feeling, however, springs from the sphere of religion. ***To this there also belongs the faith in the possibility that the regulations valid for the world of existence are rational, that is, comprehensible to reason. I cannot conceive of a genuine scientist without that profound faith.***

Albert Einstein

DEDICATION

Just hoping this is useful!

Chapter 1

Introduction

1.1 Introduction to Dark Matter

Dark matter is a hypothetical non-luminous and non-light-absorbing matter whose existence is inferred from certain astrophysical observations in the framework of the currently most well-accepted theory of gravity, i.e. the theory of general relativity[1] [2][3][4]. The phenomena which dark matter is postulated to explain very strongly suggests the insufficiency of the Standard Model of particle physics or the theory of general relativity — arguably two of the most well-tested theories of physics. The explanation of these phenomena is hence crucial to advancing our understanding of the universe from the perspective of physics.

The earliest observations which suggest the existence of dark matter are that various luminous objects (e.g. stars, gas clouds, globular clusters, or galaxies) move faster than they should according to general relativity if only visible matter[2]exists. For example, the velocity of an object moving along a circular orbit about the center of a galaxy according to Newtonian mechanics and Newtonian gravity, a sufficient approximation of the theory of general relativity in this case, should be $v \propto \sqrt{\frac{M(r)}{r}}$, where $M(r)$ is the mass enclosed in a 2-dimensional sphere of radius r centered at the center of the galaxy[3]. This implies that if all the galaxy's mass is of the visible matter, v should be proportional to $\frac{1}{\sqrt{r}}$ for r greater than the largest distance from the center of the galaxy where density of visible matter is non-negligible. However, it

[1] Although in practice Newtonian gravity and Newtonian mechanics often suffices.

[2] Matter which is luminous or not transparent.

[3] Such a plot of $v(r)$ vs r is commonly referred to as a "rotation curve" of a galaxy.

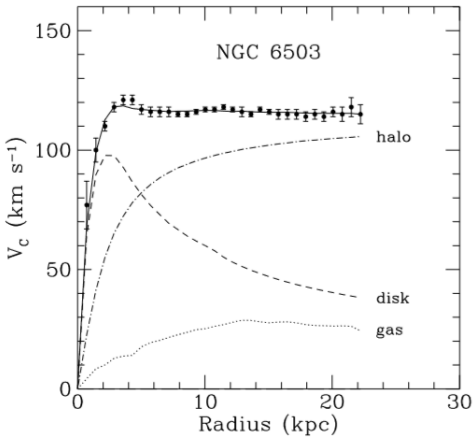

Figure 1.1: This is a plot of the rotation curve for NGC 6503 *from reference* [1]. The three labelled curves are for contributions from the respective sources as indicated.

was observed[4] that v is to a good approximation independent of r wherever rotational velocity of the objects can be measured [5] (as shown in Figure 1.1), which implies that if the theory of gravity is not to be modified, it must be the case that (approximately) $M(r) \propto r$ and therefore $\rho(r) \propto \frac{1}{r^2}$ for r larger than the radius of the visible part of the galaxy. This suggests the existence of a "halo" of dark matter which extends beyond the visible part of the galaxy. The abundance of dark matter required to resolve the discrepancy was estimated to be about 20%[5][6][7][8]. Many other evidence were subsequently found for the existence of dark matter on sub-galactic and inter-galactic scales but they will not be discussed here; for a shortlist of some of these evidence see reference [4].

Evidence for the existence of dark matter was also found from the observations of the galaxy clusters [4][2]. The total mass of a cluster can be determined by various observations which include weak gravitational lensing [9], radial velocity distribution of the galaxies[6] in the cluster and X-ray emission profile of the cluster. The fraction of mass of visible matter (which is approximately the same as that of baryonic matter[7]) in a cluster can be determined by (among other means) the temperature

[4]Usually by combining the observations from the 21cm hydrogen spectral line and optical surface photometry [4].

[5]See Chapter 3 for reference.

[6]Which is related to the gravitational potential through the virial theorem, assuming that the cluster is virialized, i.e. that the virial theorem applies to the cluster.

[7]Here baryonic matter refers to protons, neutrons and electrons — the particles which make up the ordinary atomic matter.

of the cluster at large distance from the center of the cluster[8], assuming hydrostatic equilibrium for the part of the cluster of concern — if all mass of a cluster is of the baryonic matter, the temperature of the cluster would be much higher than what was observed, hence we may infer the existence of dark matter [4]. The far from core density profile of the clusters generated by numerical simulations of collisionless dark matter agrees with that determined from the astrophysical observations, but near the cores of the clusters there is still no consensus as to whether the astrophysical observations agree with the numerical simulations of dark matter halos. For example, these numerical simulations produce the so-called "cuspy" DM halo density profiles — profiles for which the density $\rho(r)$ increases drastically as radius r becomes small, whereas observations of gravitational lensing suggest that such "cuspy" profiles are very unlikely [10]. This discrepancy suggests the possibility that dark matter has non-negligible non-gravitational elastic self-interaction, since the numerical simulations which produce "cuspy" profiles assumed that dark matter is collisionless (i.e. does not self-interact elastically except through gravity) and that the existence of such self-interaction can produce density profiles which are not "cuspy" at the central regions of the halos [6]. This possibility is one of the main motivations for the model which will be presented in this thesis and will be discussed in more detail in Chapter 2 [9].

The observation of the anisotropies of the cosmic microwave background (CMB)[10] also provides evidence for the existence of dark matter. Not only so, it is able to provide a tight constraint on the abundance[11] of dark matter (whereas the observations of the galaxies and galaxy clusters cannot) [4] — the abundance of dark matter was determined to be about 24%, a number close to the aforementioned estimate from observations on the galactic scales. See references [2][12][13] for details about the determination of the abundance of dark matter from the CMB anisotropies.

Many cosmologists consider the existence of old galaxies of redshift $z \approx 10$ to be the strongest evidence suggesting the existence of dark matter, since the matter domination era begins earlier if dark matter is present than if it is absent. This

[8] Where the temperature is approximately constant.

[9] It is to be noted however that the observation of the bullet cluster (1E0657-558) passing through another cluster gave a very small upper-bound for the allowed strength of elastic self-interaction of dark matter [3].

[10] See reference [11] for an introduction to CMB.

[11] Defined to be ρ_{DM}/ρ_{crit}, where ρ_{DM} is the energy density of the dark matter at cosmological scale and ρ_{crit} is the critical energy density of the universe. Note that at large scales the energy density is approximately spatially homogeneous.

allows cosmological density perturbation (with respect to the homogeneous density indicated by the FRW metric) to be larger in this early period (of $z \approx 10$) than in the case when dark matter is absent and thus earlier formation of galaxies [159][2].

If such a large amount of dark matter is made up of baryonic matter only, it would be difficult to explain why they cannot be directly observed through telescopes [14][6]. The baryonic content of the universe predicted by arguments concerning the big bang nucleosynthesis also suggests that it is very unlikely that the dark matter could be mostly baryonic [15][6].

Neutrinos in the Standard Model of particle physics appeared to be a good candidate of dark matter [6][16][17][18]. However, they must decouple from electrons and photons during the early stage of the formation of the first galaxies when they were so energetic that they need to be treated as relativistic particles (as such they are considered to be "hot") and this has implication on how galaxies and galaxy clusters form if they are to play the role of dark matter[12], implication which has been shown using numerical simulations to be inconsistent with observations of galaxy clustering [6][20][21]. Of course, this reasoning not only rules out Standard Model neutrinos as dark matter but also "hot" dark matter in general[13]. The standard model of cosmology nowadays is the so called ΛCDM (Λ[14] Cold Dark Matter) model [22], a model which has been very successful in accounting for many cosmological and astrophysical observations including the matter power spectrum [23][24][25] and some aspects of galaxy formation [26][27].

It is of the consensus now that there is no viable candidate for most of the dark matter from the Standard Model of particle physics. The most well-known types of viable candidates of dark matter include the so called the Weakly Interacting Massive Particles (WIMPs) and axions. These candidates are favoured because they were motivated to solve problems which are seemingly unrelated to dark matter but naturally satisfy the abundance constraint on dark matter from observation. For details about these dark matter candidates see references [31, 32, 33, 34, 35, 36, 37, 4, 38, 39] and the previously cited reviews on the subject.

One might consider instead of postulating the existence of dark matter, an al-

[12]In a universe with hot dark matter, superclusters form before galaxies according to numerical simulations [19].

[13]Note that this is based on the assumption that dark matter is all "hot"" or all "cold". It remains a possibility that some but not all dark matter is "hot". It is also possible for some or all dark matter to be neither "cold" nor "hot", but "warm". See for example references [6][28][29][30].

[14]Referring to the existence of a non-zero cosmological constant. See any well-known textbook on the theory of general relatvity or cosmology for explanation.

ternative theory of gravity which would explain the aforementioned observations. The most well-known example of such theories is the Modified Newtonian Dynamics (MOND). However, despite its success in describing the rotation curves and various other observations on galactic scales, this theory has various deficiencies which are discussed in references [40][41], including its inability to account for the CMB anisotropies and formation of large scale structures (of scales much larger than galactic scale), whereas many of the quantum field theoretic dark matter models (along with general relativity) have been successful thus far in accounting for the relevant astrophysical observations [2].

1.2 Brief Summary of the following Chapters

Chapter 2 discusses the potential problems of the ΛCDM model at galaxy or galaxy cluster scales and possible elastic self-interaction of dark matter which might resolve these potential problems as suggested by observations, simulations and semi-analytical models. This provides the main motivation for the model of dark matter which will be introduced in Chapter 4.

Chapter 3 provides a review of some of the most basic knowledge of cosmology that is required for understanding the subsequent chapters.

Chapter 4 introduces the model of dark matter and presents the results of calculations within the model and the parameter space found to satisfy the observational constraints.

Chapter 5 discusses the methods used to calculate the results and some relevant aspects of the model which have not been covered by this thesis.

Chapter 6 is mostly a summary of the results and discussions from Chapter 4.

Chapter 2

Self-interaction of Dark Matter

For a detailed and comprehensive review on the elastic self-interaction of dark matter, see [6] — **this chapter will closely follow certain parts of this reference**.

2.1 Problems of CDM model which elastic self-interaction of DM might resolve

Despite the success of the ΛCDM model on large scale, several problems on the scale of the galaxies and galaxy-clusters were discovered since the 1990s [6]. A very brief introduction to some of the problems will be given in this section.

2.1.1 "Core-Cusp" Problem

Observations of rotation curves of disk galaxies suggest that they have a "core" type density profile of roughly $\rho \propto r^0$ near the center of the galaxies, as implied by the rotation speed profile of $v(r) \propto r$ [42][43][44]. However, high-resolution simulations of CDM halos shows a "cusp" type density profile that is of roughly $\rho \propto r^{-1}$ near the center of halo [45][46][47][44], a profile well described by the Navarro-Frenk-White (NFW) profile [46][47][48]

$$\rho_{NFW}(r) = \frac{4\rho_s}{r/r_s\,(1 + r/r_s)^2}, \tag{2.1}$$

where r is the radius from the center of the halo, r_s is the characteristic scale radius of the halo defined to be the r at which

$$\frac{d[\log\rho_{NFW}(r)]}{d[\log r]} = -2 \tag{2.2}$$

and $\rho_s \equiv \rho_{NFW}(r_s)$ is the characteristic density. Since the dwarf and low-surface brightness (LSB) galaxies are highly dominated by dark matter even near the center of the DM halo, they are ideal for testing the the CDM model (as the influence of baryons is expected to be insignificant). Indeed, this problem is prevailing for these galaxies as the rotation curves of these galaxies fit better the "cored" than "cuspy" density profiles [49, 50, 51, 52, 53, 54, 55, 56, 57, 58]. However, for the dwarf galaxies, it has also been suggested that the problem could be due to that the simulations included only the DM, neglecting any influence from the baryons [59][60][61][62]. The inadequacy of the NFW profile was also found in large radii. References [63] and [64] found the halo densities of a large number of galaxies of various types and a large mass range at large radii, inferred from the rotation curves, are lower than indicated by the NFW profile. Thus it appears that the galaxies are less dense in the central regions and more dense at large radii than as indicated by the NFW profile.

There are also evidence suggesting the presence of this problem and its possible resolution within the CDM paradigm, for the satellites of the Milky Way [65, 66, 67, 64, 68, 69, 70, 71, 72, 73, 74, 75, 76, 77, 78, 79, 80, 81, 82] and galaxy clusters [10, 83, 84, 85, 86, 87, 88, 89, 90] — for a summary of these references see reference [6].

2.1.2 Diversity Problem

Since for r_s and ρ_s in equation (2.1), r_s determines ρ_s, the function $\rho_{NFW}(r)$ which determines the rotation curve is determined by only one parameter, e.g. the maximum circular speed $V_{\max}$ of the of the celestial objects orbiting about the center of the halo. In general, formation of cosmological structure in the ΛCDM model should be a self-similar process and there should be little variation in density profiles for halos of a certain mass [47][91]. However, the density profiles, i.e. $\rho(r)$, of the galaxies observed appear to be quite diverse, e.g. galaxies of the same $V_{\max}$ can have density profiles which are significantly different at small radii [92][93]. This problem is thus called the "Diversity Problem".

2.1.3 Missing Satellites Problem

Simulations of CDM suggest the structure formation of dark matter halos to be hierarchical and hence each dark matter halo should contain a large amount of subhalos [94]. But the number of subhalos as suggested by CDM simulations is far greater than the number of observed small galaxies within the Local Group. When this issue was first discovered in the Milky Way, only 10 dwarf spheroidal galaxies had been observed, while the estimate for the number of subhalos sufficiently large to host galaxies is of $O(100)$ to $O(1000)$ [95][96]. Although the problem is in fact not as severe as it was first thought to be, as more small galaxies were discovered subsequently in the Milky Way, and some galaxies associated with subhalos might be too faint to be observed due to their lack of baryonic content (mainly stars) [97][98][99]. Sloan Digital Sky Survey has speculated that there could be a factor of 5 to 20 more dwarf galaxies which are undiscovered due to faintness, limited sky coverage and luminosity bias [100][101][102]. In addition to that, the Dark Energy Survey has recently found 17 new candidate satellites.

Similar discrepancy was also found for dwarf galaxies in the field within the Local Volume[1] [103][104][105][106]. Some have suggested however that this discrepancy is due to that the HI line[2] widths are biased tracers for $V_{\max}$ of the halos, where $V_{\max}$ was used to determine the size of the galaxies[3], but whether this is the case is currently under debate [107, 108, 109, 110, 111, 27].

Note that this problem does not exist for the galactic-scale substructures in Galaxy clusters [95].

2.1.4 Too-Big-to-Fail Problem

CDM only simulations predict that the most massive subhalos should be associated with the most luminous satellites in the Milky Way. However, the central regions of these subhalos in the simulations are too dense to be consistent with the stellar dynamics of the most luminous dwarf spheroidal galaxies [112][113]. Similar discrepancies were found for dwarf galaxies in Andromeda [114] and the Local Group field [115]. The problem's name comes from the expectation that the most massive subhalos are too dense to not have generated visible galaxies within them. A similar

[1] A galaxy in the field is one that doesn't belong to any cluster of galaxies.
[2] Also called the "21-centimeter line".
[3] As the problem is of the under-abundance of *small* galaxies.

problem was also observed for dwarf field galaxies [115, 106, 116, 117, 118]. For a more detailed discussion including a discussion on the possibility that this problem might be resolved without abandoning the CDM paradigm, see reference [6].

The resolution of the "Core-Cusp" problem may also resolve this problem.

2.2 Some Resolutions of the aforementioned problems of the CDM model

2.2.1 Warm Dark Matter

A warm dark matter is a dark matter which thermally decoupled[4] in the early universe from the cosmic plasma when it was quasi-relativistic (rather than non-relativistic as was the CDM) [28][29]. Warm DM has a damped linear power spectrum due to free-streaming, suppressing the number of substructures [6]. Warm DM halos typically have density profiles that are more spread-out than the CDM halos since they form later than the CDM halos [6]. Recent high-resolution simulations of warm DM suggest that warm DM models may resolve the missing satellite problem and the too-big-to-fail problem [119][120][121]. Despite these successes, the warm dark matter models also have their inadequacies. The mass of the thermal warm DM is severely constrained by the abundance of high redshift galaxies [122] and Lyman-α forrest observations [123][124], and that the radii of the thermal warm DM halo cores, in light of the Lyman-α and lensing constraints, are significantly smaller than what is needed to solve the "Core-Cusp" problem [125].

2.2.2 Baryonic Feedback

Since the discovery of the aforementioned problems of the ΛCDM model on small scales, there had been much debate about whether they can be resolved by having the baryonic feedback processes (e.g. gas cooling, supernovae, star formation and active galactic nuclei) included in the simulations [6]. A review of the baryonic feedback is given in [6] *with a short summary*[5]. The review concluded that it is possible that the aforementioned problems in small scales cannot be resolved by baryonic feedback

[4] See Chapter 3 for definition.

[5] On page 24 of the reference.

alone. Hence it is possible that the CDM model needs to be modified at small scales by consideration of the aforementioned discrepancies.

2.2.3 Self-Interacting Dark Matter (SIDM)

A self-interacting dark matter (SIDM) is a dark matter that can have (non-gravitational) *elastic* 2 to 2 scatterings among themselves. A SIDM model was initially proposed to resolve the "cusp-core" problem and the missing satellites problem [126]. SIDM model differs significantly from collisionless CDM model in its implication on the DM halo structure at small radii. See Figure 2 of reference [6] for a comparison of the density profile of CDM halo and that of the SIDM halo. There are three important differences between a CDM halo structure and a SIDM halo structure [6][6]:

1. For CDM halo, the DM velocity dispersion at radius r decreases as r decreases in the inner halo, while SIDM's velocity dispersion is uniform with respect to radius. The velocity distribution of SIDM is closer to the Maxwell-Boltzmann distribution than that of the CDM [127].

2. SIDM halos have a "cored" rather than "cusped" density profile.

3. CDM halos are triaxial [128] while SIDM tends to be approximately spherical, since the elastic self-scattering makes the velocities of DM particles isotropic, which erases the ellipticity.

SIDM halo structure is the same as the CDM halo structure at large radii, since self-scattering rate is proportional to DM density, which becomes too small at large radii for the self-interactions to be relevant.

Many studies have been done on the effects of including elastic self-interaction in the simulations of DM halos and on the constraints for strength of the elastic self-interaction by comparing the results of the simulations with various observations [129, 130, 131, 132, 133, 134, 135, 136, 137, 138, 139, 140, 141, 142, 143, 144, 145, 146, 147, 148]. Some of the properties of the SIDM were not inferred from simulations but semi-analytical models based on Jeans-equation [148, 149, 150]. These studies suggest that introducing elastic self-interaction may resolve the "core-cusp" problem, diversity problem and the "too-big-to-fail" problem, but not the missing satellites problem. See [6] for some detailed discussions of why introducing elastic self-interaction may or may not resolve these problems. A summary of the positive observations and observational constraints are shown in Table I of reference [6]. We may infer from the table that

[6] See [6] for details.

the constraint on the elastic self-interaction strength, in terms of σ/m_{DM}, where σ is the 2 to 2 elastic self-scattering cross-section and m_{DM} is the mass of the dark matter particle, is

$$\frac{\sigma}{m_{\rm DM}} \approx 1\frac{\rm cm^2}{\rm gram} = 1.78 \times 10^{-24}\frac{\rm cm^2}{\rm GeV} = 4.59 \times 10^{3}{\rm GeV}^{-3}. \tag{2.3}$$

It is not obvious as to which cross-section should be used in place of the aforementioned σ in simulations — when the 2 to 2 elastic self-scattering amplitude is independent of the scattering angle, σ can simply be taken as the ordinary cross-section; but for some elastic 2 to 2 self-scattering processes the forward scattering can enhance the cross-section dramatically or even make it infinity (e.g. when the self-scattering may be mediated by a massless gauge boson), in which case it is computationally inefficient or impossible to take σ to be simply the cross-section. One of the the replacements for the usual cross-section here is the momentum transfer cross-section [151, 152, 153, 154, 155, 156, 157, 158], defined as:

$$\sigma_{tr} := \int (1 - \cos\theta)\,\frac{d\sigma}{d\Omega} d\Omega, \tag{2.4}$$

where $d\Omega \equiv \sin\theta d\theta$ is the solid angle measure and σ is the usual cross-section. This cross-section (approximately) measures the average loss of forward momentum in a 2 to 2 scattering, since the longitudinal momentum transfer is $\Delta p = m_{DM} v_{rel}(1-\cos\theta)$ [6], where v_{rel} is the relative velocity between the initial state particles.

Reference [152] suggested that a viscosity (or conductivity) cross-section is better at capturing the elastic self-interaction of DM, it is defined as:

$$\sigma_{vis} := \int \left(1 - \cos^2\theta\right)\frac{d\sigma}{d\Omega} d\Omega. \tag{2.5}$$

However, two of the authors of [152] claimed in [6] that considering the systematic uncertainties in the relevant astrophysical observations, both σ_{tr} and σ_{vis} are good as measures of DM elastic self-interactions. We used σ_{tr} in the calculations for our model (which will be introduced in the Chapter 4).

Chapter 3

A Brief Review of Relevant Basic Knowledge in Cosmology

This chapter will only cover some of the basic knowledge required for the following chapters and will mainly follow the "Big-Bang Cosmology" chapter of reference [2]. For a detailed and comprehensive introduction of cosmology see references [159][160]. Readers who are familiar with modern cosmology are advised to skip this chapter.

3.1 FRW Metric, Expansion of the Universe and Thermodynamics

Modern cosmology relies on the the theory of general relativity as a theory of spacetime and gravity[1]. From the perspective of general relativity, the universe is described by the metric tensor which characterizes the spacetime manifold, usually denoted as $g_{\mu\nu}$ or ds^2, and the energy-momentum-stress tensor on the spacetime manifold which characterizes matter, usually denoted as $T_{\mu\nu}$. The dynamical equation of the metric tensor *and* the energy-momentum-stress tensor is called the Einstein's equation:

$$\mathcal{R}_{\mu\nu} - \frac{1}{2}\mathcal{R}g_{\mu\nu} + \Lambda g_{\mu\nu} = \frac{8\pi G}{c^4}T_{\mu\nu}\,, \tag{3.1}$$

where $\mathcal{R}_{\mu\nu}$ is the Ricci curvature tensor, $\mathcal{R}$ is the scalar curvature, G is the gravitational constant, c is the speed of light and Λ is called the cosmological constant.

[1] For a comprehensive introduction of general relativity, see reference [161].

Astrophysical observations suggest that the matter distribution in the universe is at a large scale[2] spatially homogeneous and isotropic. The homogeneity and isotropy of the matter distribution implies the homogeneity and isotropy of the metric tensor[3]. This allows us to describe the "ultra-low-resolution" features of the spacetime of the universe with only two parameters, one giving the scaling of the metric and the other describing the curvature. This spatially homogeneous and isotropic metric tensor is called the Friedmann-Robertson-Walker (FRW) metric and is usually expressed as:

$$ds^2 = dt^2 - R^2(t)\left[\frac{dr^2}{1-kr^2} + r^2(d\theta^2 + \sin^2\theta d\phi^2)\right], \tag{3.2}$$

where we have set $c = 1$, r, θ and ϕ are 3-dimensional spherical coordinates, t is called the cosmic time, $R(t)$ is called the scale factor and is of dimension of length, k represents curvature, r is dimensionless. We also use a dimensionless scale factor $a(t) := \frac{R(t)}{R(t_0)}$ where t_0 is the present day cosmic time.

The homogeneous and isotropic matter is called a perfect fluid, defined by the energy-momentum-stress tensor:

$$T_{\mu\nu} = -pg_{\mu\nu} + (p+\rho)u_\mu u_\nu, \tag{3.3}$$

where u is the four-velocity, p is the isotropic pressure and ρ is the energy density. With the FRW metric and the energy-momentum-stress tensor of the perfect fluid, the Einstein's equation can be written as:

$$\left(\frac{\dot{a}}{a}\right)^2 = \frac{8\pi G\rho}{3} - \frac{k}{a^2} + \frac{\Lambda}{3} \tag{3.4}$$

and

$$\frac{\ddot{a}}{a} = \frac{\Lambda}{3} - \frac{4\pi G}{3}(\rho + 3p). \tag{3.5}$$

These two equations are called the Friedmann equations. $\dot{a}/a$ is called the Hubble parameter and is usually denoted as H.

We also have energy momentum conservation $\nabla_\mu T_{\mu\nu} = 0$, where ∇ is the the Levi-

[2]For definition of "large scale" see the references mentioned at the beginning of this section.
[3]Strictly speaking by Einstein's equation.

Civita connection[4]. This gives conservation of energy, or first law of thermodynamics[5]:

$$\dot{\rho} = -3H(\rho + p). \tag{3.6}$$

We may re-write equation (3.4) as

$$\frac{k}{H^2 a^2} = \Omega - 1, \tag{3.7}$$

where $\Omega := \frac{\rho}{\rho_c}$ and $\rho_c := \frac{3H^2}{8\pi G}$ is called the critical density. We may see from (3.7) that $\Omega > 1$ corresponds to $k > 0$, $\Omega = 1$ corresponds to $k = 0$ and $\Omega < 1$ corresponds to $k < 0$. It is also helpful to consider different sources of contribution to Ω — $\Omega \equiv \Omega_m + \Omega_r + \Omega_v$, where Ω_m is the contribution to Ω from non-relativistic particles (i.e. particles of sufficiently low energy; usually referred to as "matter"), Ω_r from relativistic particles (usually referred to as "radiation") and Ω_Λ from the cosmological constant.

Let $w := \frac{p}{\rho}$, then equation (3.6) becomes

$$\frac{\dot{\rho}}{\rho} = -3(1 + w)\frac{\dot{a}}{a}, \tag{3.8}$$

which can be solved to yield

$$\rho \propto a^{-3(1+w)}. \tag{3.9}$$

The spatial curvature of spacetime on large scales has been estimated to be approximately 0 with a very small margin of error [23]. We therefore may take $k = 0$. According to various astrophysical evidences [162][163][164][165][166], the matter in the universe should have been in a very hot and dense state in the past, thus the energy of the early universe was mostly of radiation and Ω_r dominates Ω_v in equation (3.7) as well[6]. Hence we may also set $\Lambda = 0$ and $w = 1/3$ during this *radiation dominated* era. Thus in early universe we have, by equation (3.9):

$$\rho \propto a^{-4}. \tag{3.10}$$

We may also derive from equation (3.4) and (3.10) that $a(t) \propto t^{\frac{1}{2}}$ in the radiation dominated era. Similarly, in the case of matter domination, we have $w = 0$ and

[4]Also referred to by many as the covariant derivative with respect to the Levi-Civita connection.
[5]Note that this equation is also implied by the Friedmann equations.
[6]That is, we may take $k = 0$ in this case.

$a(t) \propto t^{\frac{2}{3}}$. In the case when the cosmological constant dominates and is positive[7], we have $w = -1$ and $a(t) \propto e^{\sqrt{\frac{\Lambda}{3}}t}$. These equations fits naturally the astrophysical observation that the universe[8] has been expanding, and that the matter in the universe must have been in a very dense state in the past. The picture of the universe's expanding from a very hot and dense state is called the "Big-Bang" theory and has become the foundation of modern cosmology.

The phase space distribution measure of particle species i in *kinetic* equilibrium is

$$dn_{q_i} = \frac{g_i}{2\pi^2} \frac{1}{e^{-[E_i(q_i)-\mu_i]/T_i} \pm 1} q_i^2 dq_i, \tag{3.11}$$

where q_i is the momentum of the species, T_i is the temperature, g_i is the number of degrees of freedom (excluding the degrees of freedom associated with momentum), E_i is the energy, $+$ if the species is fermionic and $-$ if the species is bosonic. The number density of the species is then [159][2]

$$n_i = \int dn_{q_i}, \tag{3.12}$$

energy density is

$$\rho_i = \int E_i(q_i) dn_{q_i}, \tag{3.13}$$

pressure for an ideal gas is

$$p_i = \frac{1}{3} \int \frac{q_i^2}{E_i(q_i)} dn_{q_i}, \tag{3.14}$$

and entropy is

$$s_i = \frac{\rho_i + p_i - \mu_i n_i}{T_i}, \tag{3.15}$$

where μ is chemical potential. It is well-known that for Standard Model particles $|\mu_i| \ll T_i$ [159][2] so we may set $\mu_i = 0$ for all species i in our discussion. If a species is in *thermal* equilibrium with the cosmic plasma, then T_i would be equal to the temperature of the cosmic plasma[9], usually denoted as T (without an index).

In early universe, temperature is high enough to justify approximating the energy density ρ by only including the energy densities of the relativistic particles (i.e. those

[7] With the standard model of cosmology, $\Lambda > 0$ for our universe according to observation, although Λ is also *very* small [23].

[8] Meaning the spatial part of the metric of spacetime.

[9] And the converse is true as well.

of $m \ll T$), in which case we have [159][2]:

$$\rho = \frac{\pi^2}{30} g_*(T) T^4, \tag{3.16}$$

where

$$g_*(T) = \sum_{i \in B(T)} g_i \left(\frac{T_i}{T}\right)^4 + \frac{7}{8} \sum_{i \in F(T)} g_i \left(\frac{T_i}{T}\right)^4, \tag{3.17}$$

is called the total number of relativistic degrees of freedom associated with the energy density or simply the total number of relativistic degrees of freedom, $B(T)$ is the set of all species of bosons i with $T_i \gg m$, $F(T)$ is the set of all species of fermions i with $T_i \gg m$. The 7/8 factor is due to the difference between the Fermi-Dirac and Bose-Einstein distributions. Similarly, the entropy density is [159][2]

$$s = \frac{2\pi^2}{45} g_{*s}(T) T^3, \tag{3.18}$$

where

$$g_{*s}(T) = \sum_{i \in B(T)} g_i \left(\frac{T_i}{T}\right)^3 + \frac{7}{8} \sum_{i \in F(T)} g_i \left(\frac{T_i}{T}\right)^3 \tag{3.19}$$

is the total number of relativistic degrees of freedom associated with entropy density. Note that since for most of the history of the universe, $T_i = T$ for all species of particles [159], $g_* = g_{*s}$ except during the period of QCD phase transition in which g_* and g_{*s} differ noticeably but very slightly [167][2][10]. For the purpose of our calculations, we may take g_{*s} to be equal to g_*. With equation (3.16), we have in radiation dominated era, by equation (3.4):

$$H = \sqrt{\frac{8\pi G\rho}{3}} = 1.66 g_*^{\frac{1}{2}} T^2 / m_p, \tag{3.20}$$

where $m_p := \frac{1}{\sqrt{G}} = 1.22 \times 10^{19}$GeV is the Planck mass.

We know from elementary thermodynamics that for a system in thermal equilibrium, $dG := dp - sdT = 0$ where G is the Gibbs free energy, therefore by equation (3.15) and equation (3.6), we have the conservation of total entropy when all the particle species are in thermal equilibrium [160]:

$$\frac{d(sa^3)}{dt} = 0. \tag{3.21}$$

[10] See Figure 21.3 of the Big-Bang cosmology chapter of [2].

The conservation of entropy (3.21) and entropy as a function of temperature (3.18) implies

$$a^{-3} \propto s \propto g_{*s}(T)T^3. \tag{3.22}$$

3.2 Decoupling and WIMPs

At a sufficiently early cosmic time, all the Standard Model particles and perhaps the dark matter particles are in thermal or chemical equilibrium since the universe was sufficiently hot and dense for the scatterings among particles which enforce thermal equilibrium among particles to occur sufficiently rapidly. For certain particles (e.g. dark matter particles), the rate at which they annihilate into or interact with the cosmic plasma may become too small for them to maintain thermal or chemical equilibrium with the cosmic plasma as the universe expands and cools, in which case we say it would thermally or chemically *decouple* from the cosmic plasma[11]. A very crude criterion for decoupling is given by[12]

$$\Gamma \lesssim H, \tag{3.23}$$

where Γ is the rate of the scatterings of concern (which are the scatterings which enforce thermal or chemical equilibrium between two systems).

The CMB is made up of the earliest photons which both thermally and chemically decoupled[13] from baryonic matter at around 378,000 years after the Big-Bang[14]. This decoupling occurred roughly when the rate of Compton scattering between electron and photons became equal to H [160].

The so called WIMPs[15] [168][169][160] are one of the most well-known types of dark matter candidates. The WIMPs are initially (i.e. at sufficiently high temperatures) in thermal and chemical equilibrium with the cosmic plasma. They chemically but not thermally[16] decouple from the cosmic plasma as the universe had sufficiently

[11]The binary relation (X,Y) of "X decoupled from Y" is symmetric, i.e. (X decoupled from Y) implies (Y decoupled from X) for any X,Y.

[12]Note that since H^{-1} is the age of the universe as described by the standard Big-Bang model of cosmology [2], this criterion is the requirement that at least one such scattering occurred after the beginning of the cosmic time.

[13]The chemical decoupling occurred before the thermal decoupling.

[14]That is, 378,000 years after the earliest cosmic time.

[15]Weakly-Interacting Massive Particles.

[16]They do eventually also decouple from the cosmic plasma thermally, but this happens after the chemical decoupling.

expanded and cooled, which is roughly when

$$\Gamma_{ann} \lesssim H, \tag{3.23}$$

where Γ_{ann} is the total annihilation rate of the WIMPs. The comoving number density $a^3 n$ of the WIMPs would change little after the chemical decoupling. We therefore say that the annihilation of the WIMPs and the comoving number density have "freezed-out" after the chemical decoupling. If we take the the present day comoving number density of the WIMPs to be its equilibrium number density at the time of freeze-out (i.e. ignoring the annihilation after the freeze-out), we obtain a good estimate of the WIMPs' present day abundance in terms of its total thermally averaged annihilation cross-section $\langle \sigma v \rangle_{ann}$ [168][169][17][18]

$$\begin{aligned} \Omega h^2(\langle \sigma v \rangle_{ann}) &\approx 0.12 \frac{x_f}{30} \frac{g_*(x_f)^{\frac{1}{2}}}{10} \frac{2 \times 10^{-36} \text{cm}^2}{\langle \sigma v \rangle_{ann}} \\ &\approx 0.12 \frac{x_f}{30} \frac{g_*(x_f)^{\frac{1}{2}}}{10} \frac{4 \times 10^{-9} \text{GeV}^{-2}}{\langle \sigma v \rangle_{ann}}, \end{aligned} \tag{3.24}$$

where $x_f := m_X / T_f$ in which m_X is the mass of the WIMP particle and T_f is the temperature when "freeze-out" (i.e. chemical decoupling) occurs and g_* is given in (3.17). See also Appendix B.

The present day abundance of dark matter Ωh^2 required by observation can be taken as that of the non-baryonic matter, determined by observation of CMB anisotropies [23][2] to be

$$\Omega_{nbm} h^2 = 0.1186 \pm 0.0020 \approx 0.12. \tag{3.25}$$

Hence to satisfy the observational constraint for Ωh^2, we must have by (3.24)

$$\langle \sigma v \rangle_{ann} \approx 4 \times 10^{-9} \text{GeV}^{-2}. \tag{3.26}$$

Recall the elastic self-interaction constraint needed to resolve the problems mentioned

[17] Ωh^2 is a function of $\langle \sigma v \rangle_{ann}$ because x_f is determined by $\langle \sigma v \rangle_{ann}$.

[18] Note that reference [160] claimed that the total thermally averaged cross-section $\langle \sigma v \rangle_{ann}$ needs to be roughly of $O(10^{-39})\text{cm}^2$ for the DM abundance to be of $O(1)$ rather than $O(10^{-36})\text{cm}^2$ as indicated by 3.24. The result in 3.24 is the correct one.

in Chapter 2

$$\frac{\sigma_{tr}}{m_{\mathrm{DM}}} \approx 4.59 \times 10^{3}\mathrm{GeV}^{-3}. \tag{2.3}$$

If σ_{tr} and $\langle \sigma v \rangle_{ann}$ are of the same order in coupling constant(s)[19], we see that in order for the WIMPs to satisfy both the constraint for the abundance and the constraint for the elastic self-interaction, m_{DM} needs to be roughly of $O(10^{-12})$GeV. By arguments from Big-Bang nucleosynthesis[20] however, the mass of a thermal dark matter[21] particle must be greater than 5×10^{-4}GeV [170], hence we may safely judge that in this case the WIMPs cannot satisfy all the three aforementioned constraints.

[19] Note that they are of the same mass dimension.

[20] If the mass of dark matter is sufficiently small, it would be relativistic and therefore contribute significantly to the total energy density of the universe and thus make the Hubble parameter H significantly larger than that if the mass of dark matter isn't so small, before the freeze-out of the neutron-proton ratio. This would make the freeze-out of the neutron-proton ratio occur earlier and hence make the abundance of the neutrons higher during Big-Bang nucleosynthesis period, an effect which would change the abundance of various elements, in particular ^{4}He and ^{2}H [170]. Observations which constrain the abundance of these elements therefore provide a lower bound on the mass of dark matter.

[21] A thermal dark matter is a dark matter that had been in equilibrium with the cosmic plasma in the early universe.

Chapter 4

A Model of Self-interacting Dark Matter

We take $\hbar = c = 1$, where $\hbar$ is the reduced Planck constant and c the speed of light.

4.1 Lagrangian Density and Feynman Rules

The dark matter is in a dark sector which has an SU(2) gauge invariant Lagrangian density[1]

$$\mathcal{L} = \nabla_\mu \Phi^\dagger \nabla^\mu \Phi - \lambda \left(\Phi^\dagger \Phi - \frac{\rho^2}{2} \right)^2 - \frac{1}{4} \chi^{a\mu\nu} \chi^a_{\mu\nu}, \tag{4.1}$$

where $\Phi(x)$ is a doublet complex scalar field, ρ is a positive real number often called the vacuum expectation value (VEV), $\chi^a_{\mu\nu} = \partial_\mu A^a_\nu - \partial_\nu A^a_\mu + g\epsilon^{abc} A^b_\mu A^c_\nu$ is the field strength tensor for the gauge field $A^a_\mu(x)$ where a=1,2 or 3, ∇_μ is the gauge connection defined by $\nabla_\mu \Phi = \partial_\mu \Phi - igA^a_\mu T^a \Phi$ where $T^a = \frac{1}{2}\sigma^a$ for a=1,2,3 and σ^a are the Pauli matrices. g is a positive real number which will be referred to as the gauge coupling constant. The SU(2) gauge symmetry is often said to be spontaneously broken [175][172][174][173][2].

[1] We recommend reference [171] for a very systematic introduction to the fundamentals of quantum field theory and references [172][173][174] for an introduction to the Standard Model of particle physics.

[2] This is a very common but perhaps confusing statement. In fact, it is not possible for gauge symmetries to be spontaneously broken as proven in reference [176].

The dark sector is coupled to the Standard Model through interaction term:

$$\mathcal{L}_{int} = \lambda_{HP}\left(\Phi^\dagger\Phi\right)\left(H^\dagger H\right), \tag{4.2}$$

where H is the Standard Model Higgs field. This interaction is often referred to as the Higgs portal.

In *unitary gauge*, we have $\Phi(x) = \frac{1}{\sqrt{2}}\begin{bmatrix}0\\ \rho + h\,(x)\end{bmatrix}$ [172][174][173]. We choose ρ and h to be real without loss of generality; the quanta of h will be called the dark Higgs boson. The Lagrangian density can then be expressed as:

$$\begin{aligned}\mathcal{L} &= -\frac{1}{4}(\partial_\mu A^a_\nu - \partial_\nu A^a_\mu)(\partial^\mu A^{a\nu} - \partial^\nu A^{a\mu}) - \frac{1}{4}g^2(\epsilon^{eab}A^a_\mu A^b_\nu)(\epsilon^{ecd}A^{c\mu}A^{d\nu}) - g\epsilon^{abc}A^{b\mu}\partial_\mu A^a_\nu A^{c\nu} \\ &\quad + \partial_\mu h\partial^\mu h + \frac{g^2}{8}A^{a\mu}A^a_\mu(\rho+h)^2 - \frac{\lambda}{4}(h^2+2\rho h)^2 \\ &= -\frac{1}{4}(\partial_\mu A^a_\nu - \partial_\nu A^a_\mu)(\partial^\mu A^{a\nu} - \partial^\nu A^{a\mu}) - \frac{1}{4}g^2(\epsilon^{eab}A^a_\mu A^b_\nu)(\epsilon^{ecd}A^{c\mu}A^{d\nu}) - g\epsilon^{abc}A^{b\mu}\partial_\mu A^a_\nu A^{c\nu} \\ &\quad + \partial_\mu h\partial^\mu h + g^2A^{a\mu}A^a_\mu\left(\frac{\rho^2}{8} + \frac{\rho h}{4} + \frac{h^2}{8}\right) - \lambda\left[\rho^2h^2 + \rho h^3 + \frac{h^4}{4}\right]\end{aligned} \tag{4.3}$$

From the Lagrangian density we find that the masses of the 3 gauge bosons are all equal to $m_A = \frac{1}{2}\rho g$ and they can be treated as identical particles; the mass of the dark Higgs boson is $m_h = \rho\sqrt{2\lambda}$.

The Higgs portal will introduce a mixing of the Standard Model Higgs boson and the dark Higgs boson, hence the dark Higgs boson will decay into the Standard Model particles, with decay rate given by [177]

$$\Gamma_h = \theta^2\Gamma_{h_{SM}}(m_{h_{SM}} \to m_h), \tag{4.4}$$

where h_{SM} is the Standard Model Higgs boson and $m_{h_{SM}}$ is its mass, $\Gamma_{h_{SM}}(m_{h_{SM}} \to m_h)$ is the Standard Model Higgs boson's decay rate with the mass of the Standard Model Higgs boson $m_{h_{SM}}$ substituted with the mass of the dark Higgs boson m_h and θ is the mixing angle between the dark Higgs boson and the Standard Model Higgs boson satisfying [178]

$$\tan 2\theta = \frac{\lambda_{HP}\rho v}{\lambda\rho^2 - \lambda_H v^2}, \tag{4.5}$$

where v is the Standard Model VEV, λ_H is the coefficient associated with the Higgs

field in the Standard Model *which corresponds to* λ in our dark sector. The mixing angle must be upper-bounded by observational constraint discussed in reference [177] and *due to limitation of our consideration* be lower-bounded by the requirement that the dark sector must maintain thermal equilibrium with the cosmic plasma as we will assume, for reason which will be given in Chapter 4.3. The decay of the dark Higgs boson into the Standard Model particles would be the main venue for the dark sector to deplete its energy.

The Feynman rules [173] for the dark sector derived from the Lagrangian density are:

AAAA vertex factor:

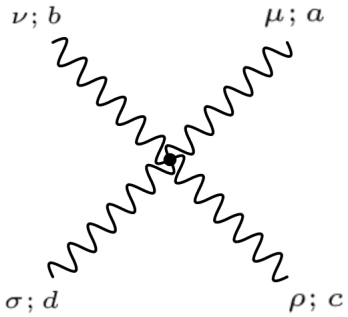

$$-ig^2[\epsilon^{abe}\epsilon^{cde}(g^{\mu\rho}g^{\nu\sigma}-g^{\mu\sigma}g^{\nu\rho})+\epsilon^{ace}\epsilon^{bde}(g^{\mu\nu}g^{\rho\sigma}-g^{\mu\sigma}g^{\nu\rho})+\epsilon^{ade}\epsilon^{bce}(g^{\mu\nu}g^{\rho\sigma}-g^{\mu\rho}g^{\nu\sigma})] \tag{4.6}$$

AAA vertex factor (with the convention that all momenta point towards the vertex):

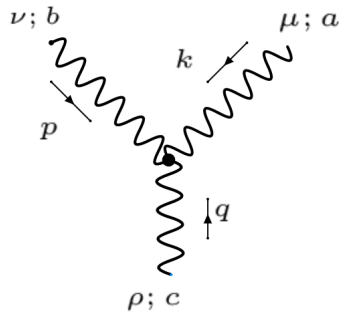

$$g\epsilon_{abc}[g^{\mu\nu}(k-p)^{\rho}+g^{\nu\rho}(p-q)^{\mu}+g^{\rho\mu}(q-k)^{\nu}] \tag{4.7}$$

AAh vertex factor:

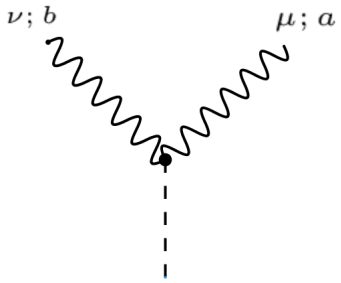

$$2!i\left(\frac{\rho g^2}{4}\right)\delta_{ab}g^{\mu\nu} = i\left(\frac{\rho g^2}{2}\right)\delta_{ab}g^{\mu\nu} \tag{4.8}$$

$AAhh$ vertex factor:

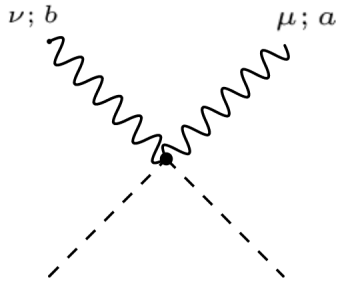

$$2!2!i\left(\frac{g^2}{8}\right)\delta_{ab}g^{\mu\nu} = i\left(\frac{g^2}{2}\right)\delta_{ab}g^{\mu\nu} \tag{4.9}$$

hhh vertex factor:

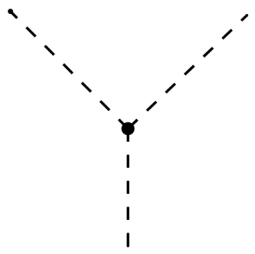

$$3!i\,(\lambda\rho) = i\,(6\lambda\rho) \tag{4.10}$$

$hhhh$ vertex factor:

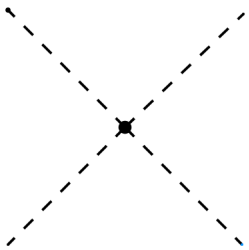

$$4!i\left(\frac{\lambda}{4}\right) = i\,(6\lambda) \tag{4.11}$$

A propagator (in unitary gauge):

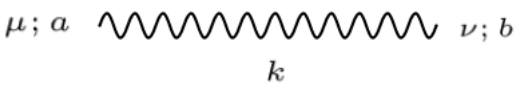

$$\frac{i}{k^2 - m_A^2 + i\epsilon}(-g^{\mu\nu} + \frac{k^\mu k^\nu}{m_A^2})\delta_{ab} \tag{4.12}$$

h propagator:

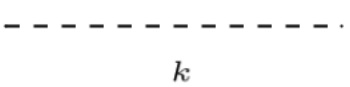

$$\frac{i}{k^2 - m_h^2 + i\epsilon} \tag{4.13}$$

As can be seen from the Feynman rules, the gauge bosons are stable (i.e. do not decay) and can have elastic 2 to 2 scattering among themselves (i.e. the scattering of $AA \to AA$)[3] at $O(g^2)$[4]. See Appendix A for the Feynman diagrams of the elastic scattering of $AA \to AA$ at lowest order in g.

The gauge bosons A's are our dark matter candidate in the model. We show in the subsequent sections the present day abundance of the gauge boson A and the elastic 2 to 2 scattering $(\sigma_{tr})_{AA\to AA}$ in terms of the parameters g, m_h and m_A and find the parameter space which satisfies observational constraint on the present day abundance of dark matter, the elastic 2 to 2 scattering and the constraint from Big-Bang nucleosynthesis considerations[5], within the domain of validity of perturbation theory (as we will only consider the regime where perturbation theory is valid and neglect non-perturbative effects)[6].

After we worked on this model for a few months, reference [181] which covered this model was published. We have done our work independently and will acknowledge some of the differences between our results and theirs.

[3] A dark matter that can have elastic 2 to 2 scattering among themselves is commonly referred to as a "self-interacting" dark matter.

[4] In the scattering amplitude.

[5] See footnote 20 of the last page of Chapter 3.

[6] This is not an observational constraint — it gives the domain of validity of our consideration rather than a parameter space excluded by observation.

4.2 The Constraint on Elastic 2 to 2 Self-Scattering of Dark Gauge Bosons

The momentum transfer cross-section for scattering $AA \to AA$ encodes the information about the elastic self-interaction of A particles [6]. It is defined to be[7] [6][2][182]:

$$\begin{aligned}(\sigma_{tr})_{AA\to AA} &:= \frac{1}{2!}\int (1-\cos\theta)\,\frac{d\sigma_{AA\to AA}}{d\Omega}d\Omega \\ &= \frac{1}{2!}\int_{t_0}^{t_1} (1-\cos\theta)\,\frac{d\sigma_{AA\to AA}}{dt}dt \\ &= \frac{1}{2!}\int_{t_0}^{t_1} \frac{t}{2\left(\frac{s}{4}-m_A^2\right)}\frac{1}{64\pi s}\frac{1}{|\mathbf{p}_{1cm}|^2}|\mathcal{M}_{AA\to AA}(s,t)|^2 dt \\ &= \frac{1}{2}\int_{t_0}^{t_1} \frac{t}{2\left(\frac{s}{4}-m_A^2\right)^2}\frac{1}{64\pi s}|\mathcal{M}_{AA\to AA}(s,t)|^2 dt,\end{aligned} \tag{4.14}$$

where $\sigma_{AA\to AA}$ is the ordinary cross-section, $s = (p_1+p_2)^2$ and $t = (p_1-p_3)^2$ are the Mandelstam variables, $\mathbf{p}_{1cm}$ is the initial 3-momentum in the center of mass frame, $t_0 = 0$ and $t_1 = 4\left(m_A^2 - \frac{s}{4}\right)$.

The non-relativistic limit of the momentum transfer cross-section for $AA \to AA$ at tree level, far from the resonance at $m_h = 2m_A$[8], was calculated to be:

$$(\sigma_{tr})_{AA\to AA} = \frac{g^4\left(320m_A^8 - 1200m_A^6m_h^2 + 8801m_A^4m_h^4 - 4208m_A^2m_h^6 + 520m_h^8\right)}{1152\pi m_A^2 m_h^4\left(m_h^2 - 4m_A^2\right)^2} \tag{4.15}$$

The correctness of the amplitude from which the above result was calculated was checked in Appendix D, in which the amplitude corresponding to only the longitudinal mode of the gauge bosons was calculated and was found to not diverge as $\rho \to 0$.

To resolve the various problems mentioned in Chapter 2 it is required that

$$\frac{\sigma}{m_{\rm DM}} \approx 1.78\times10^{-24}\frac{\rm cm^2}{\rm GeV} = 4.59\times10^{3}{\rm GeV}^{-3}, \tag{2.3}$$

where $\sigma = (\sigma_{tr})_{AA\to AA}$ and $m_{\rm DM} = m_A$ in this case.

[7] See also Chapter 2.

[8] We will only consider the case when $\frac{m_h}{m_A} > 2.05$ or $\frac{m_h}{m_A} < 1.95$ to avoid the resonance.

We will denote $(\sigma_{tr})_{AA\to AA}$ simply as σ_{tr}.

4.3 Evolution of Number Density of the Dark Matter Particles

The present day abundance of a particle species depends on its present day number density. When the dark gauge bosons are in chemical and thermal equilibrium with the cosmic plasma, the number density n_A is given by equation (3.12) with $T_A = T$. There is no reason to expect however that the gauge bosons should always be in chemical and thermal equilibrium with the cosmic plasma. The time-evolution of number density of a particle species is given by an appropriate Boltzmann equation independent of whether the species is in chemical or thermal equilibrium, but we will assume that the A's and the h's are in thermal equilibrium with the cosmic plasma, an assumption which is well justified if λ_{HP} is sufficiently large and will greatly simplify[9] this equation [179][159][160][10]. To solve the time-evolution equation for the number density of A we use a well-known ansatz [179][159][160] which is introduced in Appendix B.

The Boltzmann equation integrated over the momentum space for annihilation of the gauge bosons[11] (taking into account only the diagrams of scatterings which change the number density and of sufficiently low orders in the gauge coupling constant g), i.e. the time-evolution equation for the number density of the gauge bosons, assuming

[9] As in it would make solving the equation much easier.

[10] The original Boltzmann equation describes the time-evolution of the phase space distribution $f(t, x, p)$, but the time-evolution equation for the number density is directly implied by the time-evolution of $f(t, x, p)$.

[11] This equation will simply be referred to as the "Boltzmann equation" in the rest of the thesis.

the spatial homogeneity of the number density, is [160][179][12],

$$\begin{aligned} a^{-3}\frac{d(a^3 n_A)}{dt} =& 2(n_A^{eq})^2\langle\sigma v\rangle_{AA\to SM}\left[\frac{n_{SM}^2}{(n_{SM}^{eq})^2}-\frac{n_A^2}{(n_A^{eq})^2}\right] \\ & 2(n_A^{eq})^2\langle\sigma v\rangle_{AA\to hh}\left[\frac{n_h^2}{(n_h^{eq})^2}-\frac{n_A^2}{(n_A^{eq})^2}\right] \\ & +(n_A^{eq})^2\langle\sigma v\rangle_{AA\to Ah}\left[\frac{n_A n_h}{n_A^{eq} n_h^{eq}}-\frac{n_A^2}{(n_A^{eq})^2}\right] \\ & +(n_A^{eq})^3\langle\sigma v^2\rangle_{AAA\to AA}\left[\frac{n_A^2}{(n_A^{eq})^2}-\frac{n_A^3}{(n_A^{eq})^3}\right] \\ & +2(n_A^{eq})^3\langle\sigma v^2\rangle_{AAA\to Ah}\left[\frac{n_A n_h}{n_A^{eq} n_h^{eq}}-\frac{n_A^3}{(n_A^{eq})^3}\right] \\ & +3(n_A^{eq})^3\langle\sigma v^2\rangle_{AAA\to hh}\left[\frac{n_h^2}{(n_h^{eq})^2}-\frac{n_A^3}{(n_A^{eq})^3}\right], \end{aligned} \tag{4.16}$$

where a is the scale factor of the Friedmann-Robertson-Walker metric, n_A is the number density of (all species of) the gauge boson A, n_h is the number density of the dark Higgs boson h, n_{SM} is the number density of the relevant Standard Model particles which the A's may annihilate into through the Higgs portal, $n_{eq}{}'s$ are the corresponding number densities at both thermal and chemical equilibrium, the factors of 2 in front of the terms of $AA \to hh$ and $AAA \to Ah$ are due to that the corresponding scatterings reduce the number of gauge bosons by 2 per scattering event and the factor of 3 in front of the term of $AAA \to hh$ is due to that the corresponding scatterings reduce the number of gauge bosons by 3 per scattering event,

$$n_i^{eq}(T) := g_i \int \frac{d^3p}{(2\pi)^3} e^{-\frac{E_i}{T}} = \begin{cases} g_i \left(\frac{m_i T}{2\pi}\right)^{\frac{3}{2}} e^{-\frac{m}{T}} & \text{if } T \ll m_i \\ g_i \frac{T^3}{\pi^2} & \text{if } T \gg m_i \end{cases} \tag{4.17}$$

where i denotes the particle species which is in this case A or h, g_i is the degeneracy of the species i — $g_h = 1$ and $g_A = 3^2 = 9$ (coming from the 3 polarizations and 3 gauge group indices of A), T is the temperature of the cosmic plasma.

The $\langle\sigma v\rangle$'s are called the "thermally averaged cross-sections" and are defined for

[12] See Chapter 3 of reference [160] for a derivation of a similar equation.

the scatterings of our concern to be:

$$
\begin{aligned}
\langle\sigma v\rangle_{AA\to XX} :=& \frac{1}{\left(n_A^{eq}\right)^2}\frac{1}{2!}\frac{1}{2!}\int\left(\prod_{i=1}^{4}\frac{d^3p_i}{(2\pi)^3\,2E_i}\right)(2\pi)^4\delta^{(4)}\left(\sum_{i=1}^{i=4}p_i\right)e^{-\frac{E_1+E_2}{T}} \\
& \sum_{\epsilon,a}\left|\mathcal{M}_{AA\to XX}\right|^2 , \\
\langle\sigma v\rangle_{AA\to XY} :=& \frac{1}{\left(n_A^{eq}\right)^2}\frac{1}{2!}\int\left(\prod_{i=1}^{4}\frac{d^3p_i}{(2\pi)^3\,2E_i}\right)(2\pi)^4\delta^{(4)}\left(\sum_{i=1}^{i=4}p_i\right)e^{-\frac{E_1+E_2}{T}} \\
& \sum_{\epsilon,a}\left|\mathcal{M}_{AA\to XY}\right|^2 , \\
\langle\sigma v^2\rangle_{AAA\to XX} :=& \frac{1}{\left(n_A^{eq}\right)^3}\frac{1}{3!}\frac{1}{2!}\int\left(\prod_{i=1}^{5}\frac{d^3p_i}{(2\pi)^3\,2E_i}\right)(2\pi)^4\delta^{(4)}\left(\sum_{i=1}^{i=5}p_i\right)e^{-\frac{E_1+E_2+E_3}{T}} \\
& \sum_{\epsilon,a}\left|\mathcal{M}_{AAA\to XX}\right|^2 , \\
\langle\sigma v^2\rangle_{AAA\to XY} :=& \frac{1}{\left(n_A^{eq}\right)^3}\frac{1}{3!}\int\left(\prod_{i=1}^{5}\frac{d^3p_i}{(2\pi)^3\,2E_i}\right)(2\pi)^4\delta^{(4)}\left(\sum_{i=1}^{i=5}p_i\right)e^{-\frac{E_1+E_2+E_3}{T}} \\
& \sum_{\epsilon,a}\left|\mathcal{M}_{AAA\to XY}\right|^2 ,
\end{aligned}
\tag{4.18}
$$

where p_1, p_2 are the initial momenta, p_3, p_4 are the final momenta in the 2 to 2 scatterings and p_1, p_2, p_3 are the initial momenta, p_4, p_5 are the final momenta in the 3 to 2 scatterings, the squared amplitudes were summed over polarization and the gauge group indices, and $X, Y \in \{A, h, \text{Standard Model particles}\}$. The factorials in the expressions of thermally averaged cross-sections[13] are to take into account the "over-counting" of the phase space integration due to that there are identical particles in the initial or final states of the corresponding processes [179]. The thermal distribution used in the definitions above is the Boltzmann distribution rather than the Bose-Einstein distribution because the difference between the two distributions are negligible when $m_A > T$, which is the only relevant regime for our calculations[14] [180][179].

In this model we'd assume that the h particles were sufficiently tightly coupled to the cosmic plasma during the time period of our concern so that it was in thermal and chemical equilibrium with the cosmic plasma, an assumption which could be valid

[13]Note that $\langle\sigma v^2\rangle_{AAA\to AA}$ and $\langle\sigma v^2\rangle_{AAA\to Ah}$ have dimension of mass to the power of -5 and are therefore not cross-sections in the ordinary sense.

[14]See page 76 of [160] for reference.

given appropriate choice of λ_{HP}, ρ and λ [177]. Therefore $n_h = n_h^{eq}$, in which case (4.16) becomes:

$$\begin{aligned} a^{-3}\frac{d(a^3 n_A)}{dt} =& -2\langle\sigma v\rangle_{AA\to SM}\left[n_A^2 - (n_A^{eq})^2\right] \\ & -2\langle\sigma v\rangle_{AA\to hh}\left[n_A^2 - (n_A^{eq})^2\right] - \langle\sigma v\rangle_{AA\to Ah}\left[n_A^2 - n_A n_A^{eq}\right] \\ & -\langle\sigma v^2\rangle_{AAA\to AA}\left[n_A^3 - n_A^2 n_A^{eq}\right] \\ & -2\langle\sigma v^2\rangle_{AAA\to Ah}\left[n_A^3 - n_A\,(n_A^{eq})^2\right] \\ & -3\langle\sigma v^2\rangle_{AAA\to hh}\left[n_A^3 - (n_A^{eq})^3\right]. \end{aligned} \tag{4.19}$$

This ordinary differential equation does not admit a general closed-form solution [159][179][160] and is not easy to solve numerically. We therefore decided for the sake of efficiency to solve this equation for various cases in which some of the terms on the right-hand side can be (approximately) neglected *for the purpose of determining the present day abundance of A particles*. The terms (or alternatively, "channels") that cannot be neglected are said to *dominate* the terms which can be neglected. We determine the cases (associated with parameters g, m_A and m_h) by comparing the absolute values of the terms on the right-hand side within the *relevant* parameter spaces[15]. Also note that the following discussions are only concerned with the cases far from (i.e. unaffected by) resonances.

When $m_h \leq m_A$ or when $0 < \frac{m_h}{m_A} - 1 < 1$, the $AA \to Ah$ and $AA \to hh$ channels are not very much suppressed and dominate the $AA \to h$, $AAA \to AA$, $AAA \to Ah$ and $AAA \to hh$ channels since $AA \to h$ is impossible and that the 3 to 2 channels are exponentially suppressed by an extra Boltzmann factor from the thermal distribution, in which case the 3 to 2 channels can be neglected, hence we have:

$$\begin{aligned} a^{-3}\frac{d(a^3 n_A)}{dt} \approx& -2\langle\sigma v\rangle_{AA\to hh}\left[n_A^2 - (n_A^{eq})^2\right] \\ & -\langle\sigma v\rangle_{AA\to Ah}\left[n_A^2 - n_A n_A^{eq}\right]. \end{aligned} \tag{4.20}$$

If $\frac{m_h}{m_A} - 1 > 1$ and is sufficiently large, the 3 to 2 channels dominate the other channels since the other channels will become highly exponentially suppressed due to the phase space limitation of the initial state particles[16] and the Boltzmann factors

[15] Which will be elucidated later.

[16] Since the initial state particles need to have large enough kinetic energy to produce the heavier final state particles.

of the thermal distributions in the integral within the expression of the thermally averaged cross-sections, in which case we have:

$$\begin{aligned} a^{-3}\frac{d(a^3 n_A)}{dt} \approx & -\langle\sigma v^2\rangle_{AAA\to AA}\left[n_A^3 - n_A^2 n_A^{eq}\right] \\ & - 2\langle\sigma v^2\rangle_{AAA\to Ah}\left[n_A^3 - n_A\left(n_A^{eq}\right)^2\right] \\ & - 3\langle\sigma v^2\rangle_{AAA\to hh}\left[n_A^3 - \left(n_A^{eq}\right)^3\right]. \end{aligned} \tag{4.21}$$

When $\frac{m_h}{m_A} - 1 \geq 1$ and is sufficiently small, the $AA \to h$ channel should dominate the other channels since it is less exponentially suppressed than the other channels due to its having less mass deficit (between initial and final state particles) compared to the $AA \to hh$ and $AA \to Ah$ channels and the 3 to 2 channels' being suppressed by an extra Boltzmann factor from the thermal distribution. In this case, since h may decay into the Standard Model particles through the Higgs portal, the dominant annihilation channel would be the annihilation of two A's into the relevant Standard Model particles through the inverse decay of $AA \to h$ and the decay of h into the relevant Standard Model particles. We have:

$$a^{-3}\frac{d(a^3 n_A)}{dt} \approx -2\langle\sigma v\rangle_{AA\to SM}\left[n_A^2 - \left(n_A^{eq}\right)^2\right] \tag{4.22}$$

We call an annihilation channel that is exponentially suppressed because of the phase space limitation due to the total mass of the initial state particles' being less than that of the final state particles as in the cases discussed before a "*forbidden*" channel — when $m_h > m_A$, $AA \to Ah$ and $AA \to hh$ channels both become "forbidden". Similarly, if $m_h \geq \frac{3}{2}m_A$ then $AAA \to hh$ channel becomes "forbidden" and hence can be neglected; if $m_h \geq 2m_A$ then $AAA \to Ah$ also becomes "forbidden" and hence can be neglected, in which case the $AAA \to AA$ channel dominates the other annihilation channels for the purpose of determining the number density of dark matter. Otherwise we need to take into account all the aforementioned channels, i.e. use (4.19).

We will in this thesis investigate the case when the $AA \to hh$ and $AA \to Ah$ channels dominate and the case when the 3 to 2 channels dominate. We leave the case when the annihilation of A's into the Standard Model particles dominates to future work.

The term "2 to 2 channels" will refer to the $AA \to hh$ and $AA \to Ah$ channels in the subsequent part of the thesis.

4.4 The Case When the 2 to 2 Channels Dominate and $m_h < m_A$

When $m_h < m_A$, the case is the standard scenario for a dark matter of the WIMPs type. The WIMPs were introduced in Chapter 3.2. In this case, the annihilation is dominated by the 2 to 2 channels as discussed before, so we only need to include the 2 to 2 annihilation channels in our calculations.

Considering that $(\sigma_{tr})_{AA\to AA}$ and $\langle\sigma v\rangle_{ann}$ are both of $O(g^4/m_A^2)$, by the argument in 3.2, we conclude that in this case the parameter space satisfying the observational constraints is empty within the domain of validity of perturbation theory.

4.5 The Case When the "Forbidden" 2 to 2 Channels Dominate

To calculate the non-relativistic limit of the thermally averaged cross-section for the annihilation of $AA \to hh$ and $AA \to Ah$ when these two channels are "forbidden" and dominate (i.e. roughly when $0 < \frac{m_h}{m_A} - 1 < 1$), we follow the reference [179] for the case when $\frac{m_h}{m_A} - 1 \geq 0.1$ and [183] for the case when $0 < \frac{m_h}{m_A} - 1 < 0.1$. We let $\Delta := \frac{m_h}{m_A} - 1$.

For the case when $\Delta \geq 0.1$, we calculate the thermally averaged cross-section by equation[17] [179]

$$\begin{aligned}\langle\sigma v\rangle_{\text{total}} = \frac{1}{8m_A^2 T_f K_2^2\left(\frac{m_A}{T_f}\right)} \Bigg[&\int_{4m_h^2}^{\infty} \sigma_{AA\to hh}\left(s-4m_A^2\right)\sqrt{s}K_1\left(\frac{\sqrt{s}}{T_f}\right) \\ &+\int_{(m_A+m_h)^2}^{\infty} \sigma_{AA\to Ah}\left(s-4m_A^2\right)\sqrt{s}K_1\left(\frac{\sqrt{s}}{T_f}\right)\Bigg],\end{aligned} \tag{4.23}$$

[17] One might naively expect that since channel $AA \to Ah$ annihilates 1 particle A per scattering event whereas $AA \to hh$ annihilates 2 particles A per scattering event, there should be a factor of 2 in front of the term with $\sigma_{AA\to hh}$. But this is not true because for channel $AA \to hh$ there is also a factor of 1/2 coming from the phase space integral for the final state identical particles.

where $\langle\sigma v\rangle_{\text{total}} := 2\langle\sigma v\rangle_{AA\to hh} + 2\langle\sigma v\rangle_{AA\to Ah}$[18],

$$\langle\sigma v\rangle_{AA\to hh} := \frac{1}{2!}\frac{1}{8m_A^2 T_f K_2^2\left(\frac{m_A}{T_f}\right)}\int_{4m_h^2}^{\infty}\sigma_{AA\to hh}\left(s-4m_A^2\right)\sqrt{s}K_1\left(\frac{\sqrt{s}}{T_f}\right), \tag{4.24}$$

$$\langle\sigma v\rangle_{AA\to Ah} := \frac{1}{2!}\frac{1}{8m_A^2 T_f K_2^2\left(\frac{m_A}{T_f}\right)}\int_{(m_A+m_h)^2}^{\infty}\sigma_{AA\to hh}\left(s-4m_A^2\right)\sqrt{s}K_1\left(\frac{\sqrt{s}}{T_f}\right). \tag{4.25}$$

K_n for $n = 1, 2$ are modified Bessel functions of the second kind, $s = (p_1 + p_2)^2$ is the Mandelstam s variable and T_f is the temperature of the cosmic plasma at the so called point of freeze-out as explained in Appendix B. The $1/2!$ factors are from phase space integral of the initial state of two identical particles. $\sigma_{AA\to hh}$ is the cross-section as usually defined for the scattering $AA \to hh$ and was calculated at the lowest order in the gauge coupling constant g and the lowest order in $s - 4m_h^2$ when $m_A \leq m_h$ to be[19]

$$\begin{aligned}\sigma_{AA\to hh} =& \frac{g^4\sqrt{s-4m_h^2}}{110592\pi m_A^4 m_h^6\sqrt{m_h^2-m_A^2}} \\ & (192m_A^8 - 272m_A^6 m_h^2 + 107m_A^4 m_h^4 + 44m_A^2 m_h^6 + 4m_h^8).\end{aligned} \tag{4.26}$$

$\sigma_{AA\to Ah}$ was calculated at the lowest order in the gauge coupling constant g and lowest order in $s - (m_A + m_h)^2$ when $m_A \leq m_h$ to be

$$\begin{aligned}\sigma_{AA\to Ah} =& -\frac{g^4\sqrt{s-(m_A+m_h)^2}\sqrt{m_A m_h(m_A+m_h)^2}}{864\pi m_A^4 m_h^2(m_A+m_h)^4(2m_A+m_h)^2\sqrt{(m_h+3m_A)(m_h-m_A)}} \\ & \Big(891m_A^8 + 594m_A^7 m_h - 657m_A^6 m_h^2 - 714m_A^5 m_h^3 - 136m_A^4 m_h^4 \\ & +30m_A^3 m_h^5 - m_A^2 m_h^6 - 6m_A m_h^7 - m_h^8\Big).\end{aligned} \tag{4.27}$$

We only need these two cross-sections to the lowest order in $s - 4m_A^2$ and $s - (m_A + m_h)^2$ respectively because for the purpose of calculating the thermally averaged cross-sections, the higher order terms in $s - 4m_A^2$ and $s - (m_A + m_h)^2$ are negligible due to exponential suppression coming from the integrations in (4.23). The expression

[18]The factor of 2 here is due to the difference between the definition of the thermally averaged cross-section in this thesis and that of [179].

[19]By lowest order in g we mean lowest order in g when m_A and m_h are taken to be free parameters, or in other words, when m_A and m_h are fixed.

for $\langle\sigma v\rangle_{\text{total}}$ was obtained assuming the thermal distribution for the gauge bosons of the initial state to be the Maxwell-Boltzmann distribution rather than Bose-Einstein distribution, but the Bose-Einstein distribution can be approximated sufficiently well for our purpose by the Maxwell-Boltzmann distribution since $T_f > m_A$ [180][179]. $\langle\sigma v\rangle_{\text{total}}$ was calculated to be[20]

$$\begin{aligned}
\langle\sigma v\rangle_{\text{total}} = & \frac{g^4 e^{2x} x^2}{27648\pi^{3/2} m_A^5} \\
& \left[\frac{\sqrt{2}\left(192m_A^8 - 272m_A^6 m_h^2 + 107m_A^4 m_h^4 + 44m_A^2 m_h^6 + 4m_h^8\right) e^{-\frac{m_h x}{m_A}}}{\sqrt{m_A^5 m_h^7 x^5 \left(m_h^2 - m_A^2\right)}} \right. \\
& \left(m_h^2 x K_0(\frac{m_h}{m_A}x) + m_A^2(2\frac{m_h}{m_A} - x)K_1(\frac{m_h}{m_A}x) \right) \\
& + \frac{8\left(297m_A^6 + 396m_A^5 m_h + 144m_A^4 m_h^2 - 10m_A^3 m_h^3 - 4m_A^2 m_h^4 + 4m_A m_h^5 + m_h^6\right)}{m_A^2 m_h^{3/2} x^{5/2}(2m_A + m_h)^2} \\
& e^{-\frac{x(m_A+m_h)}{2m_A}} \sqrt{-\frac{4m_A^2}{m_A + m_h} + m_A + m_h} \\
& \left. \left((m_A + m_h)^2 x K_0\left((\frac{1}{2} + \frac{m_h}{m_A})x \right) + 4m_A^2(1 - x + \frac{m_h}{m_A}) K_1\left((\frac{1}{2} + \frac{m_h}{m_A})x \right) \right) \right].
\end{aligned} \tag{4.28}$$

To compare our results with those of reference [181], we also calculated $\sigma_{hh\to AA}$ and $\sigma_{Ah\to AA}$. The results are

$$\begin{aligned}
\sigma_{hh\to AA} = & \frac{3g^4\sqrt{m_h^2 - m_A^2}}{2048\pi m_A^4 m_h^7} \\
& \left(192m_A^8 - 272m_A^6 m_h^2 + 107m_A^4 m_h^4 + 44m_A^2 m_h^6 + 4m_h^8\right), \\
\sigma_{Ah\to AA} = & \frac{g^4\sqrt{1 - \frac{m_A}{m_h}}\sqrt{\frac{3m_A}{m_h} + 1}(m_h - m_A)(3m_A + m_h)}{384\pi m_A^5 m_h^2 (m_A + m_h)(2m_A + m_h)^2} \\
& \left(297m_A^6 + 396m_A^5 m_h + 144m_A^4 m_h^2 - 10m_A^3 m_h^3 \right. \\
& \left. -4m_A^2 m_h^4 + 4m_A m_h^5 + m_h^6\right).
\end{aligned} \tag{4.29}$$

Our result for $\sigma_{Ah\to AA}$ agrees with that from reference [181], but our result for $\sigma_{hh\to AA}$

[20] Note that $K_0(x) \propto e^{-x}$ and $K_1(x) \propto e^{-x}$, hence collecting all the exponential factors for the two terms in the square brackets of the expression yields for the first term a factor of $e^{-2\Delta x}$ and the second term a factor of $e^{-\Delta x}$.

differs from that of theirs. Their result for $\sigma_{hh\to AA}$ simplifies to

$$\sigma_{hh\to AA} = \frac{g^4\sqrt{1-\frac{m_A^2}{m_h^2}}\,(12m_A^4 - 20m_A^2m_h^2 + 11m_h^4)}{128\pi m_h^6}. \tag{4.30}$$

To ensure the correctness of our result for $\sigma_{hh\to AA}$, the high energy limit of it was checked using the Goldstone boson equivalence theorem through calculating the cross-section for the scattering in Lorenz gauge (instead of unitary gauge) of $hh \to \phi_i\phi_i$ where ϕ_i is the Goldstone boson associated with A_i [173][174]. The check confirms our result and refutes theirs. See Appendix E for details.

For the case when $0 < \Delta < 0.1$ we first calculate σv for each of the two processes and expand it in the form of $\sigma v = (a + bv^2)\, v_2$ where v denotes the relative velocity[21] of the initial state particles in the center of mass frame and v_2 denotes the velocity of each of the final state particles in the center of mass frame in the regime when $m_A \approx m_h$. From [183] we have $v_2 = z\left(\frac{v^2}{4} + \mu_+^2\right)^{\frac{1}{2}}$[22] , in which $z = m_h/m_A$ and $\mu_+ = (1-z^2)^{\frac{1}{2}}/z$. Let $(\sigma v)_{hh} = (a_{hh} + b_{hh}v^2)v_2$, $(\sigma v)_{Ah} = (a_{Ah} + b_{Ah}v^2)v_2$. Under

[21] Strictly speaking, v should be the Møller velocity [184][179], but the relative velocity is a sufficiently good approximation of the Møller velocity in this case [180].

[22] Interestingly, by definition of v_2 in reference [183], this expression of v_2 is in fact only accurate in the regime when m_h and m_A are close. It is puzzling that such an expression for v_2 was chosen instead of the exact expression of it in terms of the same variables.

the assumption that $m_h \leq 3m_A$, a_{hh}, b_{hh}, a_{Ah} and b_{Ah} were calculated to be[23]

$$\begin{aligned}
a_{hh} =& \frac{g^4\left(2816m_A^8 - 4160m_A^6m_h^2 + 2700m_A^4m_h^4 - 764m_A^2m_h^6 + 83m_h^8\right)}{27648\pi m_A^2\left(m_h^2 - 2m_A^2\right)^2\left(m_h^2 - 4m_A^2\right)^2}, \\
b_{hh} =& \frac{g^4}{331776\pi m_A^2\left(4m_A^2 - m_h^2\right)^3\left(m_h^2 - 2m_A^2\right)^4}\left(-135168m_A^{14} + 326656m_A^{12}m_h^2\right. \\
& -392128m_A^{10}m_h^4 + 259024m_A^8m_h^6 - 97664m_A^6m_h^8 + 20728m_A^4m_h^{10} \\
& \left.-2164m_A^2m_h^{12} + 61m_h^{14}\right), \\
a_{Ah} =& \frac{g^4(m_A - m_h)(m_A + m_h)\left(9m_A^2 - m_h^2\right)^{3/2}}{384\pi m_A^3\left(m_h^2 - 3m_A^2\right)^2}, \\
b_{Ah} =& \frac{g^4}{1990656\pi m_A^7\left(m_h^2 - 3m_A^2\right)^4}\sqrt{9m_A^2 - m_h^2}\left(363771m_A^{12} + 12798m_A^{10}m_h^2\right. \\
& \left.-80379m_A^8m_h^4 + 17340m_A^6m_h^6 + 2989m_A^4m_h^8 - 922m_A^2m_h^{10} + 51m_h^{12}\right).
\end{aligned} \tag{4.31}$$

Up to the order of v^2, let $\langle\sigma v\rangle_{hh} = \langle\sigma v\rangle_{hh,a} + \langle\sigma v\rangle_{hh,b}$, $\Delta := (m_2 - m_1)/m_1 \equiv z - 1$ and $x := \frac{m_A}{T}$, where from reference [183][24]

$$\langle\sigma v\rangle_{hh,a} = \begin{cases} \langle\sigma v\rangle_{hh,b\to 0,all}, & \text{if } x\Delta \leq -0.023 \\ \langle\sigma v\rangle_{hh,b\to 0,thr}, & \text{if } -0.023 < x\Delta < 0.023 \\ \langle\sigma v\rangle_{hh,b\to 0,for}, & x\Delta \geq 0.023 \end{cases} \tag{4.32}$$

for s-wave annihilation only, and

$$\langle\sigma v\rangle_{hh,b} = \begin{cases} \langle\sigma v\rangle_{hh,a\to 0,all}, & \text{if } x\Delta \leq -0.046 \\ \langle\sigma v\rangle_{hh,a\to 0,thr}, & \text{if } -0.046 < x\Delta < 0.023 \\ \langle\sigma v\rangle_{hh,a\to 0,for}, & x\Delta \geq 0.023 \end{cases} \tag{4.33}$$

[23]Note it might seem that a_{hh} and a_{Ah} are inconsistent with $\sigma_{AA\to hh}$ and $\sigma_{AA\to Ah}$ as shown previously, but these expressions are in fact consistent. For a_{hh} and $\sigma_{AA\to hh}$, the difference is due to that the series expansions are taken with respect to different variables; for a_{Ah} and $\sigma_{AA\to Ah}$, the difference is due to that the series expansions are taken with respect to different variables and the approximation that $m_h = m_A$ for the expression of v_2.

[24]For the cases of "allowed", "near threshold" and "forbidden channel".

for p-wave annihilation only, in which

$$\begin{aligned}
\langle\sigma v\rangle_{hh,all} :=& \sqrt{1-z^2}\left[a_{hh}\left(\frac{3z^2}{4x\left(1-z^2\right)}+1\right)+\frac{6b_{hh}}{x}\left(\frac{5z^2}{4x\left(1-z^2\right)}+1\right)\right], \\
\langle\sigma v\rangle_{hh,thr} :=& \frac{2z}{\sqrt{\pi x}}\left[a_{hh}(1-x\Delta)+\frac{8b_{hh}}{x}\left(1-\frac{x\Delta}{2}\right)\right], \\
\langle\sigma v\rangle_{hh,for} :=& \mu_- z e^{-\mu_-^2 x}\left[a_{hh}\left(\frac{3}{4\mu_-^2 x}+1\right)+4b_{hh}\mu_-^2\left(\frac{45}{32\mu_-^4 x^2}+\frac{9}{4\mu_-^2 x}+1\right)\right],
\end{aligned} \tag{4.34}$$

where $\mu_- := \sqrt{z^2-1}/z$.

The non-relativistic thermally averaged cross-section for channel $AA \to Ah$ cannot be directly calculated using the ansatz from [183], since the ansatz strictly speaking only applies to the case when the final state particles have the same mass[25]. However, in this case $0 < \Delta < 0.1$ so we expect the difference between m_A and m_h to be small enough for the ansatz to work well for the channel $AA \to Ah$. Using the ansatz, the expressions for the $\langle\sigma v\rangle_{Ah}$ is the same as $\langle\sigma v\rangle_{hh}$ with a_{hh} substituted with a_{Ah} and b_{hh} substituted with b_{Ah}.
The total thermally averaged cross-section is then[26]

$$\langle\sigma v\rangle_{\text{total}} = \langle\sigma v\rangle_{AA\to hh} + \langle\sigma v\rangle_{AA\to Ah} \approx \left[\left(a_{hh}+a_{Ah}\right)+\left(b_{hh}+b_{Ah}\right)v^2\right]v_2. \tag{4.35}$$

The abundance of the dark matter (i.e. the dark gauge bosons A) observed now, defined as the ratio of the energy density[27] of dark matter and the total energy density (which is equal to the critical density because we take here the spatial curvature of the universe and the cosmological constant to be both 0), is $\Omega h^2 = \rho_A h^2/\rho_c = m_A n_A h^2/\rho_c$, where $\rho_c = \frac{3H(T_0)m_p^2}{8\pi}$ is the present day critical density and where $H(T_0) = \frac{1}{4.69\times 10^{41}}\text{GeV}$ is the present day Hubble parameter. In the regime for which the 2 to 2 annihilation channels dominate, it is obtained from solving the Boltzmann equation

[25] Because v_2 in the case when the final state particles have different masses is different from that in the case when the final state particles have the same mass.

[26] One might naively expect that since channel $AA \to Ah$ annihilates 1 particle A per scattering event whereas $AA \to hh$ annihilates 2 particles A per scattering event, $\langle\sigma v\rangle_{\text{total}} \approx \left[\left(a_{hh}+\frac{1}{2}a_{Ah}\right)+\left(b_{hh}+\frac{1}{2}b_{Ah}\right)v^2\right]v_2$. But this is not true because for channel $AA \to hh$ there is also a factor of 1/2 from the phase space integral for the final state identical particles.

[27] Note that it is assumed here that the universe's energy density is homogeneous in space.

approximately to be [160][183][159][28]:

$$\Omega h^2(g, m_A, m_h) = \frac{1.07 \times 10^9 x_f g_*(x_f)^{\frac{1}{2}} \text{GeV}^{-1}}{J g_{*s}(x_f) m_p}. \tag{4.36}$$

In the above expression for the abundance, x_f is the $x := \frac{m}{T}$ at the time of the so called "freeze-out" of annihilation as explained in Appendix B [183][159]. It is defined by

$$n_A(x_f) = \sqrt{2} n_A^{eq}(x_f) \tag{4.37}$$

and is determined to be of $O(10)$[29]. $m_p = 1.22 \times 10^{19}$GeV is the Planck mass. g_* is the total number of relativistc degrees of freedom associated with the energy density as given in (3.17) and g_{*s} is the total number of relativistc degrees of freedom associated with the entropy density as given in (3.19), which are (considering that the "freeze-out" must occur before the Big Bang nucleosynthesis [170]) between 10.75 and 106.75 during the period in which the freeze-out happens;

$$J := \int_{x_f}^{\infty} \frac{\langle \sigma v \rangle_{\text{total}}}{x^2} dx \tag{4.38}$$

is called the "annihilation integral" which accounts for the annihilation after freeze-out. For the $0 < \Delta < 0.1$ case J was calculated by numerical integration, whereas for $\Delta \geq 0.1$ the expansions at infinity of the modified Bessel functions (a good approximation since x_f is of $O(10)$) were used and J was calculated analytically.

Recall that the present day abundance of non-baryonic dark matter Ωh^2 required by observation is $\Omega_{nbm} h^2 = 0.1186 \pm 0.0020$ as given in (3.25). We neglect the uncertainty of the result because it's too small to be relevant for our purpose.

Our goal was to find the parameter space of g, m_A and m_h allowed by both the observational constraints on Ωh^2 and σ_{tr}. We made plots of $\log_{10} m_A$ and $\log_{10} g$ (where g is the gauge coupling constant) which are allowed by the constraint on Ωh^2 or σ_{tr}, at various $\Delta := \frac{m_h}{m_A} - 1$. The plots are shown below. The blue curves are of the g and m_A allowed by the constraint from $\Omega h^2 = 0.1186$ [23] and the green regions are of the g and m_A allowed by the constraint from $0.5 \frac{\text{cm}^2}{\text{gram}} \leq \langle \sigma v \rangle_{tr} / m_A \leq 2 \frac{\text{cm}^2}{\text{gram}}$ [6], and

[28] Note that the abundance Ωh^2 is a function of g, m_A and m_h because J and the temperature of CMB at the time of freeze-out are both determined by g, m_A and m_h.

[29] Usually about 10 to 20.

the masses were taken to be in GeV (e.g. $\log_{10} m_A$ is in fact $\log_{10} \frac{m_A}{\text{GeV}}$). Constraints from the consideration of Big-Bang nucleosynthesis dictates that m_A, being the mass of a dark matter candidate particle, must be greater than roughly 1 MeV [170] and the region where the $m_A < 1$ MeV is coloured purple. Validity of perturbation theory requires $\alpha_g := \frac{g^2}{4\pi} < 1$ [171] and the region where $\alpha_g \geq 1$ is coloured red. To determine the exact parameter space in which the 2 to 2 channels dominate the 3 to 2 channels, we compared the x_f in the case of 2 to 2 channels only, which we shall call $(x_f)_{AA\to XY}$, with the x_f in the case of 3 to 2 channels only, which we shall call $(x_f)_{AAA\to XY}$, as well as the annihilation rate[30] of the 2 to 2 channels with that of the 3 to 2 channels at the time when all the annihilation channels freeze out. The 2 to 2 channels should dominate to a very good approximation when $(x_f)_{AA\to XY} > (x_f)_{AAA\to XY}$ or when the 2 to 2 annihilation rate is larger than the 3 to 2 annihilation rate at the time when all the annihilation channels freeze out. We found that the two criteria to agree almost perfectly within the parameter space of our concern and that the 2 to 2 channels dominate for $\{\Delta < 0.95\} \wedge \{\alpha_g \equiv \frac{g^2}{4\pi} < 1\}$[31] and for $\{1.05 < \Delta < 1.1\} \wedge \{g < 1\}$.

As can be seen from the plots, the parameters allowed by all the aforementioned

[30] Annihilation rate is defined to be $n_A \langle \sigma v \rangle$ for the 2 to 2 channels and $n_A^2 \langle \sigma v^2 \rangle$ for the 3 to 2 channels.

[31] $\alpha_g < 1$ is (approximately) equivalent to $\log_{10} g < 0.55$.

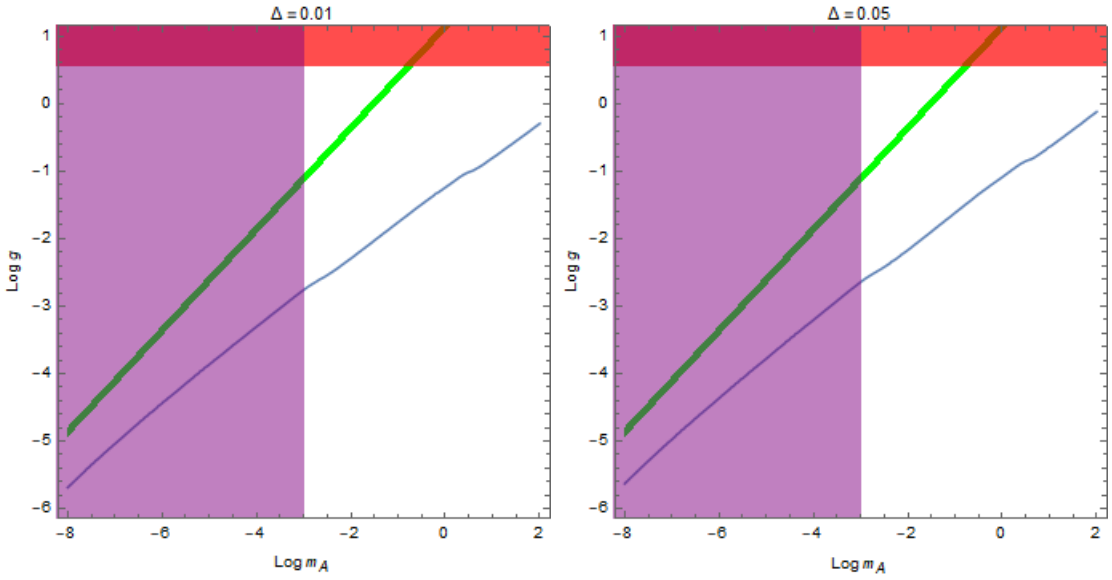

Figure 4.1: Plots of available $(\log_{10} g,\ \log_{10} m_A)$ at $\Delta = 0.01$ (left) and $\Delta = 0.05$ (right) when the 2 to 2 "forbidden" channels dominate. For more description see the second paragraph above Figure 4.1.

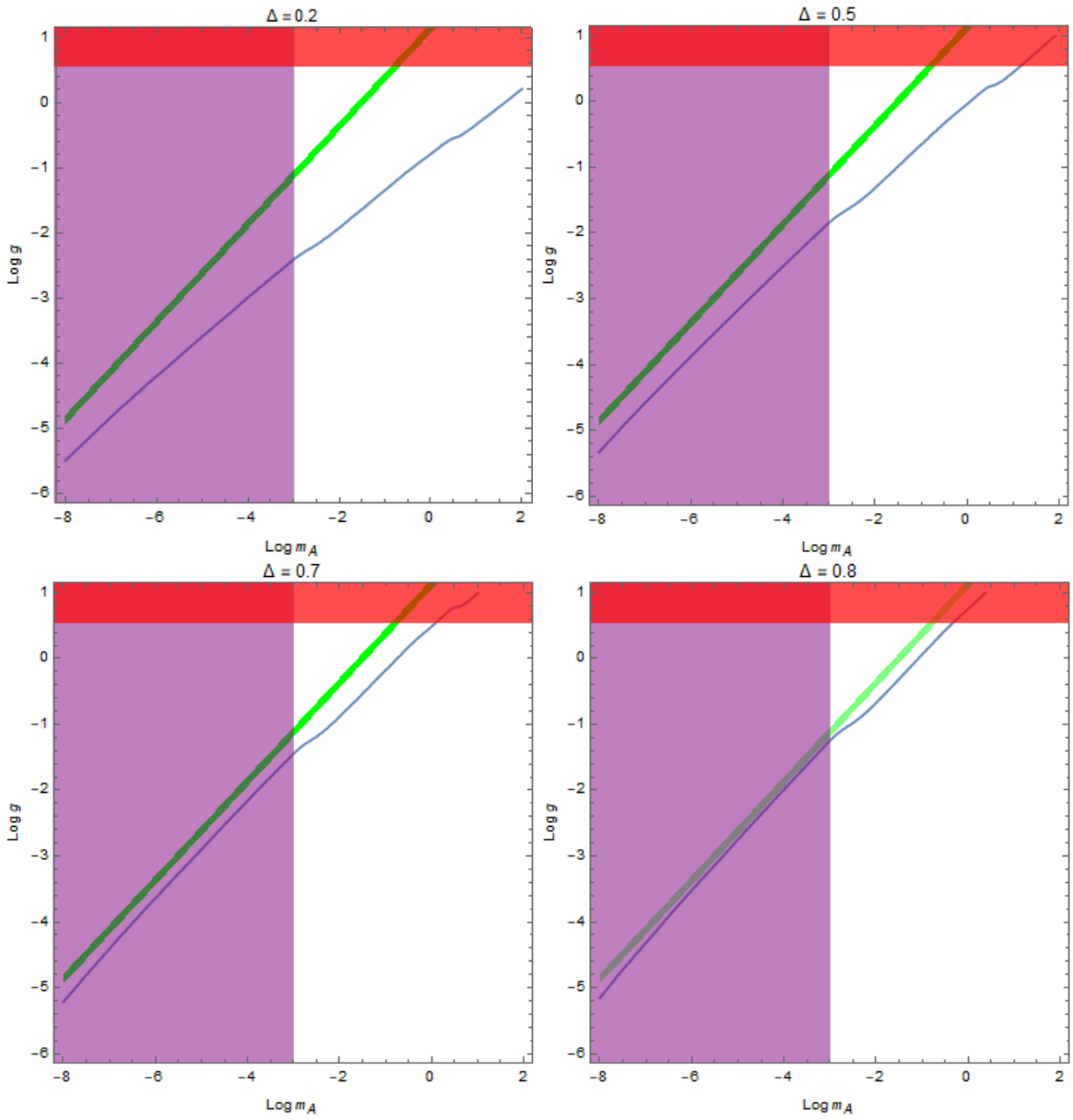

Figure 4.2: Plots of available ($\log_{10} g$, $\log_{10} m_A$) at $\Delta = 0.2$ (top left), $\Delta = 0.5$ (top right), $\Delta = 0.7$ (bottom left), $\Delta = 0.8$ (bottom right) when the 2 to 2 "forbidden" channels dominate. For more description see the second paragraph above Figure 4.1.

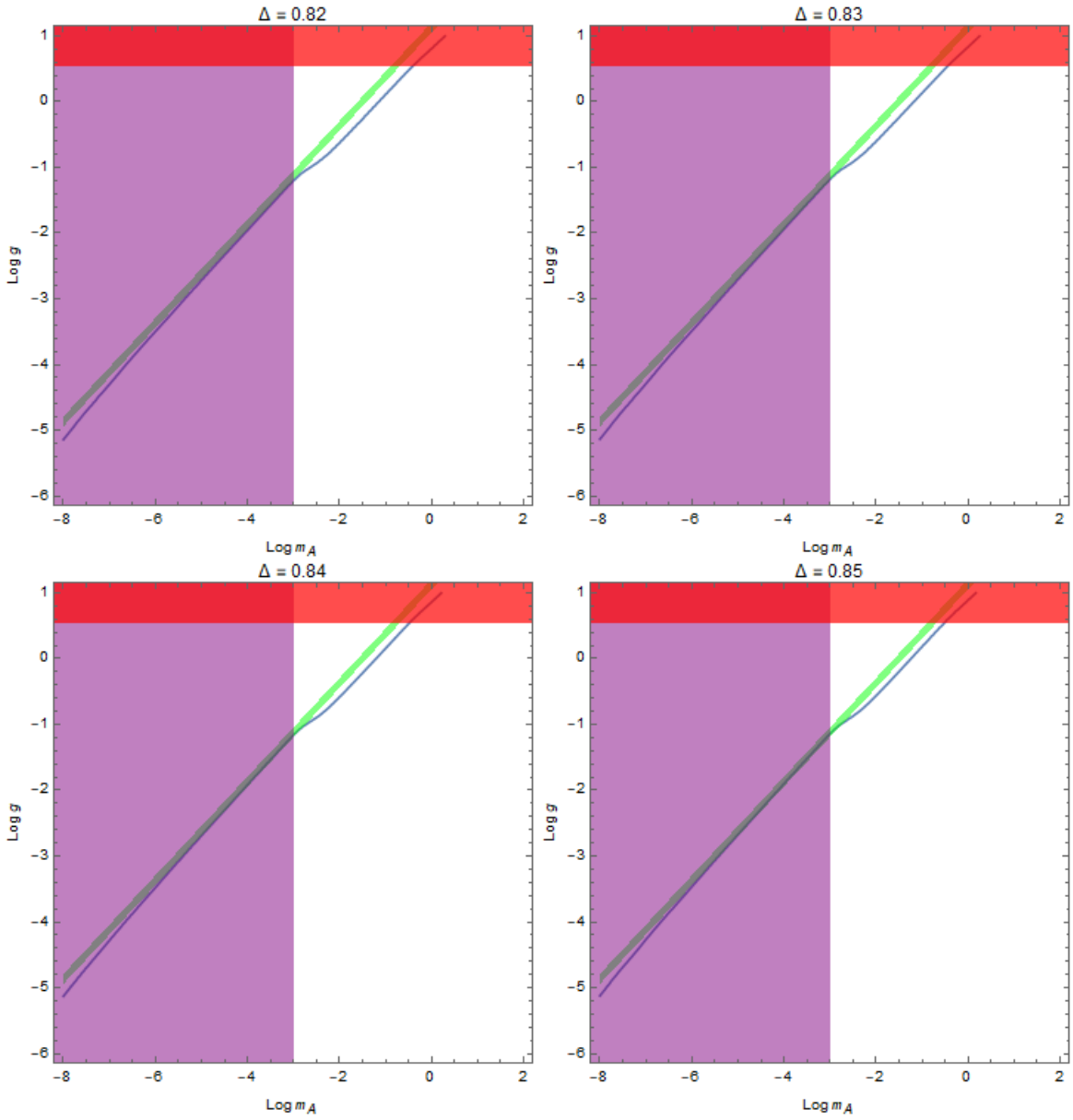

Figure 4.3: Plots of available ($\log_{10} g$, $\log_{10} m_A$) at $\Delta = 0.82$ (top left), $\Delta = 0.83$ (top right), $\Delta = 0.84$ (bottom left), $\Delta = 0.85$ (bottom right) when the 2 to 2 "forbidden" channels dominate. For more description see the second paragraph above Figure 4.1.

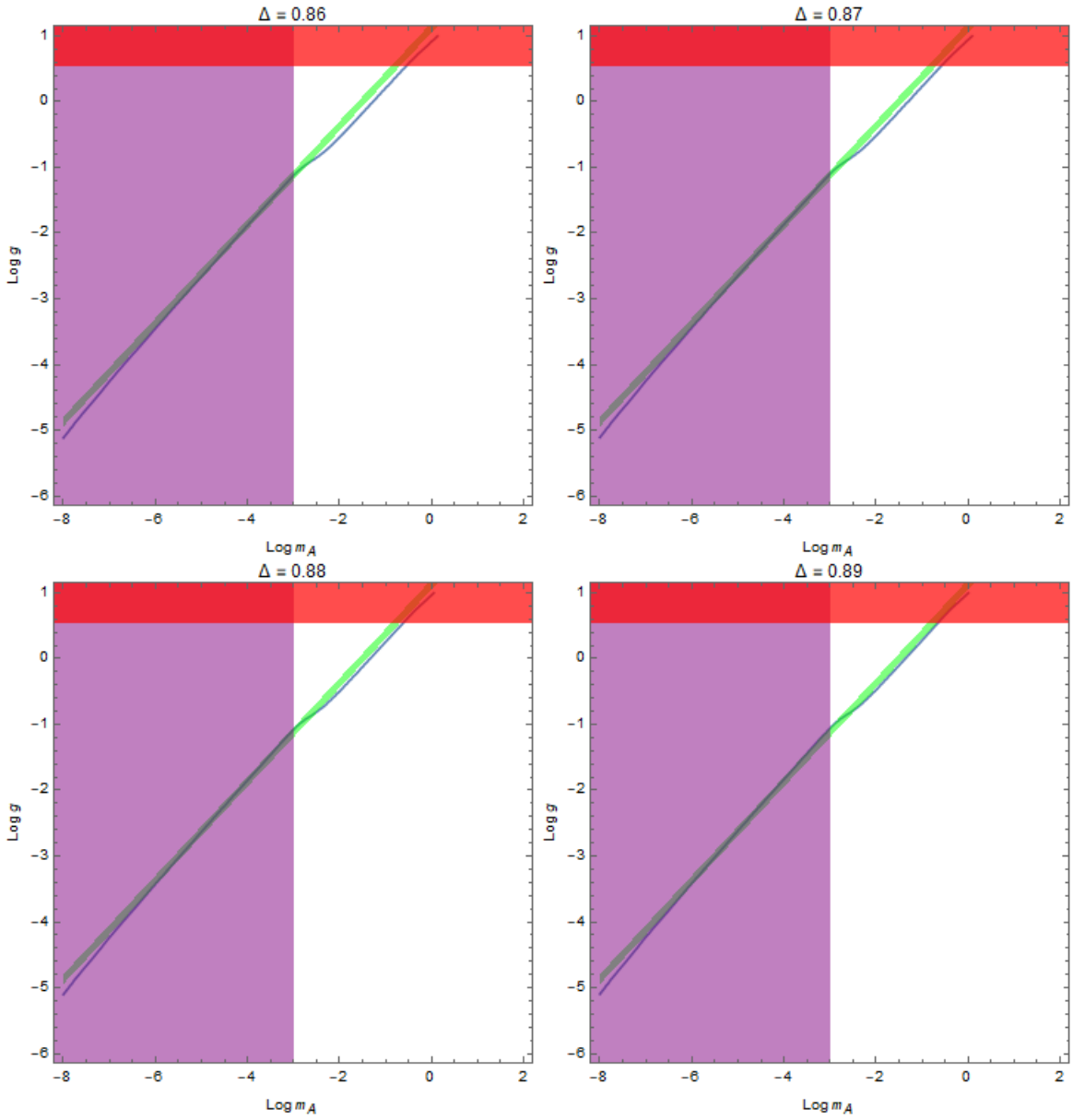

Figure 4.4: Plots of available ($\log_{10} g$, $\log_{10} m_A$) at $\Delta = 0.86$ (top left), $\Delta = 0.87$ (top right), $\Delta = 0.88$ (bottom left), $\Delta = 0.89$ (bottom right) when the 2 to 2 "forbidden" channels dominate. For more description see the second paragraph above Figure 4.1.

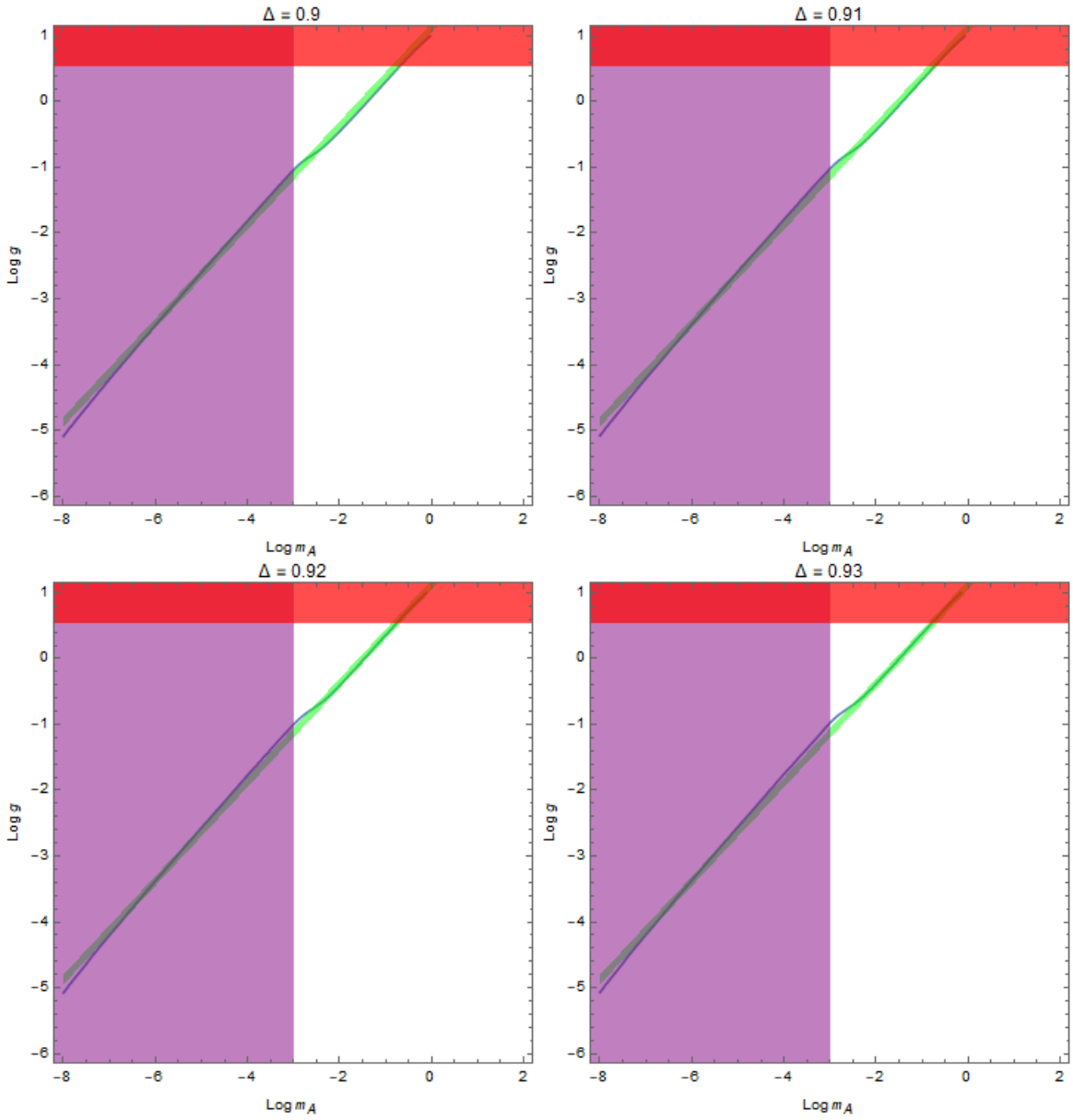

Figure 4.5: Plots of available ($\log_{10} g$, $\log_{10} m_A$) at $\Delta = 0.90$ (top left), $\Delta = 0.91$ (top right), $\Delta = 0.92$ (bottom left), $\Delta = 0.93$ (bottom right) when the 2 to 2 "forbidden" channels dominate. For more description see the second paragraph above Figure 4.1.

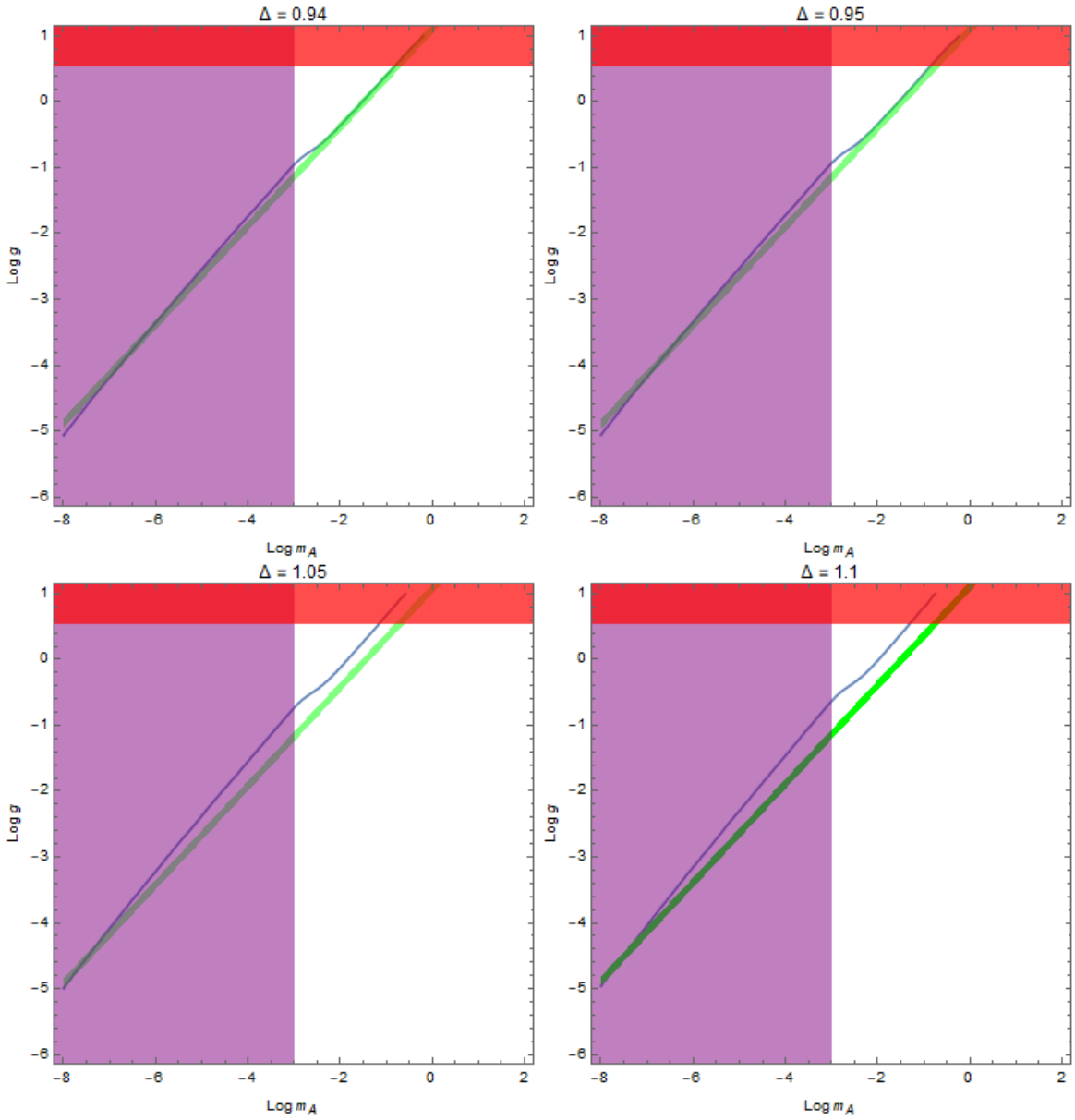

Figure 4.6: Plots of available $(\log_{10} g, \log_{10} m_A)$ at $\Delta = 0.94$ (top left), $\Delta = 0.95$ (top right), $\Delta = 1.05$ (bottom left), $\Delta = 1.10$ (bottom right) when the 2 to 2 "forbidden" channels dominate or are relevant. For more description see the second paragraph above Figure 4.1.

constraints in the regime where perturbation theory is valid and the "forbidden" channels dominate[32], when only the forbidden channels are taken into account, is non-empty roughly when $\Delta \in [0.83, 0.95]$. We observe that the mass of the dark matter is roughly in the range from 1 MeV to 500 MeV and the coupling constant in terms of α_g is roughly in the range of 10^{-3} to 1[33].

Note that both σ_{tr} and $\langle \sigma v^2 \rangle_{AAA \to Ah}$ [181] have resonance at $\Delta = 1$ and dealing with such resonances is beyond the scope of the thesis. We will therefore neglect the case when $\Delta \in (0.95, 1.05)$.

4.6 The Case When the 3 to 2 Channels Dominate

The non-relativistic limit of $\langle \sigma v^2 \rangle_{AAA \to AA}$ (of 40 distinct Feynman diagrams in total of 3 distinct "topologies") was calculated to be:

$$\begin{aligned}\langle \sigma v^2 \rangle_{AAA \to AA} =& \frac{1}{\pi} \sqrt{5} \frac{1}{2^8} \frac{1}{3^8} \frac{1}{m_A^3} \sum_{\epsilon,a} |\mathcal{M}_{AAA \to AA}|^2 \Big|_{\mathbf{p_1}=\mathbf{p_2}=\mathbf{p_3}=0} \\ =& \frac{5\sqrt{5}}{2^{15} 3^6 \pi} \frac{g^6}{m_A^5 \left(m_h^2 - 4m_A^2\right)^2 \left(m_A^2 + m_h^2\right)^2} \Big(1350224 m_A^8 \\ & + 1752472 m_A^6 m_h^2 + 118557 m_A^4 m_h^4 - 440686 m_A^2 m_h^6 \\ & + 73405 m_h^8 \Big) ,\end{aligned} \tag{4.39}$$

where

$$\begin{aligned}\sum_{\epsilon,a} |\mathcal{M}_{AAA \to AA}|^2 \Big|_{\mathbf{p_1}=\mathbf{p_2}=\mathbf{p_3}=0} =& \frac{45 g^6}{128 m_A^2 \left(m_h^2 - 4m_A^2\right)^2 \left(m_A^2 + m_h^2\right)^2} \Big(1350224 m_A^8 \\ & + 1752472 m_A^6 m_h^2 + 118557 m_A^4 m_h^4 - 440686 m_A^2 m_h^6 \\ & + 73405 m_h^8 \Big) ,\end{aligned} \tag{4.40}$$

see Appendices A and C and for details.

Note that our result for $\sum_{\epsilon,a} |\mathcal{M}_{AAA \to AA}|^2 \Big|_{\mathbf{p_1}=\mathbf{p_2}=\mathbf{p_3}=0}$ differs from the result of reference [181]. The difference is of the coefficients of the terms inside the brackets on the right of the fraction. After adjusting the overall scaling (i.e. the fraction) for the

[32] Although at $\Delta = 1.05$ and $\Delta = 1.1$ the 2 to 2 channels might not dominate the 3 to 2 channels.

[33] The region where $\alpha_g \geq 1$ is not in fact excluded but merely excluded from our consideration since we have only considered the perturbative regime of this model.

result from reference [181] to be the same as that presented above, the terms in the brackets of their result are

$$(1453880m_A^8 + 1637900m_A^6m_h^2 + 105020m_A^4m_h^4 - 437600m_A^2m_h^6 + 73405m_h^8). \quad (4.41)$$

It is expected however that this difference is too small to make a significant difference on the plots made for this thesis.
The $AAA \to hh$ channel is always sub-dominant and therefore will be neglected for our calculations — it is "forbidden" for $m_h \geq 1.5m_A$, while for $m_h < 1.5m_A$ it is dominated by the 2 to 2 forbidden channels. The $AAA \to Ah$ channel is expected to be insignificant for $\Delta > 1$ as discussed before and is therefore neglected as well.

The abundance of the dark matter, i.e. the abundance of A particles now is given by equation (B.10)

$$\Omega h^2(g, m_A, m_h) = \frac{m_A T_0^3}{\rho_c} \frac{g_{*s}(T_0)}{g_{*s}(T_f)} \sqrt{\frac{2H_0(m_A)}{\langle\sigma v^2\rangle_{\text{total}}}} \frac{x_f^2}{m_A^3} h^2, \quad (4.42)$$

where we take $h = 0.7$, $T_0 = 2.35 \times 10^{-13}$GeV is the temperature of the CMB now, $g_{*s}(T_0) = 3.36$, T_f is the temperature of the CMB at the time of "freeze-out"[34], $x_f := \frac{m_A}{T_f}$, $\langle\sigma v^2\rangle_{\text{total}} := \langle\sigma v^2\rangle_{AAA\to AA} + 2\langle\sigma v^2\rangle_{AAA\to Ah} + 3\langle\sigma v^2\rangle_{AAA\to hh}$ and for $\Delta > 1$ we may take $\langle\sigma v^2\rangle_{\text{total}} := \langle\sigma v^2\rangle_{AAA\to AA}$ for $\Delta \geq 1.05$ when both $AAA \to Ah$ and $AAA \to hh$ channels are "forbidden"; $\rho_c = \frac{3H^2(T_0)m_p^2}{8\pi}$ is the critical density of the FRW model of the universe where $m_p = 1.22 \times 10^{19}$GeV is the Planck mass, H is the Hubble parameter[35], $H_0(m_A) = 1.66g_*^{\frac{1}{2}} m_A^2/m_p$[36].

As in the case discussed previously, we made plots of $\log_{10}m_A$ and $\log_{10}g$ which are allowed by the constraint on Ωh^2 or σ_{tr}, at various $\Delta := \frac{m_h}{m_A} - 1$. They are shown in Figure 4.7 and Figure 4.8. The blue curves are of the g and m_A allowed by the constraint from $\Omega h^2 = 0.1186$ [23] and the green regions are of the g and m_A allowed by the constraint from $0.5\frac{cm^2}{g} \leq \langle\sigma v\rangle_{tr}/m_A \leq 2\frac{cm^2}{g}$ [6], and the masses were taken to be in GeV. The parameter space excluded by the constraint of Big-Bang nucleosynthesis is $m_A \leq 1$MeV [170] and is coloured purple. The parameter space excluded *from our consideration* by the perturbativity constraint is $\alpha_g := \frac{g^2}{4\pi} \geq 1$

[34] See Appendix B for definition of "freeze-out".
[35] See Chapter 3 of this thesis for definition.
[36] See Appendix B for definition of H_0.

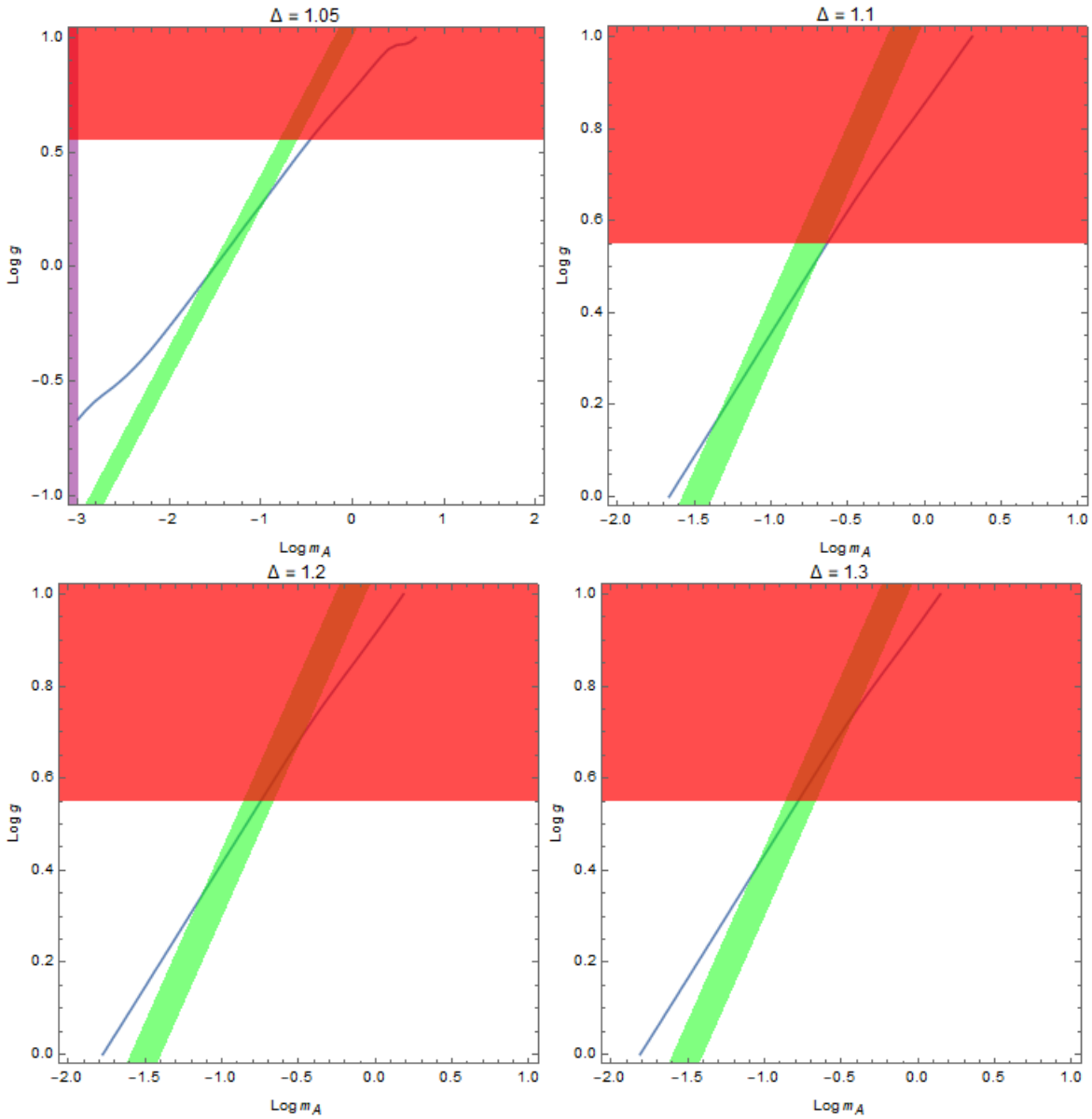

Figure 4.7: Plots of available ($\log_{10} g$, $\log_{10} m_A$) at $\Delta = 1.05$ (top left), $\Delta = 1.10$ (top right), $\Delta = 1.20$ (bottom left) and $\Delta = 1.30$ (bottom right) when the 3 to 2 channels are relevant or dominate. For more description see the first paragraph above Figure 4.7.

[171] and is coloured red.

As can be seen from Figure 4.7 and Figure 4.8, the parameter space allowed by all the aforementioned constraints (as in the case previously discussed) should be non-empty for all $\Delta \geq 1.05$, although the apparently available parameter spaces at $\Delta = 1.05$ and $\Delta = 1.1$ are not actually within the space in which the 3 to 2 channels

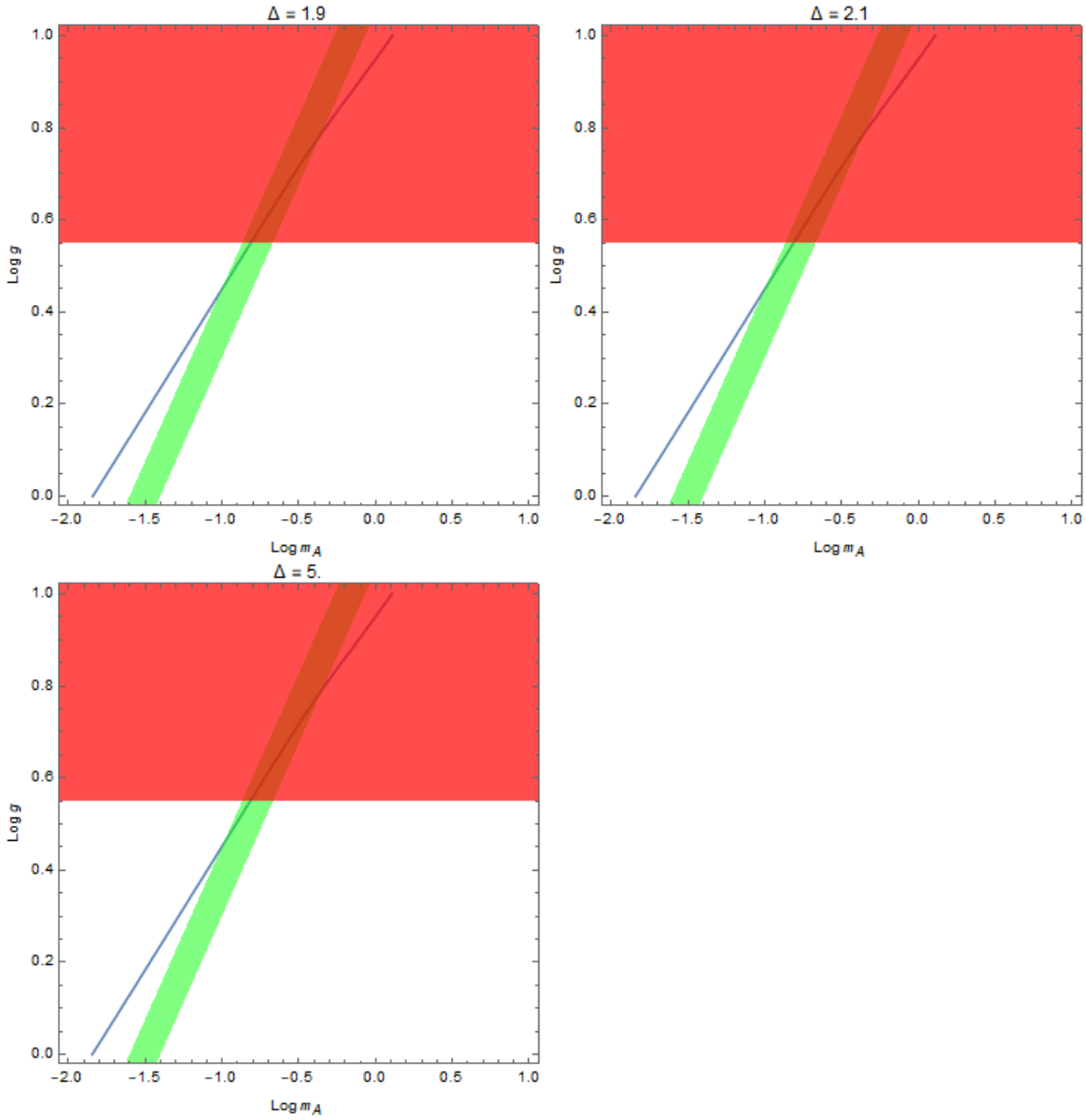

Figure 4.8: Plots of available $(\log_{10} g, \log_{10} m_A)$ for the case when the 3 to 2 channels dominate at $\Delta = 1.9$ (top left), $\Delta = 2.10$ (top right), $\Delta = 5.00$ (bottom left) when the AAA to AA channel dominate. For more description see the first paragraph above Figure 4.7.

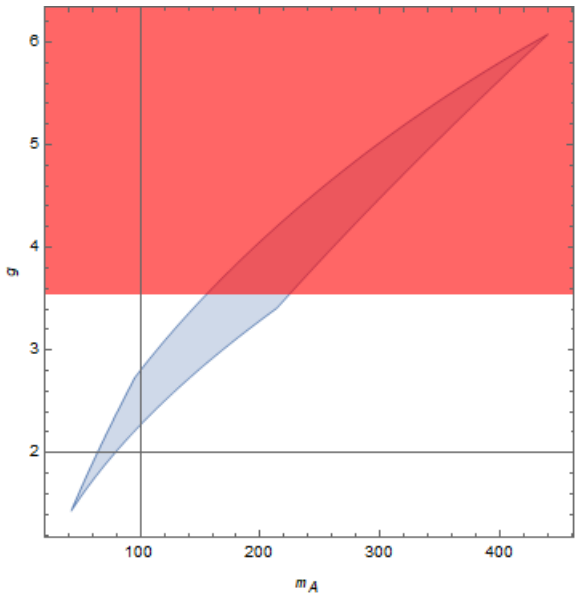

Figure 4.9: A plot of available (m_A, g) for the case when the 3 to 2 channels dominate for all Δ. This plot is in fact made only for $1.1 \leq \Delta \leq 1.6$, but since the space of (m_A, g) allowed by both the abundance and elastic self-interaction constraints changes little as Δ increases for $\Delta > 1.6$, this plot is a decent approximation for the allowed (m_A, g) for all Δ.

dominate as mentioned earlier and are therefore likely unavailable considering the previous plots for the case in which the 2 to 2 channels dominate. From Figure 4.9 we observe that the mass of the dark matter m_A is roughly in the range from 20 MeV to 200 MeV, α_g is roughly in the range from 10^{-2} to 1. We also observe that for $\Delta > 1.5$ the available parameter space is approximately independent of Δ, although this might not be the case near $\Delta = 2$ where $\langle \sigma v^2 \rangle_{AAA \to AA}$ has a resonance [181]. This is expected because at sufficiently large Δ both $\sigma_{AAA \to AA}$ and σ_{tr} are approximately independent of Δ[37].

Note that we did not discuss the decay of $h \to AA$, the inverse decay of $AA \to h$ and in any detail the decay of h's into the Standard Model particles. The $h \to AA$ channel should be significant for $\Delta > 1$, whereas the $AA \to h$ channel should be significant for $\Delta \gtrsim 1$ and will become too "forbidden" to be relevant for sufficiently large Δ. Hence for $\Delta \gtrsim 1$ (but suffciently far away from the resonance of $AAA \to Ah$), the inverse decay of $AA \to h$ and the decay of $h \to AA$ should be sufficiently fast to keep them in chemical equilibrium (i.e. $\Gamma_{AA \to h} = \Gamma_{h \to AA}$) — if the chemical equilibrium between h's and Standard Model particles cannot be maintained and that the decay of the h's into the Standard Model particles is much slower than the decay of $h \to AA$, the change in the number density of A should be governed by the decay of the h's into the Standard Model particles and the corresponding inverse decay. If Δ becomes very large (as in the case when $AAA \to AA$ dominates other channels), the h's might decay into A's very quickly so that the h's number density would become very small, to the extent that their decay into the Standard Model particles would be too slow to maintain the thermal and chemical equilibrium between them and the cosmic plasma [181], violating our previous assumption that the h's were in thermal and chemical equilibrium with the cosmic plasma during the time period of our concern. Hence we may further constrain the parameter space when $\Delta > 1$ if we treat these processes appropriately.

[37] As can be seen if we take the limit of $m_A \to 0$ while fixing m_h.

Chapter 5

Discussion of the Methods and Results

5.1 Use of Softwares

The cross-sections and plots for the allowed parameter spaces in the previous chapter were made using the software Wolfram Mathematica 11.2 Student Edition (which will simply be referred to as "Mathematica"). At first we used a package for Mathematica named FeynCalc to calculate the cross-sections of the 2 to 2 scatterings. But when we attempted to calculate $\sigma_{AAA\to AA}$ using FeynCalc, we realized it was too inefficient for the calculation, as the package was not designed for the calculation of the scattering amplitudes of non-relativistic particles[1]. We therefore wrote Mathematica codes without the aid of any packages to calculate the cross-sections of the 3 to 2 scatterings in the non-relativistic limit, and also re-calculated some of the cross-sections of the 2 to 2 scatterings in the non-relativistic limit using analogous codes. We found that the calculations of the non-relativistic limit of the cross-sections using our new code without the use of FeynCalc took significantly shorter time than those using the old codes relying on FeynCalc. The calculations of the cross-sections of the 3 to 2 scatterings were very time-consuming on our laptop computer[2] which was assigned the task to run the code. For example, the running time for the calculation of $\sum_{\epsilon,a}|\mathcal{M}_{AAA\to AA}|^2$

[1] As FeynCalc can only calculate relativistic amplitudes, and the relativistic amplitudes need then to be simplified.

[2] The processor of this laptop is Intel(R) Core(TM) M-5Y10c @ 0.80GHz 998MHz.

in the non-relativistic limit was at least 20 hours[3]. In fact, if the calculation were to be done in the most straight forward manner, the laptop would run out of memory (of 8 GB) before the calculation could be completed. To complete the calculation we had to break the scattering amplitude into 3 parts and do the sum over the indices for each of the 9 parts coming from the squaring of the amplitude separately.

5.2 Resonances of the cross-sections

We have avoided dealing with any of the resonances of the cross-sections (although this does not compromise the validy of our results). Treatments of these resonances can be found in references [179][185][186].

5.3 Coupling to the Standard Model

We have not discussed extensively the coupling to the Standard Model through the Higgs portal, in particular how the thermal and chemical equilibrium between the dark Higgs bosons and the Standard Model particles can be achieved without depleting the dark Higgs bosons, how this would constrain Δ, and the detection of this dark sector. A systematic study of dark matter coupled to the Standard Model through a Higgs portal can be found in [177] and a review on the detection of general elastically self-interacting dark matter can be found in [6]. Reference [177] suggests that there exists parameter space unexcluded by the observational constraints which would guarantee that the rate at which the dark Higgs bosons decay into the Standard Model particles be greater than the Hubble parameter, so that the dark Higgs bosons would be in thermal and chemical equilibrium with the cosmic plasma as we assumed. See also the discussion at the end of Chapter 4.

5.4 Non-perturbative regime and effects

We have employed perturbation theory in our calculations and have not explored the non-perturbative regime ($\alpha_g \geq 1$) of this model or any non-perturbative effect. See

[3]This is a conservative estimate. The actual time it took, which has not been exactly recorded, could be more than 30 hours.

[6] for discussions of non-perturbative effects in models of elastically self-interacting dark matter.

Chapter 6

Conclusions

We have investigated the possibility of that the dark gauge boson in the SU(2) gauged dark sector introduced in Chapter 4 could constitute all the non-baryonic dark matter, taking into account the recent astrophysical observations which suggest that dark matter might have significant non-gravitational elastic self-interaction. To achieve this purpose, we calculated, in the regime where perturbation theory is valid, the cross-sections and thermally averaged cross-sections for the relevant 2 to 2 and 3 to 2 annihilations of the dark gauge bosons within the dark sector, and the momentum-transfer cross-section of the 2 to 2 elastic scattering of the dark gauge bosons which encodes the strength of their elastic self-interaction. We calculated the abundance of the dark gauge bosons using a well-known ansatz and found in the regime where perturbation theory is valid that when the mass splitting between the dark gauge boson A and the dark Higgs boson h, defined as $\Delta := \frac{m_h}{m_A} - 1$, satisfies $0.83 < \Delta < 0.95$ or $\Delta > 1.20$, the dark gauge boson might be able to provide the abundance and the self-interaction needed for the dark matter. The unexcluded mass of the dark gauge boson would be roughly in the range from 1 MeV to 500 MeV and the gauge coupling fine structure constant α_g in the range from 10^{-3} to 1. The unexcluded mass of the dark gauge boson might not be determined accurately for a given Δ above 0.9 since the unexcluded mass range is very large for each such Δ (which may span as much as about two orders of magnitude), due to that the curve allowed by abundance constraint's being almost parallel to the curve allowed by the self-interaction constraint.

Note that for $\Delta \leq 0$, the dark gauge boson would be a standard WIMP, and the required elastic self-interaction momentum transfer cross-section (2.3) in conjunction with the required total thermally averaged annihilation cross-section (4.23) implies

m_A to be roughly of $O(10^{-12})$GeV[1], severely violating the constraint from Big-Bang nucleosynthesis that $m_A > 0.5$MeV. That the aforementioned constraints could be consistent with each other relied on the suppression of the thermally averaged annihilation cross-sections due to the channels' being "forbidden" — the coupling constant can be sufficiently large so that the elastic self-interaction constraint can be satisfied while the annihilation cross-sections are not too large for the abundance constraint to be satisfied.

The coupling of the dark sector to the Standard Model, the decay of $h \to AA$ and the inverse decay of $AA \to h$ have not been extensively discussed in this thesis. Further investigations on the decay of dark Higgs bosons into Standard Model particles, the decay $h \to AA$ and the inverse decay $AA \to h$ may provide constraint on the strength of the Higgs portal coupling λ_{HP} and tighter constraint on the parameter space of g, m_A, and Δ.

[1]That is, satisfying the elastic self-interaction constraint would make the annihilation rate too high for the abundance constraint to be satisfied, provided that the dark gauge boson is not too light.

Appendix A

Feynman diagrams for the scatterings

For 2 to 2 scatterings, the default configuration is

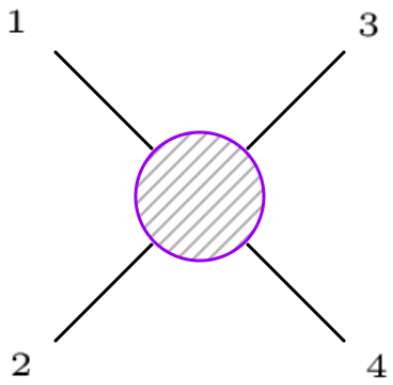

in which 1,2 denote the initial state particles and 3,4 denote the final state particles. A diagram may be labeled by a label below it. If a diagram has any label, e.g. f, then $f(i \leftrightarrow j)$ for $i, j \in \{1, 2, 3, 4\}$ denotes a diagram that is f with labels i and j switched, for example:

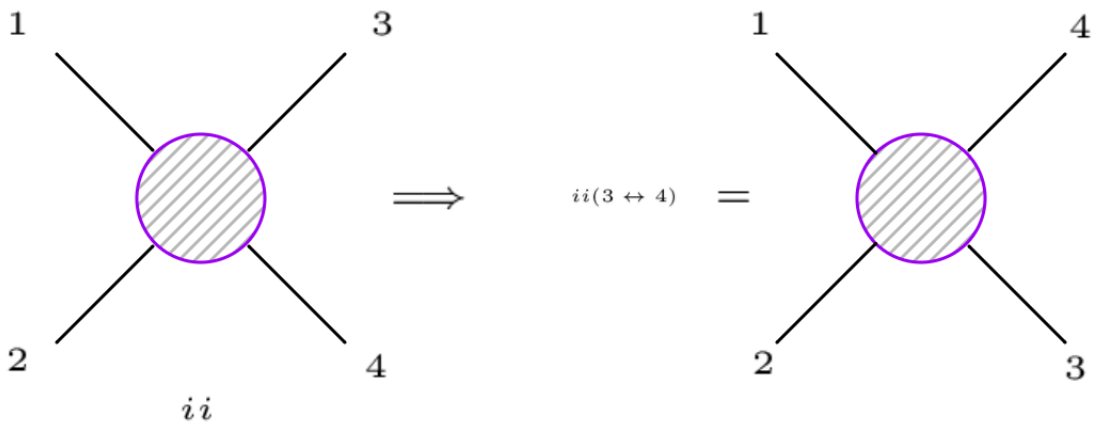

ii

For $AA \to Ah$:

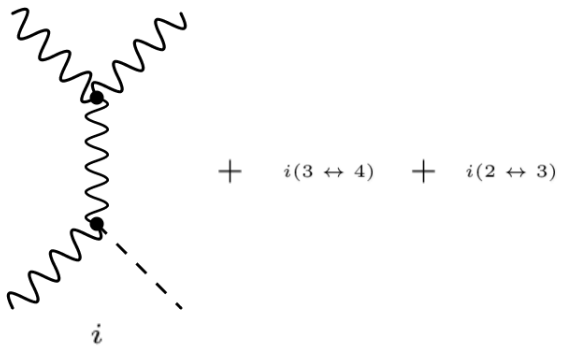

For $AA \to hh$:

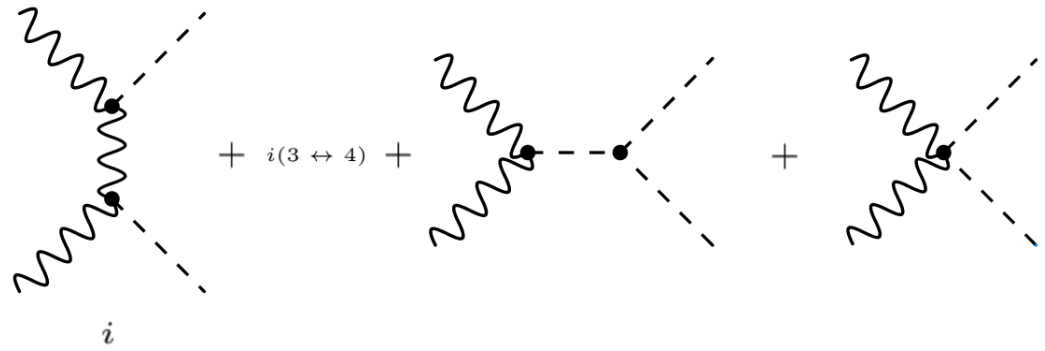

For $AA \to AA$:

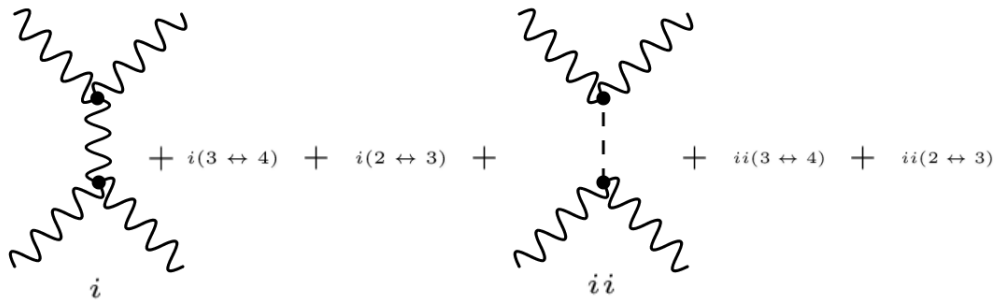

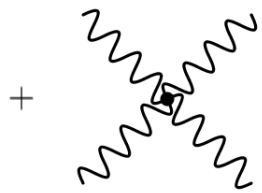

The default configuration for 3 to 2 scattering is:

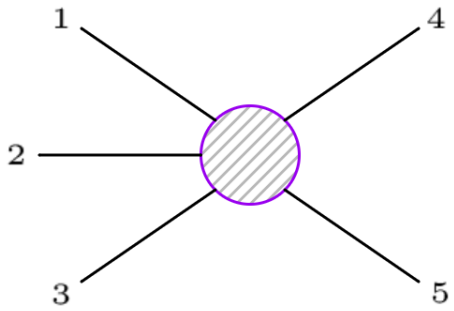

in which 1,2,3 denote the initial state particles and 4,5 denote the final state particle. For any label f of a diagram, let $f[1,2,3,4,5]$ denote the diagram of default configuration where $1,2,3,4,5$ are labels of the particles as described above for 3 to 2 scattering and that for any element p of the symmetric group S_5, $f[p(1,2,3,4,5)]$ be the diagram which the diagram $f[1,2,3,4,5]$ becomes when the array of labels 1,2,3,4,5 are permuted to $p(1,2,3,4,5)$.

For $AAA \to AA$:

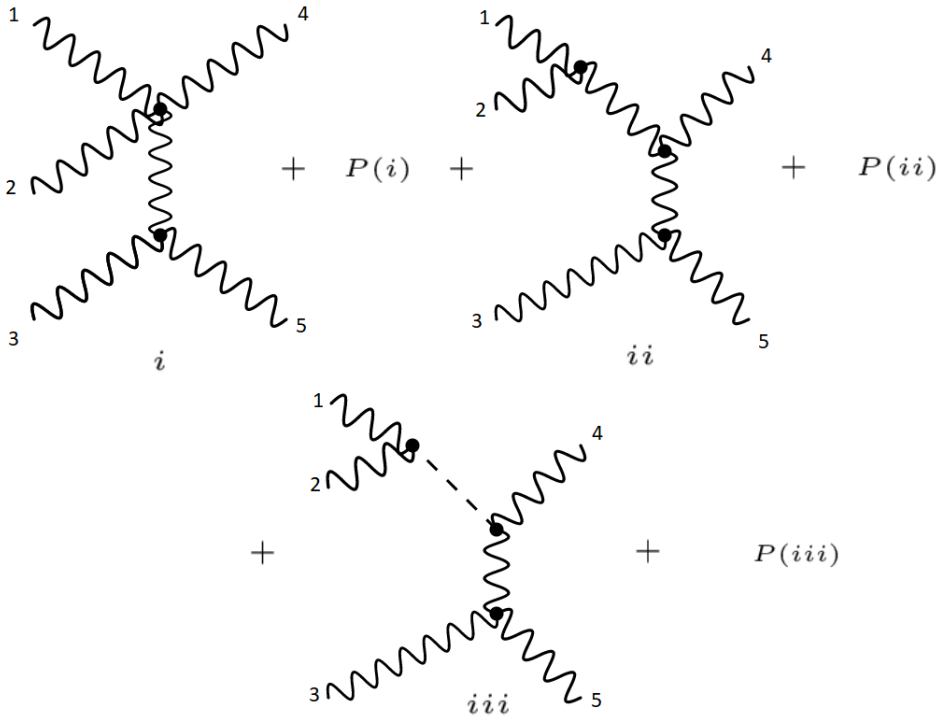

in which

$$
\begin{aligned}
P(i) = {} & i[1,2,4,3,5] + i[1,2,5,3,4] + i[1,3,4,2,5] + i[1,3,5,2,4] + i[3,2,4,1,5] \\
& + i[3,2,5,1,4] + i[4,5,3,1,2] + i[4,5,2,1,3] + i[4,5,1,3,2], \\
P(ii) = {} & ii[1,2,3,5,4] + ii[1,3,2,4,5] + ii[1,3,2,5,4] + ii[2,3,1,4,5] \\
& + ii[2,3,1,5,4] + ii[1,4,5,2,3] + ii[3,4,5,2,1] + ii[1,4,5,3,2] \\
& + ii[2,4,5,3,1] + ii[2,4,5,1,3] + ii[3,4,5,1,2] + ii[4,5,1,3,2] \\
& + ii[4,5,1,2,3] + ii[4,5,2,1,3], \\
P(iii) = {} & iii[1,2,3,5,4] + iii[1,3,2,4,5] + iii[1,3,2,5,4] + iii[2,3,1,4,5] \\
& + iii[2,3,1,5,4] + iii[1,4,5,2,3] + iii[3,4,5,2,1] + iii[1,4,5,3,2] \\
& + iii[2,4,5,3,1] + iii[2,4,5,1,3] + iii[3,4,5,1,2] + iii[4,5,1,3,2] \\
& + iii[4,5,1,2,3] + iii[4,5,2,1,3].
\end{aligned}
\tag{A.1}
$$

Appendix B

Derivation of expressions of relic abundance from Boltzmann equation

For the case when the 2 to 2 channels dominate, recall

$$\begin{aligned} a^{-3}\frac{d(a^3 n_A)}{dt} =& -2\langle\sigma v\rangle_{AA\to hh}\left[n_A^2-(n_A^{eq})^2\right] \\ & -\langle\sigma v\rangle_{AA\to Ah}\left[n_A^2-n_A n_A^{eq}\right]. \end{aligned} \tag{4.20}$$

We may rewrite this equation [160][159] with the assumption $a \propto T^{-1}$ (which is only approximately true as will be explained later) as

$$\frac{dY}{dt} = -T^3\left[2\langle\sigma v\rangle_{AA\to hh}\left(Y^2-Y_{eq}^2\right)-\langle\sigma v\rangle_{AA\to Ah}\left(Y^2-YY_{eq}\right)\right], \tag{B.1}$$

where $Y := n_A/T^3$, $Y_{eq} := n_A^{eq}/T^3$.
Since the thermally averaged cross-section $\langle\sigma v\rangle$ is written in terms of temperature, it is preferable to further rewrite the equation using $x := m_A/T$[1] in place of time t in the equation. Since $a \propto T^{-1}$, i.e. $T = k/a$ for some constant k, we have $\frac{dx}{dt} = \frac{d}{dt}\left(\frac{m_A}{T}\right) = m_A\frac{dT}{dt}\left(-\frac{1}{T^2}\right) = m_A\frac{d}{dt}\left(\frac{k}{a}\right)\left(-\frac{1}{T^2}\right) = km_A\left(-\frac{da}{dt}\,/\,a^2\right)\left(-\frac{1}{T^2}\right) = m_A\left(\frac{k}{a}\right)H\frac{1}{T^2} = H\frac{m_A}{T} = Hx$. It is required by observaton that the dark matter be produced in the radiation dominated era [160][159], hence we may assume $H \propto T^2$, which allows us to express

[1]Here m_A is chosen for convenience and can be replaced by other mass scales.

H (as in 3.20) as $H = H_0\left(m_A\right)/x^2$ for $H_0(m_A) := Hx^2 = 1.66 g_*^{\frac{1}{2}} m_A^2/m_p$. Therefore

$$\begin{aligned}\frac{dY}{dx} &= \frac{dY}{dt}\frac{dt}{dx} = \frac{1}{Hx}\frac{dY}{dt} \\ &= -\frac{T^3}{Hx}\left[2\langle\sigma v\rangle_{AA\to hh}\left(Y^2 - Y_{eq}^2\right) - \langle\sigma v\rangle_{AA\to Ah}\left(Y^2 - YY_{eq}\right)\right] \\ &= -\frac{m_A^3}{H_0\left(m_A\right)x^2}\left[2\langle\sigma v\rangle_{AA\to hh}\left(Y^2 - Y_{eq}^2\right) - \langle\sigma v\rangle_{AA\to Ah}\left(Y^2 - YY_{eq}\right)\right].\end{aligned} \tag{B.2}$$

The above ordinary differential equation is a kind of *Riccati equation* which admits no general closed-form solutions, but the qualitative behavior of it is well-known [159][180][187][185][179][160]:

1. $Y(x) \approx Y_{eq}(x)$ for sufficiently small x.

2. As x increases to approximately when $Y(x) - Y_{eq}(x) = cY_{eq}(x)$ for some real number c of O(1), $Y_{eq}(x)/Y(x)$ begins to drop approximately exponentially with respect to x — $Y(x)$ decreases more and more slowly and approaches an asymptotic value as x increases. The time for which $Y(x) - Y_{eq}(x) = cY_{eq}(x)$ is usually referred to as the time of "freeze-out". The later the freeze-out occurs, the lower is the asymptotic value that $Y(x)$ approaches. This criterion agrees very well with the criterion given by equation (3.23) when Γ in equation (3.23) is set to be the total annihilation rate.

The choice of c is insignificant for temperature-insensitive annihilation cross-sections and we will take $c = \sqrt{2} - 1$ following [183][159]. The value of x at the time of freeze-out x_f is determined by solving for x the evolution equation (B.2) (i.e. the Boltzmann equation for annihilation) in conjunction with the freeze-out condition $Y(x) - Y_{eq}(x) = cY_{eq}(x)$. Let $\delta(x) := Y(x) - Y_{eq}(x)$ and rewrite $Y(x)$ as $Y(x) = \delta(x) + Y_{eq}(x)$ in equation (B.2). The equation can be solved without our knowing the solution for $Y(x)$ if we make the assumption that $\frac{d\delta}{dx} = 0$. This assumption had been justified by examination of the (very reliable) numerical solutions of the ODE and is reasonable considering that before the freeze-out $Y(x) \approx Y_{eq}(x)$. We will also take the assumption that x_f is of $O(10)$, an assumption which is justified by astrophysical observations[2] and allows us to take the limit of n_A^{eq} (as in (4.17)) when $m_i \gg T$.

This qualitative behavior allows us to solve the equation to good approximation

[2]See in Chapter 1 the discussion about "Cold" vs. "Hot" dark matter and the references therein.

for $Y(x=\infty)$ while taking $Y_{eq}=0$ for the equation, in which case we obtain

$$\frac{dY}{dx}=-\frac{\kappa}{x^2}\langle\sigma v\rangle_{\text{total}}Y^2, \tag{B.3}$$

where $\kappa:=\frac{m_A^3}{H_0(m_A)}$ and $\langle\sigma v\rangle_{\text{total}}:=2\langle\sigma v\rangle_{AA\to hh}+\langle\sigma v\rangle_{AA\to Ah}$. The above equation can then be solved by separation of variables to obtain $Y(x=\infty)$:

$$\begin{aligned}\int_{Y(x_f)}^{Y(\infty)}\frac{1}{Y^2}dY&=-\kappa\int_{x_f}^{\infty}\frac{\langle\sigma v\rangle_{\text{total}}}{x^2}dx\\ \implies -\frac{1}{Y}\Big|_{Y(x_f)}^{Y(\infty)}&=-\kappa\int_{x_f}^{\infty}\frac{\langle\sigma v\rangle_{\text{total}}}{x^2}dx\end{aligned} \tag{B.4}$$

It is also well-known that $Y(x_f)\gg Y(\infty)$ [179][160][159], hence we may take $\frac{1}{Y(x_f)}=0$ and obtain

$$Y(\infty)=\left(\kappa\int_{x_f}^{\infty}\frac{\langle\sigma v\rangle_{\text{total}}}{x^2}\right)^{-1}:=Y_\infty. \tag{B.5}$$

When $m_A\gg T_f$, $\langle\sigma v\rangle_{\text{total}}$ can be taken to be independent of temperature (see Appendix C for details), therefore[3]

$$\begin{aligned}Y_\infty&=\left(\kappa\langle\sigma v\rangle_{\text{total}}\int_{x_f}^{\infty}\frac{1}{x^2}\right)^{-1}\\&=\frac{x_f}{\kappa\langle\sigma v\rangle_{\text{total}}}\equiv\frac{H_0(m_A)\,x_f}{m_A^3\langle\sigma v\rangle_{\text{total}}}.\end{aligned} \tag{B.6}$$

If indeed $T\propto a^{-1}$ always holds, the dark matter density today should be

$$\rho_A=m_AY_\infty T_0^3, \tag{B.7}$$

where T_0 is the temperature of the CMB now. But $T\propto a^{-1}$ does not always hold to good approximation[4] since by equation (3.21) and (3.18)

$$g_{*s}T^3\propto s\propto a^{-3} \tag{B.8}$$

[3]Note that it would appear by consideration of the expression below that Y_∞ is proportional to x_f, contradicting the previous claim that the later the freeze-out occurs, the lower is Y_∞. However, we would find that this is not the case considering that $\langle\sigma v\rangle_{\text{total}}$ determines x_f and is therefore a function of x_f.

[4]A "good approximation" is an approximation whose error is negligible for our purpose.

where g_{*s} is *not* constant as T varies — our previous assumption that $T \propto a^{-1}$ amounts to that g_{*s} is constant. What normally happens and we shall assume is what happens for our model is that during a time period for which g_{*s} is approximately constant, annihilation would "freeze out" and Y would approach (to very good approximation) a value which is the Y_∞ we had before, and then g_{*s} would significantly decrease, which implies that $Y(x)$ would decrease as well (as will be elucidated soon) — note that the Y_∞ we had before is *not* equal to $Y(\infty)$ in this case, since the Y_∞ before was obtained with the assumption that g_{*s} is constant, which is not true after Y approximately reaches Y_∞ in this case. This means that the previously obtained Y_∞ is in fact the value of $Y(x)$ just before g_{*s} begins to change significantly (i.e. can no longer be treated as a constant) rather than $Y(\infty)$ with this consideration. Despite that the "freeze-out" behavior was observed in the above discussion for equation (B.3) only when g_{*s} was assumed to be constant, it is well-known that even though g_{*s} is not constant, the comoving number density $n_A a^3$ stays (approximately) constant after Y has reached (approximately) Y_∞ [160]. This implies

$$n_A(T_0) = n_A(T_1)\left(\frac{a_1}{a_0}\right)^3 = Y(x_1)T_1^3\left(\frac{a_1}{a_0}\right)^3, \tag{B.9}$$

where T_0 is the temperature now, T_1 is the temperature after Y (approximately) reaches Y_∞ just before g_{*s} can no longer be treated as a constant and $x_1 := m_A/T_1$; note that $Y(x_1) = Y_\infty$ by definition and $g_{*s}(T_1) = g_{*s}(T_f)$[5].
Hence dark matter abundance now is

$$\Omega(x_0) = \frac{\rho_A}{\rho_c} = \frac{m_A Y(x_1) T_0^3}{\rho_c}\left(\frac{a_1 T_1}{a_0 T_0}\right)^3 = \frac{m_A Y_\infty T_0^3}{\rho_c}\frac{g_{*s}(T_0)}{g_{*s}(T_f)}. \tag{B.10}$$

The temperature of the CMB now $T_0 = 2.7255K \pm 0.0006K \approx 2.35 \times 10^{-13}$GeV [188] and $g_{*s}(T_0) \approx 3.36$ [2][160][159].

[5]Note that reference [160]'s account of what was explained in this paragraph can be confusing, as it claims that Y reaches its asymptotic value after the "freeze-out" but then describes how Y shouldn't have have been constant after it approximately reaches Y_∞ because $T \propto a^{-1}$ no longer holds to good approximation.

Similarly, when the 3 to 2 channels dominate, we have the equation

$$\begin{aligned} a^{-3}\frac{d(a^3 n_A)}{dt} = &- \langle\sigma v^2\rangle_{AAA\to AA}\left[n_A^3 - n_A^2 n_A^{eq}\right] \\ &- 2\langle\sigma v^2\rangle_{AAA\to Ah}\left[n_A^3 - n_A\left(n_A^{eq}\right)^2\right] \\ &- 3\langle\sigma v^2\rangle_{AAA\to hh}\left[n_A^3 - \left(n_A^{eq}\right)^3\right]. \end{aligned} \tag{4.21}$$

For the purpose of solving the equation for $Y\left(x=\infty\right)$ when g_{*s} is approximately constant, we have

$$\frac{dY}{dx} = -\frac{\gamma}{x^5}\langle\sigma v^2\rangle_{\text{total}} Y^3, \tag{B.11}$$

where $\gamma := \frac{m_A^6}{H_0(m_A)}$, $\langle\sigma v^2\rangle_{\text{total}} := \langle\sigma v^2\rangle_{AAA\to AA} + 2\langle\sigma v^2\rangle_{AAA\to Ah} + 3\langle\sigma v^2\rangle_{AAA\to hh}$, and when $m_A \gg T_f$,

$$\begin{aligned} Y\left(\infty\right) &= \left(2\gamma\langle\sigma v^2\rangle_{\text{total}}\int_{x_f}^{\infty}\frac{1}{x^5}\right)^{-\frac{1}{2}} \\ &= \frac{2x_f^2}{\sqrt{2\gamma\langle\sigma v^2\rangle_{\text{total}}}} \equiv \sqrt{\frac{2H_0\left(m_A\right)}{\langle\sigma v^2\rangle_{\text{total}}}}\frac{x_f^2}{m_A^3}. \end{aligned} \tag{B.12}$$

The dark matter abundance now is as before given by equation (B.10).

Note that the constant c in the definition of x_f for the case when the 3 to 2 channels dominate is probably not best chosen to be the same as in the case when the 2 to 2 channels dominate. However, x_f depends on c only logarithmically and therefore it is expected that it wouldn't introduce a significant error if we use $c = \sqrt{2} - 1$ in the calculations for the case when the 3 to 2 channels dominate. We therefore simply used $c = \sqrt{2} - 1$ for the case when the 3 to 2 channels dominate as well.

Appendix C

Derivation of thermally averaged cross-sections of 3 to 2 scatterings in terms of $\Sigma_{\epsilon,a}|\mathcal{M}|^2$

Recall from equations (4.18) that

$$\langle\sigma v^2\rangle_{AAA\to AA} := \frac{1}{(n_A^{eq})^3}\frac{1}{3!}\frac{1}{2!}\int\left(\prod_{i=1}^{5}\frac{d^3p_i}{(2\pi)^3\,2E_i}\right)(2\pi)^4\delta^4\left(\sum_{i=1}^{i=5}p_i\right)e^{-\frac{E_1+E_2+E_3}{T}} \sum_{\epsilon,a}|\mathcal{M}_{AAA\to AA}|^2, \tag{4.18}$$

where from equations (4.17)

$$n_i^{eq}(T) := g_A\int\frac{d^3p}{(2\pi)^3}e^{-\frac{E_A}{T}}. \tag{4.17}$$

For the purpose of determining the relic abundance, we only need to consider the case when $m_A \gg T$ and $m_h \gg T$, for which the pre-factor of the exponent of $e^{-\frac{E}{T}}$ is very large, which justifies:

1. A non-relativistic approximation of the energy $E = m + \frac{p^2}{2m}$ for the energy of the initial state particles.

2. Treating the part of the integrand excluding the thermal Boltzmann factor as being independent of the initial state momenta and evaluated at initial state 3-momenta equal to 0 while applying the constraint of conservation of 4-momenta.

Therefore we have (implicitly assuming 4-momenta conservation for the evaluations

at $\mathbf{p_1} = \mathbf{p_2} = \mathbf{p_3} = 0$)

$$
\begin{aligned}
\langle \sigma v^2 \rangle_{AAA\to AA} :=& \frac{(2\pi)^4}{\left[3^2 e^{-\frac{m_A}{T}} \int \frac{d^3p}{(2\pi)^3} e^{-\frac{p^2}{T}}\right]^3} \frac{1}{2^2}\frac{1}{3} \left(\prod_{i=1}^{5} \frac{1}{(2\pi)^3\, 2E_i}\right)\Bigg|_{\mathbf{p_1}=\mathbf{p_2}=\mathbf{p_3}=\mathbf{0}} e^{-\frac{3m_A}{T}} \\
& \left(\sum_{\epsilon,a} |\mathcal{M}_{AAA\to AA}|^2\right)\Bigg|_{\mathbf{p_1}=\mathbf{p_2}=\mathbf{p_3}=\mathbf{0}} \int \left(\prod_{i=1}^{5} d^3p_i\right) e^{-\frac{p_1^2+p_2^2+p_3^3}{T}} \\
& \delta^{(4)}\left(\sum_{i=1}^{i=5} p_i\right)\Bigg|_{\mathbf{p_1}=\mathbf{p_2}=\mathbf{p_3}=\mathbf{0}} \\
=& \frac{(2\pi)^{-2}}{\left(\int d^3p\, e^{-\frac{p^2}{T}}\right)^3} \frac{1}{2^2}\frac{1}{3^7} \left(\frac{1}{2m_A}\right)^3 \left(\frac{1}{3m_A}\right)^2 \\
& \left(\sum_{\epsilon,a} |\mathcal{M}_{AAA\to AA}|^2\right)\Bigg|_{\mathbf{p_1}=\mathbf{p_2}=\mathbf{p_3}=\mathbf{0}} \left[\int \left(\prod_{i=1}^{3} d^3p_i\right) e^{-\frac{p_1^2+p_2^2+p_3^3}{T}}\right] \\
& \left[\int d^3p_4 d^3p_5\, \delta^{(1)}\left(3m_A - E_4 - E_5\right) \delta^{(3)}\left(-\mathbf{p_4} - \mathbf{p_5}\right)\right] \\
=& \frac{1}{\pi^2}\frac{1}{2^7}\frac{1}{3^9}\frac{1}{m_A^5} \left(\sum_{\epsilon,a} |\mathcal{M}_{AAA\to AA}|^2\right)\Bigg|_{\mathbf{p_1}=\mathbf{p_2}=\mathbf{p_3}=\mathbf{0}} \\
& \int d^3p_4 d^3p_5\, \delta^{(1)}\left(3m_A - \sqrt{m_A^2 + \mathbf{p_4}^2} - \sqrt{m_A^2 + \mathbf{p_5}^2}\right) \\
& \delta^{(3)}\left(-\mathbf{p_4} - \mathbf{p_5}\right).
\end{aligned}
\tag{C.1}
$$

Since

$$
\begin{aligned}
& \int d^3p_4 d^3p_5\, \delta^{(1)}\left(3m_A - \sqrt{m_A^2 + \mathbf{p_4}^2} - \sqrt{m_A^2 + \mathbf{p_5}^2}\right) \delta^{(3)}\left(-\mathbf{p_4} - \mathbf{p_5}\right) \\
=& 4\pi \int_0^\infty dr\, r^2 \delta^{(1)}\left(3m_A - 2\sqrt{m_A^2 + r^2}\right) \\
=& 4\pi \left.\frac{r^2}{\left|\frac{d}{dr}\left(3m_A - 2\sqrt{m_A^2 + r^2}\right)\right|}\right|_{3m_A = 2\sqrt{m_A^2+r^2}} \\
=& 4\pi \left.\frac{r\sqrt{m_A^2 + r^2}}{2}\right|_{\sqrt{m_A+r^2} = \frac{3}{2}m_A} \\
=& 2\pi \left(\frac{\sqrt{5}}{2} m_A\right)\left(\frac{3}{2} m_A\right) \\
=& \frac{3}{2}\sqrt{5}\,\pi m_A^2,
\end{aligned}
\tag{C.2}
$$

we finally have

$$\langle\sigma v^2\rangle_{AAA\to AA} = \frac{1}{\pi}\sqrt{5}\frac{1}{2^8}\frac{1}{3^8}\frac{1}{m_A^3}\sum_{\epsilon,a}|\mathcal{M}_{AAA\to AA}|^2\Big|_{\mathbf{p_1}=\mathbf{p_2}=\mathbf{p_3}=\mathbf{0}}. \tag{C.3}$$

Similarly we may obtain for $m_h \leq \frac{3}{2}m_A$ (i.e. when the $AAA \to hh$ channel isn't "forbidden")

$$\begin{aligned}\langle\sigma v^2\rangle_{AAA\to hh} =& \frac{1}{\pi^2}\frac{1}{2^7}\frac{1}{3^9}\frac{1}{m_A^5}3\pi\sqrt{\frac{9}{4}m_A^2 - m_h^2}\, m_A \sum_{\epsilon,a}|\mathcal{M}_{AAA\to hh}|^2\Big|_{\mathbf{p_1}=\mathbf{p_2}=\mathbf{p_3}=\mathbf{0}} \\ =& \frac{1}{\pi}\frac{1}{2^7}\frac{1}{3^8}\frac{1}{m_A^4}\sqrt{\frac{9}{4}m_A^2 - m_h^2}\sum_{\epsilon,a}|\mathcal{M}_{AAA\to hh}|^2\Big|_{\mathbf{p_1}=\mathbf{p_2}=\mathbf{p_3}=\mathbf{0}},\end{aligned} \tag{C.4}$$

and for $m_h \leq 2m_A$

$$\begin{aligned}\langle\sigma v^2\rangle_{AAA\to Ah} =& \frac{1}{\pi^2}\frac{1}{2^6}\frac{1}{3^9}\frac{1}{m_A^5}\frac{\pi\left(80m_A^4 + 2m_A^2m_h^2 - m_h^4\right)\sqrt{64m_A^4 - 20m_A^2m_h^2 + m_h^4}}{162m_A^4} \\ & \sum_{\epsilon,a}|\mathcal{M}_{AAA\to Ah}|^2\Big|_{\mathbf{p_1}=\mathbf{p_2}=\mathbf{p_3}=\mathbf{0}} \\ =& \frac{1}{\pi}\frac{1}{2^7}\frac{1}{3^{13}}\frac{1}{m_A^9}\left(80m_A^4 + 2m_A^2m_h^2 - m_h^4\right)\sqrt{64m_A^4 - 20m_A^2m_h^2 + m_h^4} \\ & \sum_{\epsilon,a}|\mathcal{M}_{AAA\to Ah}|^2\Big|_{\mathbf{p_1}=\mathbf{p_2}=\mathbf{p_3}=\mathbf{0}}.\end{aligned} \tag{C.5}$$

Appendix D

Checking of the result for $\mathcal{M}_{AA\to AA}$

To ensure the correctness of the expression of the amplitude from which $(\sigma_{tr})_{AA\to AA}$ was calculated, the high energy limit of the amplitude for the case in which all of the external A's are longitudinally polarized was calculated, yielding a result which doesn't diverge as $\rho \to 0$:

$$\begin{aligned}\mathcal{M}_{AA\to AA,L} =& \frac{i}{2st\,(s+t)}\Big[(s+t)\delta_{ad}\delta_{bc}\left(g^2(s^2+st+t^2)-4\lambda st\right)\\ &-t\delta_{ac}\delta_{bd}\left(g^2(s^2+st+t^2)+4\lambda s(s+t)\right)\\ &-\,s\delta_{ab}\delta_{cd}\left(g^2(s^2+st+t^2)+4\lambda t(s+t)\right)\Big]+O(\rho^2),\end{aligned} \tag{D.1}$$

The longitudinal polarization vectors used in the calculation of $\mathcal{M}_{AA\to AA,L}$ were expressed as:

$$\begin{aligned}\epsilon^{\mu}_{1L} &= \frac{1}{m_A}\sqrt{1-4\frac{m_A^2}{s}}\left[p_1^{\mu}\left(1+2\frac{m_A^2}{s-4m_A^2}\right)-p_2^{\mu}\frac{2m_A^2}{s-4m_A^2}\right]\\ \epsilon^{\mu}_{2L} &= \frac{1}{m_A}\sqrt{1-4\frac{m_A^2}{s}}\left[p_2^{\mu}\left(1+2\frac{m_A^2}{s-4m_A^2}\right)-p_1^{\mu}\frac{2m_A^2}{s-4m_A^2}\right]\\ \epsilon^{\mu}_{3L} &= \frac{1}{m_A}\sqrt{1-4\frac{m_A^2}{s}}\left[p_3^{\mu}\left(1+2\frac{m_A^2}{s-4m_A^2}\right)-p_4^{\mu}\frac{2m_A^2}{s-4m_A^2}\right]\\ \epsilon^{\mu}_{4L} &= \frac{1}{m_A}\sqrt{1-4\frac{m_A^2}{s}}\left[p_4^{\mu}\left(1+2\frac{m_A^2}{s-4m_A^2}\right)-p_3^{\mu}\frac{2m_A^2}{s-4m_A^2}\right]\end{aligned} \tag{D.2}$$

The cancellation of the terms which diverge as $\rho \to 0$ is unlikely if the amplitude is incorrect. The cancellation of the highest order divergent $O(\rho^{-4})$ terms from the

gauge boson only diagrams is necessitated by gauge invariance. The $O(\rho^{-2})$ terms from gauge boson only diagrams canceled with the $O(\rho^{-2})$ terms from the Higgs boson exchange diagrams [173].

Appendix E

Checking of the result for $\mathcal{M}_{AA\to hh}$ using Goldstone boson equivalence theorem

The theorem states, in the context of quantum field theory, that the amplitude for the emission or absorption of a longitudinally polarized gauge boson in a "spontaneously broken" gauge theory is equal to the amplitude of the emission or absorption of the corresponding Goldstone boson (which was "eaten" by the gauge boson) [174] at the high energy limit. This theorem implies that $\mathcal{M}_{hh\to A_iA_i} = \mathcal{M}_{hh\to\phi_i\phi_i}$ at the high energy limit if A_i is longitudinally polarized, where ϕ_i is the Goldstone boson associated with A_i.

Let $\Phi(x) = \frac{1}{\sqrt{2}}\begin{bmatrix} -i(\phi_1 - i\phi_2) \\ \rho + (h + i\phi_3) \end{bmatrix}$ [174], then the term in the Lagrangian density of the dark sector which gives the interaction between the Goldstone boson ϕ_i's and h is

$$\mathcal{L}_\Phi = -\lambda\left(\Phi^\dagger\Phi - \frac{\rho^2}{2}\right)^2. \tag{E.1}$$

Since the gauge bosons are identical except for their group indices, the coupling between h and ϕ_i must be the same for every i — this can also be derived by a direct calculation. We may therefore refer to all the ϕ_i's simply as ϕ in the subsequent part of this appendix. We find from $\mathcal{L}_\Phi$ that the interaction between h and ϕ for each ϕ_i

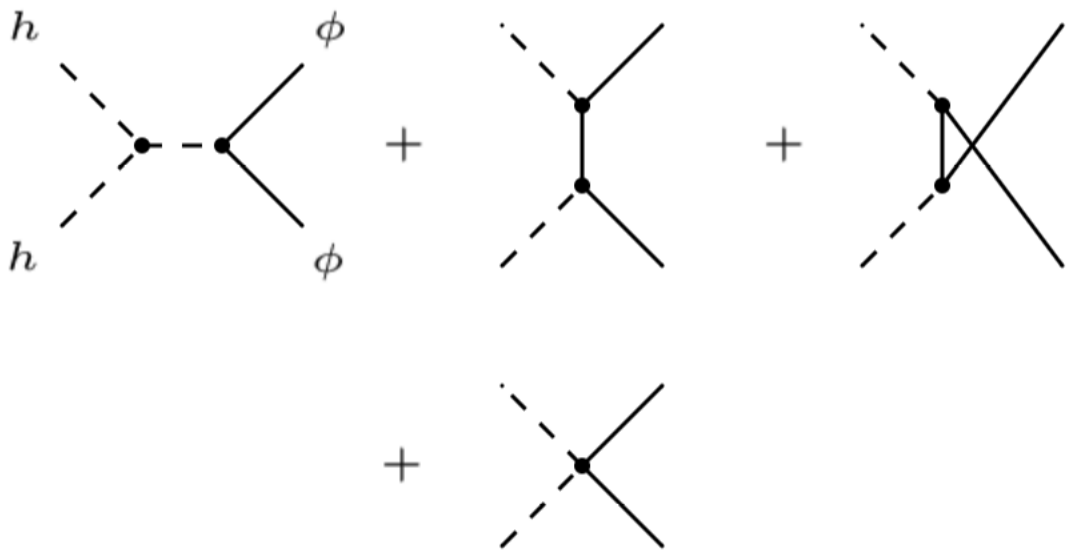

Figure E.1: Diagrams contributing to $\mathcal{M}_{hh\to\phi\phi}$ at lowest order in g if g, m_A and m_h are taken to be free parameters.

is given by

$$\begin{aligned}\mathcal{L}_{h\phi} =& -\lambda\left(\frac{1}{2}\left[\rho+(h+i\phi)\right]\left[\rho+(h-i\phi)\right]-\frac{\rho^2}{2}\right)^2 \\ =& -\frac{\lambda}{4}(h^2+2h\rho+\phi^2)^2 \\ =& -\frac{\lambda}{4}h^4-\lambda h^2\rho^2-\frac{\lambda}{4}\phi^4-\lambda h^3\rho-\lambda h\phi^2\rho-\frac{\lambda}{2}h^2\phi^2.\end{aligned} \tag{E.2}$$

If we take g, m_A and m_h to be the free parameters, the diagrams contributing to $\mathcal{M}_{hh\to\phi\phi}$ at lowest order in g are shown in Figure E.1. We calculated the non-relativistic limit of $\sigma_{hh\to\phi\phi}$ (summed over the group index) at lowest order in g in Lorenz gauge in which the Goldstone bosons are massless (i.e. have massless propagators) and obtained

$$\sigma_{hh\to\phi\phi}=\frac{3g^4m_h^2}{512\pi m_A^4}. \tag{E.3}$$

Recall

$$\sigma_{hh\to AA} = \frac{3g^4\sqrt{m_h^2 - m_A^2}}{2048\pi m_A^4 m_h^7} \left(192m_A^8 - 272m_A^6 m_h^2 + 107m_A^4 m_h^4 + 44m_A^2 m_h^6 + 4m_h^8\right). \tag{4.29}$$

The high energy limit can also be seen as the limit of $\rho \to 0$[1]. If we now take $\rho \to 0$ and $g \to 0$ while fixing λ[2], we would have $\frac{m_A}{m_h} \to 0$, in which case the contribution to $\mathcal{M}_{hh\to A_iA_i}$ from the transverse modes of A becomes negligible compared to that from the longitudinal mode since (at the high energy limit) the longitudinal polarization is proportional to m_A^{-1}, whereas the transverse polarizations are proportional to ${m_A}^0$. We find in this limit that

$$\sigma_{hh\to AA} = \frac{3g^4 m_h^2}{512\pi m_A^4} = \sigma_{hh\to\phi\phi}, \tag{E.4}$$

confirming (4.29).

Take the same limit for (4.30) and we find the result refuted by the check.

[1] As when g and λ are fixed, ρ which is of dimension Energy^{-1} sets the energy scale.

[2] Note that we are not taking limit in a mathematically rigorous sense but only considering the case when g and ρ are sufficiently close to 0.

Bibliography

[1] G. Battaglia et al., *The DART imaging and CaT survey of the Fornax Dwarf Spheroidal Galaxy*, *Astron. Astrophys.* **459** (2006) 423 [astro-ph/0608370].

[2] Particle Data Group collaboration, C. Patrignani et al., *Review of Particle Physics*, *Chin. Phys.* **C40** (2016) 100001.

[3] J. Silk et al., *Particle Dark Matter: Observations, Models and Searches*. Cambridge Univ. Press, Cambridge, 2010, 10.1017/CBO9780511770739.

[4] G. Bertone, D. Hooper and J. Silk, *Particle dark matter: Evidence, candidates and constraints*, *Phys. Rept.* **405** (2005) 279 [hep-ph/0404175].

[5] K. G. Begeman, A. H. Broeils and R. H. Sanders, *Extended rotation curves of spiral galaxies: Dark haloes and modified dynamics*, *Mon. Not. Roy. Astron. Soc.* **249** (1991) 523.

[6] S. Tulin and H.-B. Yu, *Dark Matter Self-interactions and Small Scale Structure*, *Phys. Rept.* **730** (2018) 1 [1705.02358].

[7] J. P. Ostriker, P. J. E. Peebles and A. Yahil, *The size and mass of galaxies, and the mass of the universe*, *Astrophysical Journal* **193** (1974) L1.

[8] J. Einasto, A. Kaasik and E. Saar, *Dynamic evidence on massive coronas of galaxies*, *Nature* **250** (1974) 309.

[9] J. A. Tyson, G. P. Kochanski and I. P. Dell'Antonio, *Detailed mass map of cl 0024+1654 from strong lensing*, *The Astrophysical Journal Letters* **498** (1998) L107.

[10] D. J. Sand, T. Treu and R. S. Ellis, *The dark matter density profile of the lensing cluster ms2137-23: a test of the cold dark matter paradigm*, *Astrophys. J.* **574** (2002) L129 [astro-ph/0207048].

[11] D. Samtleben, S. Staggs and B. Winstein, *The Cosmic microwave background for pedestrians: A Review for particle and nuclear physicists*, *Ann. Rev. Nucl. Part. Sci.* **57** (2007) 245 [0803.0834].

[12] W. Hu and S. Dodelson, *Cosmic microwave background anisotropies*, *Annual Review of Astronomy and Astrophysics* **40** (2002) 171 [https://doi.org/10.1146/annurev.astro.40.060401.093926].

[13] W. Hu, N. Sugiyama and J. Silk, *The Physics of microwave background anisotropies*, *Nature* **386** (1997) 37 [astro-ph/9604166].

[14] D. J. Hegyi and K. A. Olive, *Can galactic halos be made of baryons?*, *Physics Letters B* **126** (1983) 28 .

[15] R. V. Wagoner, *Big-Bang Nucleosynthesis Revisited*, *Astrophysical Journal* **179** (1973) 343.

[16] S. S. Gershtein and Ya. B. Zeldovich, *Rest Mass of Muonic Neutrino and Cosmology*, *JETP Lett.* **4** (1966) 120.

[17] R. Cowsik and J. McClelland, *An upper limit on the neutrino rest mass*, *Phys. Rev. Lett.* **29** (1972) 669.

[18] A. S. Szalay and G. Marx, *Neutrino rest mass from cosmology*, *Astronomy and Astrophysics* **49** (1976) 437.

[19] J. R. Primack and M. A. K. Gross, *Hot dark matter in cosmology*, astro-ph/0007165.

[20] S. D. M. White, C. S. Frenk and M. Davis, *Clustering in a neutrino-dominated universe*, *Astrphysical Journal* **274** (1983) L1.

[21] P. Hut and S. D. M. White, *Can a neutrino-dominated Universe be rejected?*, *Nature* **310** (1984) 637.

[22] N. A. Bahcall, J. P. Ostriker, S. Perlmutter and P. J. Steinhardt, *The Cosmic triangle: Assessing the state of the universe*, *Science* **284** (1999) 1481 [astro-ph/9906463].

[23] Planck collaboration, P. A. R. Ade et al., *Planck 2015 results. XIII. Cosmological parameters*, *Astron. Astrophys.* **594** (2016) A13 [1502.01589].

[24] SDSS collaboration, M. Tegmark et al., *The 3-D power spectrum of galaxies from the SDSS*, *Astrophys. J.* **606** (2004) 702 [astro-ph/0310725].

[25] SDSS collaboration, M. Tegmark et al., *Cosmological parameters from SDSS and WMAP*, *Phys. Rev.* **D69** (2004) 103501 [astro-ph/0310723].

[26] V. Springel, C. S. Frenk and S. D. M. White, *The large-scale structure of the Universe*, *Nature* **440** (2006) 1137 [astro-ph/0604561].

[27] S. Trujillo-Gomez, A. Schneider, E. Papastergis, D. S. Reed and G. Lake, *Another baryon miracle? Testing solutions to the âĂŸmissing dwarfsâĂŹ problem*, *Mon. Not. Roy. Astron. Soc.* **475** (2018) 4825 [1610.09335].

[28] S. Colombi, S. Dodelson and L. M. Widrow, *Large scale structure tests of warm dark matter*, *Astrophys. J.* **458** (1996) 1 [astro-ph/9505029].

[29] P. Bode, J. P. Ostriker and N. Turok, *Halo formation in warm dark matter models*, *Astrophys. J.* **556** (2001) 93 [astro-ph/0010389].

[30] S. F. King and A. Merle, *Warm Dark Matter from keVins*, *JCAP* **1208** (2012) 016 [1205.0551].

[31] H. Goldberg, *Constraint on the Photino Mass from Cosmology*, *Phys. Rev. Lett.* **50** (1983) 1419.

[32] G. Jungman, M. Kamionkowski and K. Griest, *Supersymmetric dark matter*, *Phys. Rept.* **267** (1996) 195 [hep-ph/9506380].

[33] G. Servant and T. M. P. Tait, *Is the lightest Kaluza-Klein particle a viable dark matter candidate?*, *Nucl. Phys.* **B650** (2003) 391 [hep-ph/0206071].

[34] H.-C. Cheng, J. L. Feng and K. T. Matchev, *Kaluza-Klein dark matter*, *Phys. Rev. Lett.* **89** (2002) 211301 [hep-ph/0207125].

[35] J. Preskill, M. B. Wise and F. Wilczek, *Cosmology of the Invisible Axion*, *Phys. Lett.* **B120** (1983) 127.

[36] R. D. Peccei and H. R. Quinn, *CP Conservation in the Presence of Instantons*, *Phys. Rev. Lett.* **38** (1977) 1440.

[37] B. W. Lee and S. Weinberg, *Cosmological Lower Bound on Heavy Neutrino Masses*, *Phys. Rev. Lett.* **39** (1977) 165.

[38] J. L. Feng, *Dark Matter Candidates from Particle Physics and Methods of Detection*, *Ann. Rev. Astron. Astrophys.* **48** (2010) 495 [1003.0904].

[39] N. A. Graf, M. E. Peskin and J. L. Rosner, eds., *Proceedings, 2013 Community Summer Study on the Future of U.S. Particle Physics: Snowmass on the Mississippi (CSS2013)*, 2013.

[40] M. Mordehai, *Mond theory*, *Canadian Journal of Physics* **93** (2015) 107 [https://doi.org/10.1139/cjp-2014-0211].

[41] L. Bernard and L. Blanchet, *Phenomenology of dark matter via a bimetric extension of general relativity*, *Phys. Rev. D* **91** (2015) 103536.

[42] R. A. Flores and J. R. Primack, *Observational and theoretical constraints on singular dark matter halos*, *Astrophys. J.* **427** (1994) L1 [astro-ph/9402004].

[43] B. Moore, *Evidence against dissipationless dark matter from observations of galaxy haloes*, *Nature* **370** (1994) 629.

[44] B. Moore, T. R. Quinn, F. Governato, J. Stadel and G. Lake, *Cold collapse and the core catastrophe*, *Mon. Not. Roy. Astron. Soc.* **310** (1999) 1147 [astro-ph/9903164].

[45] J. Dubinski and R. G. Carlberg, *The structure of cold dark matter halos*, *Astrophysical Journal* **378** (1991) 496.

[46] J. F. Navarro, C. S. Frenk and S. D. M. White, *The Structure of cold dark matter halos*, *Astrophys. J.* **462** (1996) 563 [astro-ph/9508025].

[47] J. F. Navarro, C. S. Frenk and S. D. M. White, *A Universal density profile from hierarchical clustering*, *Astrophys. J.* **490** (1997) 493 [astro-ph/9611107].

[48] E. Romano-Diaz, Y. Hoffman, C. Heller, A. Faltenbacher, D. Jones and I. Shlosman, *Evolution of Characteristic Quantities for Dark Matter Halo Density Profiles*, *Astrophys. J.* **657** (2007) 56 [astro-ph/0610090].

[49] F. C. van den Bosch and R. A. Swaters, *Dwarf galaxy rotation curves and the core problem of dark matter halos*, *Mon. Not. Roy. Astron. Soc.* **325** (2001) 1017 [astro-ph/0006048].

[50] A. Borriello and P. Salucci, *The Dark matter distribution in disk galaxies*, *Mon. Not. Roy. Astron. Soc.* **323** (2001) 285 [astro-ph/0001082].

[51] W. J. G. de Blok, S. S. McGaugh and V. C. Rubin, *High-Resolution Rotation Curves of Low Surface Brightness Galaxies. II. Mass Models*, *Astron. J.* **122** (2001) 2396.

[52] W. J. G. de Blok, S. S. McGaugh, A. Bosma and V. C. Rubin, *Mass density profiles of LSB galaxies*, *Astrophys. J.* **552** (2001) L23 [astro-ph/0103102].

[53] D. Marchesini, E. D'Onghia, G. Chincarini, C. Firmani, P. Conconi, E. Molinari et al., *Halpha rotation curves: the soft core question*, *Astrophys. J.* **575** (2002) 801 [astro-ph/0202075].

[54] G. Gentile, A. Burkert, P. Salucci, U. Klein and F. Walter, *The dwarf galaxy DDO 47 as a dark matter laboratory: testing cusps hiding in triaxial halos*, *Astrophys. J. Lett.* **634** (2005) L145 [astro-ph/0506538].

[55] G. Gentile, P. Salucci, U. Klein and G. L. Granato, *NGC 3741: Dark halo profile from the most extended rotation curve*, *Mon. Not. Roy. Astron. Soc.* **375** (2007) 199 [astro-ph/0611355].

[56] R. Kuzio de Naray, S. S. McGaugh, W. J. G. de Blok and A. Bosma, *High Resolution Optical Velocity Fields of 11 Low Surface Brightness Galaxies*, *Astrophys. J. Suppl.* **165** (2006) 461 [astro-ph/0604576].

[57] R. Kuzio de Naray, S. S. McGaugh and W. J. G. de Blok, *Mass Models for Low Surface Brightness Galaxies with High Resolution Optical Velocity Fields*, *Astrophys. J.* **676** (2008) 920 [0712.0860].

[58] P. Salucci, A. Lapi, C. Tonini, G. Gentile, I. Yegorova and U. Klein, *The Universal Rotation Curve of Spiral Galaxies. 2. The Dark Matter Distribution out to the Virial Radius*, *Mon. Not. Roy. Astron. Soc.* **378** (2007) 41 [astro-ph/0703115].

[59] J. F. Navarro, V. R. Eke and C. S. Frenk, *The cores of dwarf galaxy halos*, *Mon. Not. Roy. Astron. Soc.* **283** (1996) L72 [astro-ph/9610187].

[60] S.-H. Oh, C. Brook, F. Governato, E. Brinks, L. Mayer, W. J. G. de Blok et al., *The central slope of dark matter cores in dwarf galaxies: Simulations vs. THINGS*, *Astron. J.* **142** (2011) 24 [1011.2777].

[61] J. J. Dalcanton and A. Stilp, *Pressure Support in Galaxy Disks: Impact on Rotation Curves and Dark Matter Density Profiles*, *Astrophys. J.* **721** (2010) 547 [1007.2535].

[62] J. C. B. Pineda, C. C. Hayward, V. Springel and C. Mendes de Oliveira, *Rotation curve fitting and its fatal attraction to cores in realistically simulated galaxy observations*, *Monthly Notices of the Royal Astronomical Society* **466** (2017) 63 [1602.07690].

[63] S. S. McGaugh, W. J. G. de Blok, J. M. Schombert, R. K. de Naray and J. H. Kim, *The Rotation Velocity Attributable to Dark Matter at Intermediate Radii in Disk Galaxies*, *Astrophys. J.* **659** (2007) 149 [astro-ph/0612410].

[64] G. Gentile, C. Tonini and P. Salucci, *Lambda CDM Halo Density Profiles: Where do actual halos converge to NFW ones?*, *Astron. Astrophys.* **467** (2007) 925 [astro-ph/0701550].

[65] H. Katz, F. Lelli, S. S. McGaugh, A. Di Cintio, C. B. Brook and J. M. Schombert, *Testing feedback-modified dark matter haloes with galaxy rotation curves: estimation of halo parameters and consistency with ÎŻCDM scaling relations*, *Mon. Not. Roy. Astron. Soc.* **466** (2017) 1648 [1605.05971].

[66] G. Gentile, P. Salucci, U. Klein, D. Vergani and P. Kalberla, *The Cored distribution of dark matter in spiral galaxies*, *Mon. Not. Roy. Astron. Soc.* **351** (2004) 903 [astro-ph/0403154].

[67] F. Donato, G. Gentile, P. Salucci, C. F. Martins, M. I. Wilkinson, G. Gilmore et al., *A constant dark matter halo surface density in galaxies*, *Mon. Not. Roy. Astron. Soc.* **397** (2009) 1169 [0904.4054].

[68] M. G. Walker, M. Mateo, E. W. Olszewski, J. Penarrubia, N. W. Evans and G. Gilmore, *A Universal Mass Profile for Dwarf Spheroidal Galaxies*, *Astrophys. J.* **704** (2009) 1274 [0906.0341].

[69] J. Wolf, G. D. Martinez, J. S. Bullock, M. Kaplinghat, M. Geha, R. R. Munoz et al., *Accurate Masses for Dispersion-supported Galaxies*, *Mon. Not. Roy. Astron. Soc.* **406** (2010) 1220 [0908.2995].

[70] G. Battaglia, A. Helmi, E. Tolstoy, M. Irwin, V. Hill and P. Jablonka, *The kinematic status and mass content of the Sculptor dwarf spheroidal galaxy*, *Astrophys. J.* **681** (2008) L13 [0802.4220].

[71] N. C. Amorisco and N. W. Evans, *Dark Matter Cores and Cusps: The Case of Multiple Stellar Populations in Dwarf Spheroidals*, *Mon. Not. Roy. Astron. Soc.* **419** (2012) 184 [1106.1062].

[72] M. G. Walker and J. Penarrubia, *A Method for Measuring (Slopes of) the Mass Profiles of Dwarf Spheroidal Galaxies*, *Astrophys. J.* **742** (2011) 20 [1108.2404].

[73] L. E. Strigari, C. S. Frenk and S. D. M. White, *Dynamical Models for the Sculptor Dwarf Spheroidal in a ÎŻCDM Universe*, *Astrophys. J.* **838** (2017) 123 [1406.6079].

[74] M. A. Breddels and A. Helmi, *Model comparison of the dark matter profiles of Fornax, Sculptor, Carina and Sextans*, *Astron. Astrophys.* **558** (2013) A35 [1304.2976].

[75] N. C. Amorisco, A. Agnello and N. W. Evans, *The core size of the Fornax dwarf Spheroidal*, *Mon. Not. Roy. Astron. Soc.* **429** (2013) L89 [1210.3157].

[76] J. T. Kleyna, M. I. Wilkinson, G. Gilmore and N. W. Evans, *A dynamical fossil in the ursa minor dwarf spheroidal galaxy*, *Astrophys. J.* **588** (2003) L21 [astro-ph/0304093].

[77] M. G. Walker, M. Mateo, E. W. Olszewski, J. K. Pal, B. Sen and M. Woodroofe, *On Kinematic Substructure in the Sextans Dwarf Spheroidal Galaxy*, *Astrophys. J.* **642** (2006) L41 [astro-ph/0603694].

[78] V. Lora, E. K. Grebel, F. J. Sanchez-Salcedo and A. Just, *Sextans' cold substructures as a dynamical judge: Core, Cusp or MOND?*, *Astrophys. J.* **777** (2013) 65 [1309.1565].

[79] F. J. Sanchez-Salcedo, J. Reyes-Iturbide and X. Hernandez, *An extensive study of dynamical friction in dwarf galaxies: the role of stars, dark matter, halo profiles and mond*, *Mon. Not. Roy. Astron. Soc.* **370** (2006) 1829 [astro-ph/0601490].

[80] T. Goerdt, B. Moore, J. I. Read, J. Stadel and M. Zemp, *Does the fornax dwarf spheroidal have a central cusp or core?*, *Mon. Not. Roy. Astron. Soc.* **368** (2006) 1073 [astro-ph/0601404].

[81] J. I. Read, T. Goerdt, B. Moore, A. P. Pontzen, J. Stadel and G. Lake, *Dynamical friction in constant density cores: A failure of the Chandrasekhar formula*, *Mon. Not. Roy. Astron. Soc.* **373** (2006) 1451 [astro-ph/0606636].

[82] D. R. Cole, W. Dehnen, J. I. Read and M. I. Wilkinson, *The mass distribution of the Fornax dSph: constraints from its globular cluster distribution*, *Mon. Not. Roy. Astron. Soc.* **426** (2012) 601 [1205.6327].

[83] D. J. Sand, T. Treu, G. P. Smith and R. S. Ellis, *The dark matter distribution in the central regions of galaxy clusters: Implications for CDM*, *Astrophys. J.* **604** (2004) 88 [astro-ph/0309465].

[84] A. B. Newman, T. Treu, R. S. Ellis, D. J. Sand, J. Richard, P. J. Marshall et al., *The Distribution of Dark Matter Over 3 Decades in Radius in the Lensing Cluster Abell 611*, *Astrophys. J.* **706** (2009) 1078 [0909.3527].

[85] A. B. Newman, T. Treu, R. S. Ellis and D. J. Sand, *The Dark Matter Distribution in Abell 383: Evidence for a Shallow Density Cusp from Improved Lensing, Stellar Kinematic and X-ray Data*, *Astrophys. J.* **728** (2011) L39 [1101.3553].

[86] A. B. Newman, T. Treu, R. S. Ellis, D. J. Sand, C. Nipoti, J. Richard et al., *The Density Profiles of Massive, Relaxed Galaxy Clusters: I. The Total Density Over 3 Decades in Radius*, *Astrophys. J.* **765** (2013) 24 [1209.1391].

[87] A. B. Newman, T. Treu, R. S. Ellis and D. J. Sand, *The Density Profiles of Massive, Relaxed Galaxy Clusters: II. Separating Luminous and Dark Matter in Cluster Cores*, *Astrophys. J.* **765** (2013) 25 [1209.1392].

[88] D. Martizzi, R. Teyssier, B. Moore and T. Wentz, *The effects of baryon physics, black holes and AGN feedback on the mass distribution in clusters of galaxies*, *Mon. Not. Roy. Astron. Soc.* **422** (2012) 3081 [1112.2752].

[89] D. Martizzi, R. Teyssier and B. Moore, *Cusp-core transformations induced by AGN feedback in the progenitors of cluster galaxies*, *Mon. Not. Roy. Astron. Soc.* **432** (2013) 1947 [1211.2648].

[90] M. Schaller, C. S. Frenk, R. G. Bower, T. Theuns, J. Trayford, R. A. Crain et al., *The effect of baryons on the inner density profiles of rich clusters*, *Mon. Not. Roy. Astron. Soc.* **452** (2015) 343 [1409.8297].

[91] J. S. Bullock, T. S. Kolatt, Y. Sigad, R. S. Somerville, A. V. Kravtsov, A. A. Klypin et al., *Profiles of dark haloes. Evolution, scatter, and environment*, *Mon. Not. Roy. Astron. Soc.* **321** (2001) 559 [astro-ph/9908159].

[92] K. A. Oman et al., *The unexpected diversity of dwarf galaxy rotation curves*, *Mon. Not. Roy. Astron. Soc.* **452** (2015) 3650 [1504.01437].

[93] R. Kuzio de Naray, G. D. Martinez, J. S. Bullock and M. Kaplinghat, *The Case Against Warm or Self-Interacting Dark Matter as Explanations for Cores in Low Surface Brightness Galaxies*, *Astrophys. J.* **710** (2010) L161 [0912.3518].

[94] G. Kauffmann, S. D. M. White and B. Guiderdoni, *The Formation and Evolution of Galaxies Within Merging Dark Matter Haloes*, *Mon. Not. Roy. Astron. Soc.* **264** (1993) 201.

[95] B. Moore, S. Ghigna, F. Governato, G. Lake, T. R. Quinn, J. Stadel et al., *Dark matter substructure within galactic halos*, *Astrophys. J.* **524** (1999) L19 [astro-ph/9907411].

[96] A. A. Klypin, A. V. Kravtsov, O. Valenzuela and F. Prada, *Where are the missing Galactic satellites?*, *Astrophys. J.* **522** (1999) 82 [astro-ph/9901240].

[97] A. A. Thoul and D. H. Weinberg, *Hydrodynamic simulations of galaxy formation. 2. Photoionization and the formation of low mass galaxies*, *Astrophys. J.* **465** (1996) 608 [astro-ph/9510154].

[98] J. S. Bullock, A. V. Kravtsov and D. H. Weinberg, *Reionization and the abundance of galactic satellites*, *Astrophys. J.* **539** (2000) 517 [astro-ph/0002214].

[99] A. Dekel and J. Silk, *The origin of dwarf galaxies, cold dark matter, and biased galaxy formation*, *Astrophys. J.* **303** (1986) 39.

[100] E. J. Tollerud, J. S. Bullock, L. E. Strigari and B. Willman, *Hundreds of Milky Way Satellites? Luminosity Bias in the Satellite Luminosity Function*, *Astrophys. J.* **688** (2008) 277 [0806.4381].

[101] S. Walsh, B. Willman and H. Jerjen, *The Invisibles: A Detection Algorithm to Trace the Faintest Milky Way Satellites*, *Astron. J.* **137** (2009) 450 [0807.3345].

[102] J. S. Bullock, K. R. Stewart, M. Kaplinghat and E. J. Tollerud, *Stealth Galaxies in the Halo of the Milky Way*, *Astrophys. J.* **717** (2010) 1043 [0912.1873].

[103] S. Trujillo-Gomez, A. Klypin, J. Primack and A. J. Romanowsky, *Galaxies in LCDM with Halo Abundance Matching: luminosity-velocity relation, baryonic mass-velocity relation, velocity function and clustering*, *Astrophys. J.* **742** (2011) 16 [1005.1289].

[104] J. Zavala, Y. P. Jing, A. Faltenbacher, G. Yepes, Y. Hoffman, S. Gottlober et al., *The velocity function in the local environment from LCDM and LWDM constrained simulations*, *Astrophys. J.* **700** (2009) 1779 [0906.0585].

[105] M. A. Zwaan, M. J. Meyer and L. Staveley-Smith, *The velocity function of gas-rich galaxies*, *Mon. Not. Roy. Astron. Soc.* **403** (2010) 1969 [0912.1754].

[106] A. Klypin, I. Karachentsev, D. Makarov and O. Nasonova, *Abundance of Field Galaxies*, *Mon. Not. Roy. Astron. Soc.* **454** (2015) 1798 [1405.4523].

[107] S. Cole and N. Kaiser, *Biased clustering in the cold dark matter cosmogony*, *Mon. Not. Roy. Astron. Soc.* **237** (1989) 1127.

[108] K. Shimasaku, *Velocity functions of galaxies and clusters of galaxies.*, in *Evolution of the Universe and its Observational Quest* (K. Sato, ed.), pp. 531–532, 1994.

[109] C. Brook and F. Shankar, *A matter of measurement: rotation velocities and the velocity function of dwarf galaxies*, *Mon. Not. Roy. Astron. Soc.* **455** (2016) 3841 [1506.00655].

[110] A. V. MacciÃš, S. M. Udrescu, A. A. Dutton, A. Obreja, L. Wang, G. R. Stinson et al., *NIHAO X: reconciling the local galaxy velocity function with cold dark matter via mock HâĂŹLI observations*, *Mon. Not. Roy. Astron. Soc.* **463** (2016) L69 [1607.01028].

[111] A. M. Brooks, E. Papastergis, C. R. Christensen, F. Governato, A. Stilp, T. R. Quinn et al., *How to Reconcile the Observed Velocity Function of Galaxies with Theory*, *Astrophys. J.* **850** (2017) 97 [1701.07835].

[112] M. Boylan-Kolchin, J. S. Bullock and M. Kaplinghat, *Too big to fail? The puzzling darkness of massive Milky Way subhaloes*, *Mon. Not. Roy. Astron. Soc.* **415** (2011) L40 [1103.0007].

[113] M. Boylan-Kolchin, J. S. Bullock and M. Kaplinghat, *The Milky Way's bright satellites as an apparent failure of LCDM*, *Mon. Not. Roy. Astron. Soc.* **422** (2012) 1203 [1111.2048].

[114] E. J. Tollerud, M. Boylan-Kolchin and J. S. Bullock, *M31 Satellite Masses Compared to LCDM Subhaloes*, *Mon. Not. Roy. Astron. Soc.* **440** (2014) 3511 [1403.6469].

[115] S. Garrison-Kimmel, M. Boylan-Kolchin, J. S. Bullock and E. N. Kirby, *Too Big to Fail in the Local Group*, *Mon. Not. Roy. Astron. Soc.* **444** (2014) 222 [1404.5313].

[116] I. Ferrero, M. G. Abadi, J. F. Navarro, L. V. Sales and S. Gurovich, *The dark matter halos of dwarf galaxies: a challenge for the LCDM paradigm?*, *Mon. Not. Roy. Astron. Soc.* **425** (2012) 2817 [1111.6609].

[117] E. Papastergis, R. Giovanelli, M. P. Haynes and F. Shankar, *Is there a âĂIJtoo big to failâĂİ problem in the field?*, *Astron. Astrophys.* **574** (2015) A113 [1407.4665].

[118] C. B. Brook and A. Di Cintio, *Expanded haloes, abundance matching and too-big-to-fail in the Local Group*, *Mon. Not. Roy. Astron. Soc.* **450** (2015) 3920 [1410.3825].

[119] M. R. Lovell, V. Eke, C. S. Frenk, L. Gao, A. Jenkins, T. Theuns et al., *The Haloes of Bright Satellite Galaxies in a Warm Dark Matter Universe*, *Mon. Not. Roy. Astron. Soc.* **420** (2012) 2318 [1104.2929].

[120] M. R. Lovell, C. S. Frenk, V. R. Eke, A. Jenkins, L. Gao and T. Theuns, *The properties of warm dark matter haloes*, *Mon. Not. Roy. Astron. Soc.* **439** (2014) 300 [1308.1399].

[121] S. Horiuchi, B. Bozek, K. N. Abazajian, M. Boylan-Kolchin, J. S. Bullock, S. Garrison-Kimmel et al., *Properties of resonantly produced sterile neutrino dark matter subhaloes*, *Mon. Not. Roy. Astron. Soc.* **456** (2016) 4346 [1512.04548].

[122] N. Menci, A. Grazian, M. Castellano and N. G. Sanchez, *A Stringent Limit on the Warm Dark Matter Particle Masses from the Abundance of z=6 Galaxies in the Hubble Frontier Fields*, *Astrophys. J.* **825** (2016) L1 [1606.02530].

[123] V. IrÅąiÄĐ et al., *New Constraints on the free-streaming of warm dark matter from intermediate and small scale Lyman-α forest data*, *Phys. Rev.* **D96** (2017) 023522 [1702.01764].

[124] M. Viel, G. D. Becker, J. S. Bolton and M. G. Haehnelt, *Warm dark matter as a solution to the small scale crisis: New constraints from high redshift Lyman-Îś forest data*, *Phys. Rev.* **D88** (2013) 043502 [1306.2314].

[125] A. V. Maccio, S. Paduroiu, D. Anderhalden, A. Schneider and B. Moore, *Cores in warm dark matter haloes: a Catch 22 problem*, *Mon. Not. Roy. Astron. Soc.* **424** (2012) 1105 [1202.1282].

[126] D. N. Spergel and P. J. Steinhardt, *Observational evidence for selfinteracting cold dark matter*, *Phys. Rev. Lett.* **84** (2000) 3760 [astro-ph/9909386].

[127] M. Vogelsberger and J. Zavala, *Direct detection of self-interacting dark matter*, *Mon. Not. Roy. Astron. Soc.* **430** (2013) 1722 [1211.1377].

[128] J. Dubinski and R. G. Carlberg, *The Structure of cold dark matter halos*, *Astrophys. J.* **378** (1991) 496.

[129] B. Moore, S. Gelato, A. Jenkins, F. R. Pearce and V. Quilis, *Collisional versus collisionless dark matter*, *Astrophys. J.* **535** (2000) L21 [astro-ph/0002308].

[130] N. Yoshida, V. Springel, S. D. M. White and G. Tormen, *Collisional dark matter and the structure of dark halos*, *Astrophys. J.* **535** (2000) L103 [astro-ph/0002362].

[131] A. Burkert, *The Structure and evolution of weakly selfinteracting cold dark matter halos*, *Astrophys. J.* **534** (2000) L143 [astro-ph/0002409].

[132] C. S. Kochanek and M. J. White, *A Quantitative study of interacting dark matter in halos*, *Astrophys. J.* **543** (2000) 514 [astro-ph/0003483].

[133] N. Yoshida, V. Springel, S. D. M. White and G. Tormen, *Weakly self-interacting dark matter and the structure of dark halos*, *Astrophys. J.* **544** (2000) L87 [astro-ph/0006134].

[134] R. Dave, D. N. Spergel, P. J. Steinhardt and B. D. Wandelt, *Halo properties in cosmological simulations of selfinteracting cold dark matter*, *Astrophys. J.* **547** (2001) 574 [astro-ph/0006218].

[135] P. Colin, V. Avila-Reese, O. Valenzuela and C. Firmani, *Structure and subhalo population of halos in a selfinteracting dark matter cosmology*, *Astrophys. J.* **581** (2002) 777 [astro-ph/0205322].

[136] J. Miralda-Escude, *A test of the collisional dark matter hypothesis from cluster lensing*, *Astrophys. J.* **564** (2002) 60 [astro-ph/0002050].

[137] M. Meneghetti, N. Yoshida, M. Bartelmann, L. Moscardini, V. Springel, G. Tormen et al., *Giant cluster arcs as a constraint on the scattering cross-section of dark matter*, *Mon. Not. Roy. Astron. Soc.* **325** (2001) 435 [astro-ph/0011405].

[138] S. W. Randall, M. Markevitch, D. Clowe, A. H. Gonzalez and M. Bradac, *Constraints on the Self-Interaction Cross-Section of Dark Matter from Numerical Simulations of the Merging Galaxy Cluster 1E 0657-56*, *Astrophys. J.* **679** (2008) 1173 [0704.0261].

[139] C. Firmani, E. D'Onghia, V. Avila-Reese, G. Chincarini and X. Hernandez, *Evidence of self-interacting cold dark matter from galactic to galaxy cluster scales*, *Mon. Not. Roy. Astron. Soc.* **315** (2000) L29 [astro-ph/0002376].

[140] C. Firmani, E. D'Onghia, G. Chincarini, X. Hernandez and V. Avila-Reese, *Constraints on dark matter physics from dwarf galaxies through galaxy cluster haloes*, *Mon. Not. Roy. Astron. Soc.* **321** (2001) 713 [astro-ph/0005001].

[141] M. Vogelsberger, J. Zavala and A. Loeb, *Subhaloes in Self-Interacting Galactic Dark Matter Haloes*, *Mon. Not. Roy. Astron. Soc.* **423** (2012) 3740 [1201.5892].

[142] J. Zavala, M. Vogelsberger and M. G. Walker, *Constraining Self-Interacting Dark Matter with the Milky Way's dwarf spheroidals*, *Mon. Not. Roy. Astron. Soc.* **431** (2013) L20 [1211.6426].

[143] O. D. Elbert, J. S. Bullock, S. Garrison-Kimmel, M. Rocha, J. OÃśorbe and A. H. G. Peter, *Core formation in dwarf haloes with self-interacting dark matter: no fine-tuning necessary*, *Mon. Not. Roy. Astron. Soc.* **453** (2015) 29 [1412.1477].

[144] M. Vogelsberger, J. Zavala, C. Simpson and A. Jenkins, *Dwarf galaxies in CDM and SIDM with baryons: observational probes of the nature of dark matter*, *Mon. Not. Roy. Astron. Soc.* **444** (2014) 3684 [1405.5216].

[145] A. B. Fry, F. Governato, A. Pontzen, T. Quinn, M. Tremmel, L. Anderson et al., *All about baryons: revisiting SIDM predictions at small halo masses*, *Mon. Not. Roy. Astron. Soc.* **452** (2015) 1468 [1501.00497].

[146] G. A. Dooley, A. H. G. Peter, M. Vogelsberger, J. Zavala and A. Frebel, *Enhanced Tidal Stripping of Satellites in the Galactic Halo from Dark Matter Self-Interactions*, *Mon. Not. Roy. Astron. Soc.* **461** (2016) 710 [1603.08919].

[147] D. Harvey, R. Massey, T. Kitching, A. Taylor and E. Tittley, *The non-gravitational interactions of dark matter in colliding galaxy clusters*, *Science* **347** (2015) 1462 [1503.07675].

[148] M. Kaplinghat, S. Tulin and H.-B. Yu, *Dark Matter Halos as Particle Colliders: Unified Solution to Small-Scale Structure Puzzles from Dwarfs to Clusters*, *Phys. Rev. Lett.* **116** (2016) 041302 [1508.03339].

[149] M. Kaplinghat, R. E. Keeley, T. Linden and H.-B. Yu, *Tying Dark Matter to Baryons with Self-interactions*, *Phys. Rev. Lett.* **113** (2014) 021302 [1311.6524].

[150] A. Kamada, M. Kaplinghat, A. B. Pace and H.-B. Yu, *How the Self-Interacting Dark Matter Model Explains the Diverse Galactic Rotation Curves*, *Phys. Rev. Lett.* **119** (2017) 111102 [1611.02716].

[151] J. L. Feng, M. Kaplinghat and H.-B. Yu, *Halo Shape and Relic Density Exclusions of Sommerfeld-Enhanced Dark Matter Explanations of Cosmic Ray Excesses*, *Phys. Rev. Lett.* **104** (2010) 151301 [0911.0422].

[152] S. Tulin, H.-B. Yu and K. M. Zurek, *Beyond Collisionless Dark Matter: Particle Physics Dynamics for Dark Matter Halo Structure*, *Phys. Rev.* **D87** (2013) 115007 [1302.3898].

[153] K. Schutz and T. R. Slatyer, *Self-Scattering for Dark Matter with an Excited State*, *JCAP* **1501** (2015) 021 [1409.2867].

[154] M. R. Buckley and P. J. Fox, *Dark Matter Self-Interactions and Light Force Carriers*, *Phys. Rev.* **D81** (2010) 083522 [0911.3898].

[155] A. Loeb and N. Weiner, *Cores in Dwarf Galaxies from Dark Matter with a Yukawa Potential*, *Phys. Rev. Lett.* **106** (2011) 171302 [1011.6374].

[156] S. Tulin, H.-B. Yu and K. M. Zurek, *Resonant Dark Forces and Small Scale Structure*, *Phys. Rev. Lett.* **110** (2013) 111301 [1210.0900].

[157] R. N. Mohapatra, S. Nussinov and V. L. Teplitz, *Mirror matter as selfinteracting dark matter*, *Phys. Rev.* **D66** (2002) 063002 [hep-ph/0111381].

[158] M. Ibe and H.-b. Yu, *Distinguishing Dark Matter Annihilation Enhancement Scenarios via Halo Shapes*, *Phys. Lett.* **B692** (2010) 70 [0912.5425].

[159] E. W. Kolb and M. S. Turner, *The Early Universe*, *Front. Phys.* **69** (1990) 1.

[160] S. Dodelson, *Modern Cosmology*. Academic Press, Amsterdam, 2003.

[161] R. M. Wald, *General Relativity*. Chicago Univ. Pr., Chicago, USA, 1984, 10.7208/chicago/9780226870373.001.0001.

[162] G. Gamow, *Expanding universe and the origin of elements*, *Phys. Rev.* **70** (1946) 572.

[163] R. A. Alpher, H. Bethe and G. Gamow, *The origin of chemical elements*, *Phys. Rev.* **73** (1948) 803.

[164] R. A. Alpher and R. C. Herman, *On the relative abundance of the elements*, *Phys. Rev.* **74** (1948) 1737.

[165] R. A. Alpher and R. C. Herman, *Remarks on the evolution of the expanding universe*, *Phys. Rev.* **75** (1949) 1089.

[166] A. A. Penzias and R. W. Wilson, *A Measurement of Excess Antenna Temperature at 4080 Mc/s.*, *Astrophysical Journal* **142** (1965) 419.

[167] M. Srednicki, R. Watkins and K. A. Olive, *Calculations of Relic Densities in the Early Universe*, *Nucl. Phys.* **B310** (1988) 693.

[168] T. Plehn, *Yet Another Introduction to Dark Matter*, 1705.01987.

[169] L. Roszkowski, E. M. Sessolo and S. Trojanowski, *WIMP dark matter candidates and searchesâĂŤcurrent status and future prospects*, *Rept. Prog. Phys.* **81** (2018) 066201 [1707.06277].

[170] K. M. Nollett and G. Steigman, *BBN And The CMB Constrain Light, Electromagnetically Coupled WIMPs*, *Phys. Rev.* **D89** (2014) 083508 [1312.5725].

[171] S. Weinberg, *The Quantum theory of fields. Vol. 1: Foundations*. Cambridge University Press, 2005.

[172] S. Weinberg, *The quantum theory of fields. Vol. 2: Modern applications*. Cambridge University Press, 2013.

[173] M. D. Schwartz, *Quantum Field Theory and the Standard Model*. Cambridge University Press, 2014.

[174] M. E. Peskin and D. V. Schroeder, *An Introduction to quantum field theory*. Addison-Wesley, Reading, USA, 1995.

[175] P. W. Higgs, *Broken symmetries and the masses of gauge bosons*, *Phys. Rev. Lett.* **13** (1964) 508.

[176] S. Elitzur, *Impossibility of spontaneously breaking local symmetries*, *Phys. Rev. D* **12** (1975) 3978.

[177] G. Krnjaic, *Probing Light Thermal Dark-Matter With a Higgs Portal Mediator*, *Phys. Rev.* **D94** (2016) 073009 [1512.04119].

[178] B. Batell, D. McKeen and M. Pospelov, *Singlet Neighbors of the Higgs Boson*, *JHEP* **10** (2012) 104 [1207.6252].

[179] P. Gondolo and G. Gelmini, *Cosmic abundances of stable particles: Improved analysis*, *Nucl. Phys.* **B360** (1991) 145.

[180] R. J. Scherrer and M. S. Turner, *On the relic, cosmic abundance of stable, weakly interacting massive particles*, *Phys. Rev. D* **33** (1986) 1585.

[181] S.-M. Choi, Y. Hochberg, E. Kuflik, H. M. Lee, Y. Mambrini, H. Murayama et al., *Vector SIMP dark matter*, *JHEP* **10** (2017) 162 [1707.01434].

[182] L. D. Landau and L. M. Lifshitz, *Quantum Mechanics Non-Relativistic Theory, Third Edition: Volume 3*. Butterworth-Heinemann, 3 ed., Jan., 1981.

[183] K. Griest and D. Seckel, *Three exceptions in the calculation of relic abundances*, *Phys. Rev. D* **43** (1991) 3191.

[184] S. R. De Groot, *Relativistic Kinetic Theory. Principles and Applications*. 1980.

[185] K. Griest and D. Seckel, *Cosmic Asymmetry, Neutrinos and the Sun*, *Nucl. Phys.* **B283** (1987) 681.

[186] S.-M. Choi, H. M. Lee and M.-S. Seo, *Cosmic abundances of SIMP dark matter*, *JHEP* **04** (2017) 154 [1702.07860].

[187] G. Steigman, *Cosmology Confronts Particle Physics*, *Ann. Rev. Nucl. Part. Sci.* **29** (1979) 313.

[188] H. K. Eriksen, C. Dickinson, C. R. Lawrence, C. Baccigalupi, A. J. Banday, K. M. GÃşrski et al., *Cosmic microwave background component separation by parameter estimation*, *The Astrophysical Journal* **641** (2006) 665.